

Supporting Information for

Leveraging the monomer structure for high-performance chemically recyclable semiaromatic polyesters

Hua-Zhong Fan,^a Xing Yang,^a Yan-Chen Wu,^a Qing Cao,^a Zhongzheng Cai,^{*a} Jian-Bo Zhu^{*a}

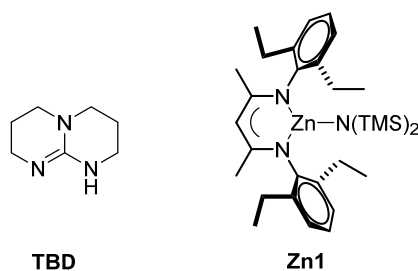
^aNational Engineering Laboratory of Eco-Friendly Polymeric Materials (Sichuan), College of Chemistry, Sichuan University, 29 Wangjiang Road, Chengdu, 610064, People's Republic of China

| TABLE OF CONTENTS | | Page(s) |
|--|---|----------------|
| Materials and Methods | | S3-S4 |
| General Monomer Preparations | | S5-S9 |
| Fig. S1 | ¹ H NMR (CDCl ₃ , 25 °C) spectrum of DHB-Me | S10 |
| Fig. S2 | ¹ H NMR (CDCl ₃ , 25 °C) spectrum of (<i>R</i>)-DHB-Me | S11 |
| Fig. S3 | ¹³ C NMR (CDCl ₃ , 25 °C) spectrum of (<i>R</i>)-DHB-Me | S11 |
| Fig. S4 | ¹ H NMR (CDCl ₃ , 25 °C) spectrum of (<i>S</i>)-DHB-Me | S12 |
| Fig. S5 | ¹³ C NMR (CDCl ₃ , 25 °C) spectrum of (<i>S</i>)-DHB-Me | S12 |
| Fig. S6 | ¹ H NMR (CDCl ₃ , 25 °C) spectrum of DHB-Et | S13 |
| Fig. S7 | ¹³ C NMR (CDCl ₃ , 25 °C) spectrum of DHB-Et | S13 |
| Fig. S8 | ¹ H NMR (CDCl ₃ , 25 °C) spectrum of DHN-Me | S14 |
| Fig. S9 | ¹³ C NMR (CDCl ₃ , 25 °C) spectrum of DHN-Me | S14 |
| Fig. S10 | ¹ H NMR (CDCl ₃ , 25 °C) spectrum of (<i>R</i>)-DHN-Me | S15 |
| Fig. S11 | ¹³ C NMR (CDCl ₃ , 25 °C) spectrum of (<i>R</i>)-DHN-Me | S15 |
| Fig. S12 | ¹ H NMR (CDCl ₃ , 25 °C) spectrum of (<i>S</i>)-DHN-Me | S16 |
| Fig. S13 | ¹³ C NMR (CDCl ₃ , 25 °C) spectrum of (<i>S</i>)-DHN-Me | S16 |
| Fig. S14 | ¹ H NMR (CDCl ₃ , 25 °C) spectrum of DHN-Et | S17 |
| Fig. S15 | ¹³ C NMR (CDCl ₃ , 25 °C) spectrum of DHN-Et | S17 |
| General Polymerization Procedures | | S18 |
| Table S1 | Results for the copolymerization of DHB-Me and DHB-Et | S18 |
| Polymer Characterization | | |
| Fig. S16 | ¹ H NMR (CDCl ₃ , 25 °C) spectrum of P(DHB-Me) | S19 |
| Fig. S17 | ¹³ C NMR (CDCl ₃ , 25 °C) spectrum of P(DHB-Me) | S19 |
| Fig. S18 | ¹ H NMR (CDCl ₃ , 25 °C) spectrum of P[(<i>R</i>)-DHB-Me] | S20 |
| Fig. S19 | ¹³ C NMR (CDCl ₃ , 25 °C) spectrum of P[(<i>R</i>)-DHB-Me] | S20 |
| Fig. S20 | ¹ H NMR (CDCl ₃ , 25 °C) spectrum of P[(<i>S</i>)-DHB-Me] | S21 |
| Fig. S21 | ¹³ C NMR (CDCl ₃ , 25 °C) spectrum of P[(<i>S</i>)-DHB-Me] | S21 |
| Fig. S22 | ¹ H NMR (CDCl ₃ , 25 °C) spectrum of P(DHB-Et) | S22 |
| Fig. S23 | ¹³ C NMR (CDCl ₃ , 25 °C) spectrum of P(DHB-Et) | S22 |
| Fig. S24 | ¹ H NMR (CDCl ₃ , 25 °C) spectrum of P(DHN-Me) | S23 |
| Fig. S25 | ¹³ C NMR (CDCl ₃ , 25 °C) spectrum of P(DHN-Me) | S23 |
| Fig. S26 | ¹ H NMR (CDCl ₃ , 25 °C) spectrum of P P[(<i>R</i>)-DHN-Me] | S24 |
| Fig. S27 | ¹³ C NMR (CDCl ₃ , 25 °C) spectrum of P[(<i>R</i>)-DHN-Me] | S24 |
| Fig. S28 | ¹ H NMR (CDCl ₃ , 25 °C) spectrum of P P[(<i>S</i>)-DHN-Me] | S25 |
| Fig. S29 | ¹³ C NMR (CDCl ₃ , 25 °C) spectrum of P[(<i>S</i>)-DHN-Me] | S25 |
| Fig. S30 | ¹ H NMR (CDCl ₃ , 25 °C) spectrum of P(DHN-Et) | S26 |
| Fig. S31 | ¹³ C NMR (CDCl ₃ , 25 °C) spectrum of P(DHN-Et) | S26 |
| Fig. S32 | ¹ H NMR (CDCl ₃ , 25 °C) spectrum of P(DHB-Me-co-DHB-Et) | S27 |
| Fig. S33 | ¹³ C NMR (CDCl ₃ , 25 °C) spectrum of P(DHB-Me-co-DHB-Et) | S27 |
| Fig. S34 | MALDI-TOF MS spectrum (top) of the low-molecular-weight P(DHB- | S28 |

| | | |
|---|--|-----|
| | Me) | |
| Fig. S35 | TGA and DTG curves for P(DHB-Me) | S29 |
| Fig. S36 | TGA and DTG curves for P[(<i>R</i>)-DHB-Me] | S29 |
| Fig. S37 | TGA and DTG curves for P(DHB-Et) | S30 |
| Fig. S38 | TGA and DTG curves for P[(<i>R</i>)-DHN-Me] | S30 |
| Fig. S39 | TGA and DTG curves for P(DHN-Me) | S31 |
| Fig. S40 | TGA and DTG curves for P(DHN-Et) | S31 |
| Fig. S41 | TGA and DTG curves for P(DHB-Me-co-DHB-Et) | S32 |
| Fig. S42 | DSC curves for P(DHB-Me) | S32 |
| Fig. S43 | DSC curves for P[(<i>R</i>)-DHB-Me] | S33 |
| Fig. S44 | DSC curves for P(DHB-Et) | S33 |
| Fig. S45 | DSC curves for P(DHN-Me) | S34 |
| Fig. S46 | DSC curves for P[(<i>R</i>)-DHN-Me] | S34 |
| Fig. S47 | DSC curves for P(DHN-Et) | S35 |
| Fig. S48 | DSC curves for P(DHB-Me-co-DHB-Et) | S35 |
| Fig. S49 | GPC trace of P(DHB-Me) | S36 |
| Fig. S50 | GPC trace of P[(<i>R</i>)-DHB-Me] | S36 |
| Fig. S51 | GPC trace of P(DHB-Et) | S37 |
| Fig. S52 | GPC trace of P(DHN-Me) | S37 |
| Fig. S53 | GPC trace of P[(<i>R</i>)-DHN-Me] | S38 |
| Fig. S54 | GPC trace of P(DHN-Et) | S38 |
| Fig. S55 | GPC trace of P(DHB-Me-co-DHB-Et) | S39 |
| General Stereocomplexation procedures | | |
| Fig. S56 | DSC and PXRD spectra of P(DHB-Me)s and P(DHN-Me)s | S40 |
| Mechanical Property | | |
| Table S2 | Summary of mechanical properties of polymers | S41 |
| Table S3 | Summary of mechanical properties of P(DHB-Me) | S41 |
| Fig. S57 | Stress-strain curves of P(DHB-Me) | S41 |
| Table S4 | Summary of mechanical properties of P(DHB-Me)s | S42 |
| Fig. S58 | Stress-strain curves of P(DHB-Me)s | S42 |
| Table S5 | Summary of mechanical properties of P(DHB-Et) | S43 |
| Fig. S59 | Stress-strain curves of P(DHB-Et) | S43 |
| Table S6 | Summary of mechanical properties of P(DHN-Me) | S44 |
| Fig. S60 | Stress-strain curves of P(DHN-Me) | S44 |
| Table S7 | Summary of mechanical properties of P(DHN-Et) | S45 |
| Fig. S61 | Stress-strain curves of P(DHN-Et) | S45 |
| Table S8 | Summary of mechanical properties of P(DHB-Me-co-DHB-Et) | S46 |
| Fig. S62 | Stress-strain curves of P(DHB-Me-co-DHB-Et) | S46 |
| Thermodynamic Study | | |
| Table S9 | Raw data over equilibrium conversion at various temperature for DHB-Me | S47 |
| Fig. S63 | Van't Hoff plot of $\ln[\text{DHB-Me}]_{\text{eq}}$ vs. reciprocal of the absolute temperature (T^{-1}). | S47 |
| General procedure for the depolymerization of polymers in dilute solutions | | |
| Table S10 | Results for depolymerization of P(M)s in dilute solutions | S48 |
| Fig. S64 | ^1H NMR spectra of the depolymerization products of P(DHB-Et) | S48 |
| Fig. S65 | ^1H NMR spectra of the depolymerization products of P(DHN-Me) | S49 |
| Fig. S66 | ^1H NMR spectra of the depolymerization products of P(DHN-Et) | S49 |
| References | | |
| | | S50 |

Materials and Methods

All synthesis and manipulations of air- and moisture-sensitive materials were carried out in an argon-filled glovebox. All reagents from Adamas-beta and Energy Chemical were used as received unless otherwise stated. High-performance liquid chromatography (HPLC)-grade organic solvents were dried by Vigor YJC-5 and then stored over activated 4 Å molecular sieves. The initiator *p*-tolylmethanol was purchased from adamas and sublimed at 55 °C prior to use. 1,5,7-triazabicyclo[4.4.0]dec-5-ene (TBD) was sublimed under vacuum at 60 °C prior to use. 2,6-diethylphenyl substituted β -diiminate zinc trimethylsilyl complex **Zn1** was prepared according to literature procedures.^[1]



NMR ¹H and ¹³C NMR spectra were recorded on an Agilent 400-MR DD2 or a Bruker Advance 400 spectrometer (¹H: 400 MHz, ¹³C: 100 MHz). Chemical shifts (δ) for ¹H and ¹³C NMR spectra are given in ppm relative to TMS. The residual solvent signals were used as references for ¹H and ¹³C NMR spectra and the chemical shifts converted to the TMS scale. The following abbreviations were used to explain the multiplicities: s = singlet, d = doublet, t = triplet, q = quartet, m = multiplet.

Size Exclusion Chromatography (SEC) Measurements of polymer absolute weight-average molecular weight (M_w), number average molecular weight (M_n), and molecular weight distributions or dispersity indices ($\mathcal{D} = M_w/M_n$) were performed via size exclusion chromatography (SEC). The SEC instrument consisted of an Agilent LC system equipped with one guard column and two PL gel 5 μ m mixed-C gel permeation columns and coupled with an Agilent G7162A 1260 Infinity II RI detector. The analysis was performed at 40 °C using THF as the eluent at a flow rate of 1.0 mL/min. The instrument was calibrated with nine polystyrene standards, and chromatograms were processed with Agilent OpenLab CDS Acquisition 2.5 molecular weight characterization software.

Differential scanning calorimetry (DSC) Melting-transition temperature (T_m) and glass-transition temperature (T_g) of purified and thoroughly dried polymer samples were measured by differential scanning calorimetry (DSC) on a TRIOS DSC25, TA Instrument. All T_g values were obtained from a second scan after the thermal history was removed from the first scan.

Thermo-gravimetric analysis (TGA) Decomposition onset temperatures (T_{onset}) and maximum rate decomposition temperatures (T_{max}) of the polymers were measured by thermal gravimetric analysis (TGA) on a TGA55 Analyzer, TA Instrument. Polymer samples were heated from ambient temperature to 600 °C at a heating rate of 10 °C/min. Values of T_{max} were obtained from derivative (wt%/°C) vs. temperature (°C) plots and defined by the peak values, while T_{onset} values were obtained from wt% vs. temperature (°C) plots and defined by the temperature of 5% weight loss.

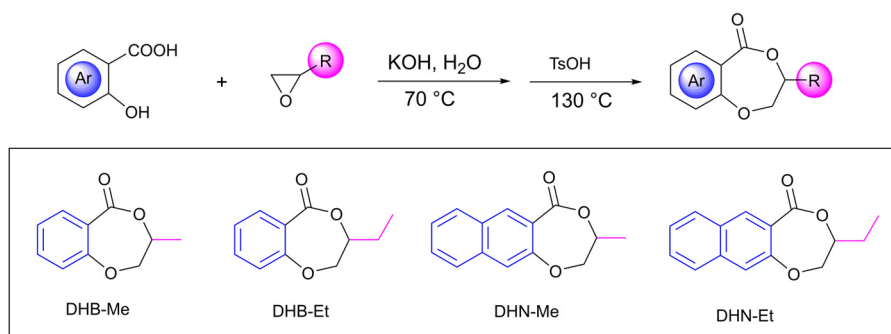
Matrix-assisted laser desorption/ionization time-of-flight mass spectroscopy

(MALDI-TOF MS). An AXIMA performance instrument was used in reflection mode with dithranol as the matrix. A thin layer of a 1% NaI solution was first deposited on the target plate, followed by the solutions of matrix (5 μ L, 5 mg/mL in dichloromethane) and polymer (2 μ L, 5 mg/mL in dichloromethane) were mixed together. The mixed solution was spotted on the MALDI sample plate and air-dried. The raw data was processed in the Shimadzu Biotech MALDI-MS software.

Wide angle X-ray diffraction (WXR) Powder X-ray diffraction data were obtained using a Bruker D2 Phaser diffractometer with Cu-K α radiation ($\lambda = 1.5416$ A) at 30 kV and 10 mA (scan of $2\theta = 5-30^\circ$ with a speed of $2^\circ/\text{min}$).

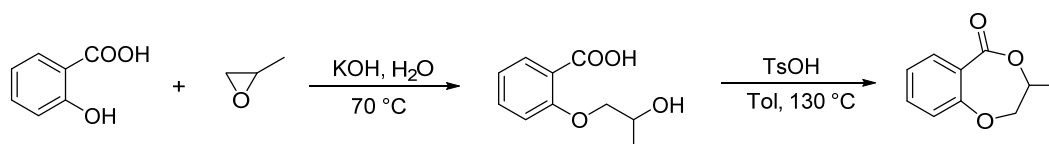
Mechanical Analysis. Tensile stress/strain testing was performed by an Instron 34SC-1 universal testing system. Samples were made by melt press in a steel mold ($50 \times 4 \times 0.4$ mm³) and were stretched at a strain rate of 10 mm/min at ambient temperature until break. The measurements were performed 3-5 times for each test, and the values reported are averaged from the measured data.

General Monomer Preparations



Scheme S1. Synthesis of monomers.

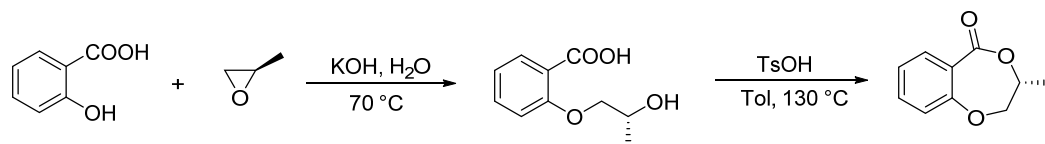
Synthesis of DHB-Me



A 75 mL pressure tube equipped with a stir bar was charged with salicylic acid (6.9 g, 0.05 mol), KOH (5.6 g, 0.1 mol), H₂O (3.6 mL, 0.2 mol) and propylene oxide (14.0 mL, 0.2 mol). After stirring for 12 h at 70 °C, the reaction was quenched by the addition of 12 M HCl (9 mL) slowly and diluted with water (30 mL), then the mixture was extracted with ethyl acetate (3 × 50 mL). The combined organic layers were dried over anhydrous Na₂SO₄, filtrated, and concentrated in vacuo. The crude product was directly used for the next step.

In a 500 mL flask which connected to a Dean-Stark trap, the above crude product was dissolved in 300 mL toluene and 1.9 g TsOH was used as catalyst. After refluxing for 12 h at 130 °C, the reaction mixture was cooled to room temperature and concentrated in vacuo. The crude product was purified by flash chromatography (petroleum ether/ethyl acetate = 20: 1) to afford DHB-Me as white solid (5.0 g, 56% for two steps). ¹H NMR (400 MHz, CDCl₃): δ 7.86 (d, *J* = 7.9 Hz, 1H), 7.47 (t, *J* = 7.8 Hz, 1H), 7.13 – 7.09 (m, 1H), 7.00 (dd, *J* = 8.3, 1.3 Hz, 1H), 4.75 – 4.68 (m, 1H), 4.36 – 4.26 (m, 2H), 1.40 (d, *J* = 6.7 Hz, 3H).

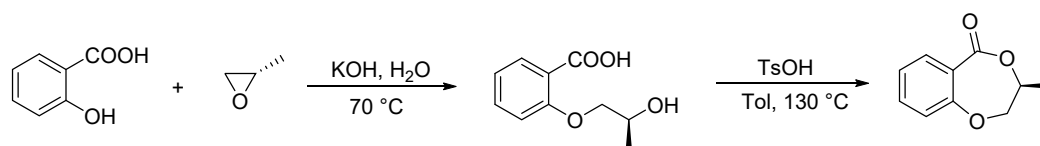
Synthesis of (*R*)-DHB-Me



A 75 mL pressure tube equipped with a stir bar was charged with salicylic acid (6.9 g, 0.05 mol), KOH (5.6 g, 0.1 mol), H₂O (3.6 mL, 0.2 mol) and (*R*)-propylene oxide (12.9 mL, 0.2 mol). After stirring for 12 h at 70 °C, the reaction was quenched by the addition of 12 M HCl (9 mL) slowly and diluted with water (30 mL), then the mixture was extracted with ethyl acetate (3 × 50 mL). The combined organic layers were dried over anhydrous Na₂SO₄, filtrated, and concentrated in vacuo. The crude product was directly used for the next step.

In a 500 mL flask which connected to a Dean-Stark trap, the above crude product was dissolved in 300 mL toluene and 1.9 g TsOH was used as catalyst. After refluxing for 12 h at 130 °C, the reaction mixture was cooled to room temperature and concentrated in vacuo. The crude product was purified by flash chromatography (petroleum ether/ethyl acetate = 20: 1) to afford (*R*)-DHB-Me as white solid (4.4 g, 49% for two steps). ¹H NMR (400 MHz, CDCl₃): δ 7.86 (dd, J = 7.9, 1.8 Hz, 1H), 7.50 – 7.46 (m, 1H), 7.14 – 7.10 (m, 1H), 7.00 (d, J = 8.3 Hz, 1H), 4.76 – 4.68 (m, 1H), 4.36 – 4.26 (m, 2H), 1.40 (d, J = 6.6 Hz, 3H). ¹³C NMR (100 MHz, CDCl₃): δ 168.5, 155.0, 134.7, 133.2, 122.9, 120.9, 120.4, 75.6, 72.4, 16.3. ESI-MS: calculated m/z 179.0708; found m/z 179.0706 [M + H]⁺.

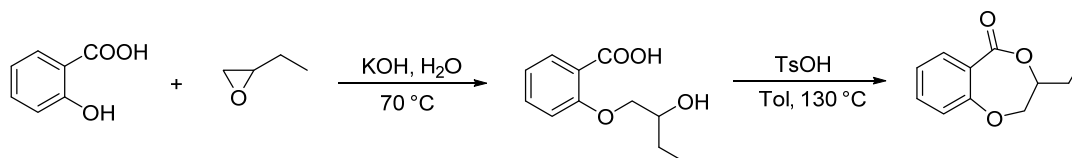
Synthesis of (*S*)-DHB-Me



A 75 mL pressure tube equipped with a stir bar was charged with salicylic acid (6.9 g, 0.05 mol), KOH (5.6 g, 0.1 mol), H₂O (3.6 mL, 0.2 mol) and (*S*)-propylene oxide (12.9 mL, 0.2 mol). After stirring for 12 h at 70 °C, the reaction was quenched by the addition of 12 M HCl (9 mL) slowly and diluted with water (30 mL), then the mixture was extracted with ethyl acetate (3 × 50 mL). The combined organic layers were dried over anhydrous Na₂SO₄, filtrated, and concentrated in vacuo. The crude product was directly used for the next step.

In a 500 mL flask which connected to a Dean-Stark trap, the above crude product was dissolved in 300 mL toluene and 1.9 g TsOH was used as catalyst. After refluxing for 12 h at 130 °C, the reaction mixture was cooled to room temperature and concentrated in vacuo. The crude product was purified by flash chromatography (petroleum ether/ethyl acetate = 20: 1) to afford (*S*)-DHB-Me as white solid (3.8 g, 43% for two steps). ¹H NMR (400 MHz, CDCl₃): δ 7.87 (dd, J = 8.0, 1.6 Hz, 1H), 7.51-7.46 (m, 1H), 7.12 (dd, J = 8.1, 7.1 Hz, 1H), 7.01 (d, J = 8.3 Hz, 1H), 4.76-4.69 (m, 1H), 4.37-4.27 (m, 2H), 1.41 (d, J = 6.6 Hz, 3H). ¹³C NMR (100 MHz, CDCl₃): δ 168.5, 155.1, 134.8, 133.3, 122.9, 120.9, 120.4, 75.6, 72.4, 16.3. ESI-MS: calculated m/z 179.0708; found m/z 179.0706 [M + H]⁺.

Synthesis of DHB-Et

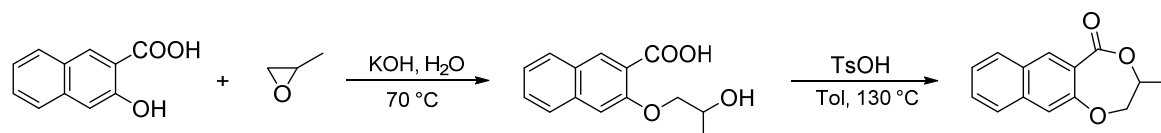


A 75 mL pressure tube equipped with a stir bar was charged with salicylic acid (6.9 g, 0.05 mol), KOH (5.6 g, 0.1 mol), H₂O (3.6 mL, 0.2 mol) and 1,2-epoxybutane (16.4 mL, 0.2 mol). After stirring for 24 h at 70 °C, the reaction was quenched by the addition of 12 M HCl (9 mL) slowly and diluted with water (30 mL), then the mixture was extracted with ethyl acetate (3 × 50 mL). The combined organic layers were dried over anhydrous Na₂SO₄, filtrated, and concentrated in vacuo. The crude product was directly used for the next step.

In a 500 mL flask which connected to a Dean-Stark trap, the above crude product was dissolved in 300 mL toluene, and 1.9 g TsOH was used as catalyst. After refluxing for 24 h at

130 °C, the reaction mixture was cooled to room temperature and concentrated in vacuo. The crude product was purified by flash chromatography (petroleum ether/ethyl acetate = 20: 1) to afford DHB-Et as white solid (4.4 g, 46% for two steps). ¹H NMR (400 MHz, CDCl₃): δ 7.89 (dd, *J* = 7.9, 1.8 Hz, 1H), 7.50-7.46 (m, 1H), 7.14-7.10 (m, 1H), 7.00 (dd, *J* = 8.2, 1.2 Hz, 1H), 4.47-4.43 (m, 1H), 4.38-4.33 (m, 2H), 1.84-1.62 (m, 2H), 1.06 (t, *J* = 7.5 Hz, 3H). ¹³C NMR (100 MHz, CDCl₃): δ 168.6, 155.2, 134.7, 133.4, 122.7, 120.8, 120.1, 77.4, 74.4, 24.0, 9.7. ESI-MS: calculated *m/z* 193.0865; found *m/z* 193.0862 [M + H]⁺.

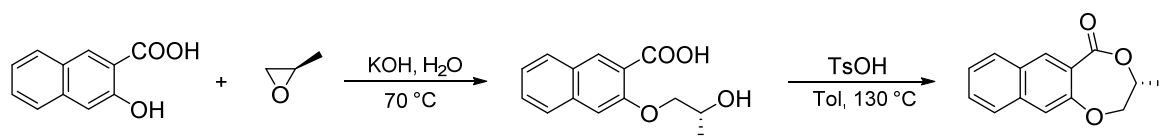
Synthesis of DHN-Me



A 75 mL pressure tube equipped with a stir bar was charged with 3-Hydroxy-2-naphthoic acid (9.4 g, 0.05 mol), KOH (5.6 g, 0.1 mol), H₂O (10 mL) and propylene oxide (14.0 mL, 0.2 mol). After stirring for 12 h at 70 °C, the reaction was quenched by the addition of 12 M HCl (9 mL) slowly and diluted with water (30 mL), then the mixture was extracted with ethyl acetate (3 × 50 mL). The combined organic layers were dried over anhydrous Na₂SO₄, filtrated, and concentrated in vacuo. The crude product was directly used for the next step.

In a 500 mL flask which connected to a Dean-Stark trap, the above crude product was dissolved in 300 mL toluene, and 1.9 g TsOH was used as catalyst. After refluxing for 12 h at 130 °C, the reaction mixture was cooled to room temperature and concentrated in vacuo. The crude product was purified by flash chromatography (petroleum ether/ethyl acetate = 20: 1) to afford DHN-Me as white solid (7.4 g, 65% for two steps). ¹H NMR (400 MHz, CDCl₃): δ 8.31 (s, 1H), 7.87 (d, *J* = 8.2 Hz, 1H), 7.76 (d, *J* = 8.3 Hz, 1H), 7.56-7.53 (m, 1H), 7.46 (d, *J* = 7.9 Hz, 2H), 4.70-4.62 (m, 1H), 4.33-4.17 (m, 2H), 1.37 (d, *J* = 6.4 Hz, 3H). ¹³C NMR (100 MHz, CDCl₃): δ 168.9, 150.4, 136.4, 133.4, 129.9, 128.8, 128.7, 126.8, 125.8, 124.6, 118.0, 76.3, 71.8, 15.6. ESI-MS: calculated *m/z* 229.0865; found *m/z* 229.0855 [M + H]⁺.

Synthesis of (*R*)-DHN-Me

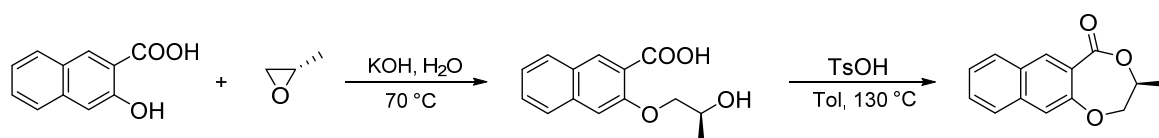


A 75 mL pressure tube equipped with a stir bar was charged with 3-Hydroxy-2-naphthoic acid (9.4 g, 0.05 mol), KOH (5.6 g, 0.1 mol), H₂O (15 mL) and (*R*)-propylene oxide (12.9 mL, 0.2 mol). After stirring for 12 h at 70 °C, the reaction was quenched by the addition of 12 M HCl (9 mL) slowly and diluted with water (30 mL), then the mixture was extracted with ethyl acetate (3 × 50 mL). The combined organic layers were dried over anhydrous Na₂SO₄, filtrated, and concentrated in vacuo. The crude product was directly used for the next step.

In a 500 mL flask which connected to a Dean-Stark trap, the above crude product was dissolved in 300 mL toluene, and 1.9 g TsOH was used as catalyst. After refluxing for 24 h at 130 °C, the reaction mixture was cooled to room temperature and concentrated in vacuo. The crude product was purified by flash chromatography (petroleum ether/ethyl acetate = 20: 1) to

afford (*R*)-DHN-Me as white solid (5.0 g, 44% for two steps). ¹H NMR (400 MHz, CDCl₃): δ 8.32 (s, 1H), 7.89 (d, *J* = 8.3 Hz, 1H), 7.77 (d, *J* = 8.3 Hz, 1H), 7.58-7.54 (m, 1H), 7.49-7.45 (m, 2H), 4.72-4.64 (m, 1H), 4.32 (t, *J* = 11.1 Hz, 1H), 4.19 (dd, *J* = 11.5, 3.1 Hz, 1H), 1.39 (d, *J* = 6.4 Hz, 3H). ¹³C NMR (100 MHz, CDCl₃): δ 168.9, 150.5, 136.5, 133.4, 130.0, 128.9, 128.7, 126.9, 125.9, 124.6, 118.0, 76.4, 71.8, 15.7. ESI-MS: calculated *m/z* 229.0865; found *m/z* 229.0883 [M + H]⁺.

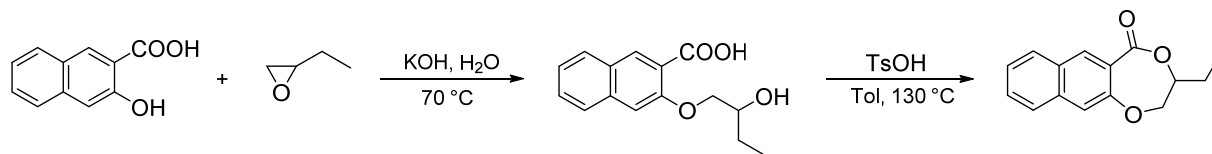
Synthesis of (*S*)-DHN-Me



A 75 mL pressure tube equipped with a stir bar was charged with 3-Hydroxy-2-naphthoic acid (9.4 g, 0.05 mol), KOH (5.6 g, 0.1 mol), H₂O (15 mL) and (*S*)-propylene oxide (12.9 mL, 0.2 mol). After stirring for 12 h at 70 °C, the reaction was quenched by the addition of 12 M HCl (9 mL) slowly and diluted with water (30 mL), then the mixture was extracted with ethyl acetate (3 × 50 mL). The combined organic layers were dried over anhydrous Na₂SO₄, filtrated, and concentrated in vacuo. The crude product was directly used for the next step.

In a 500 mL flask which connected to a Dean-Stark trap, the above crude product was dissolved in 300 mL toluene, and 1.9 g TsOH was used as catalyst. After refluxing for 24 h at 130 °C, the reaction mixture was cooled to room temperature and concentrated in vacuo. The crude product was purified by flash chromatography (petroleum ether/ethyl acetate = 20: 1) to afford (*S*)-DHN-Me as white solid (6.3 g, 55% for two steps). ¹H NMR (400 MHz, CDCl₃): δ 8.32 (s, 1H), 7.89 (dd, *J* = 8.2, 1.2 Hz, 1H), 7.77 (dd, *J* = 8.4, 1.1 Hz, 1H), 7.58-7.54 (m, 1H), 7.49-7.45 (m, 2H), 4.72-4.64 (m, 1H), 4.32 (t, *J* = 11.1 Hz, 1H), 4.19 (dd, *J* = 11.5, 3.1 Hz, 1H), 1.39 (d, *J* = 6.4 Hz, 3H). ¹³C NMR (100 MHz, CDCl₃): δ 168.9, 150.5, 136.5, 133.4, 130.0, 128.9, 128.7, 126.9, 125.9, 124.6, 118.0, 76.4, 71.8, 15.7. ESI-MS: calculated *m/z* 229.0865; found *m/z* 229.0880 [M + H]⁺.

Synthesis of DHN-Et



A 75 mL pressure tube equipped with a stir bar was charged with 3-hydroxy-2-naphthoic Acid (9.4 g, 0.05 mol), KOH (5.6 g, 0.1 mol), H₂O (3.6 mL, 0.2 mol) and 1,2-epoxybutane (16.4 mL, 0.2 mol). After stirring for 24 h at 70 °C, the reaction was quenched by the addition of 12 M HCl (9 mL) slowly and diluted with water (30 mL), then the mixture was extracted with ethyl acetate (3 × 50 mL). The combined organic layers were dried over anhydrous Na₂SO₄, filtrated, and concentrated in vacuo. The crude product was directly used for the next step.

In a 500 mL flask which connected to a Dean-Stark trap, the above crude product was dissolved in 300 mL toluene, and 1.9 g TsOH was used as catalyst. After refluxing for 24 h at 130 °C, the reaction mixture was cooled to room temperature and concentrated in vacuo. The crude product was purified by flash chromatography (petroleum ether/ethyl acetate = 20:1) to

afford DHN-Et as white solid (4.1 g, 34% for two steps). ¹H NMR (400 MHz, CDCl₃): δ 8.34 (s, 1H), 7.90 (d, *J* = 8.2 Hz, 1H), 7.78 (d, *J* = 8.3 Hz, 1H), 7.58 – 7.54 (m, 1H), 7.49 – 7.45 (m, 2H), 4.45 – 4.40 (m, 1H), 4.36 (t, *J* = 10.8 Hz, 1H), 4.24 – 4.20 (m, 1H), 1.82 – 1.60 (m, 2H), 1.04 (t, *J* = 7.4 Hz, 3H). ¹³C NMR (100 MHz, CDCl₃): δ 169.1, 150.5, 136.4, 133.4, 129.9, 128.9, 128.7, 126.8, 125.8, 124.6, 118.0, 76.7, 75.1, 23.4, 9.8. ESI-MS: calculated *m/z* 243.1021; found *m/z* 243.1012 [M + H]⁺.

NMR spectra of monomers

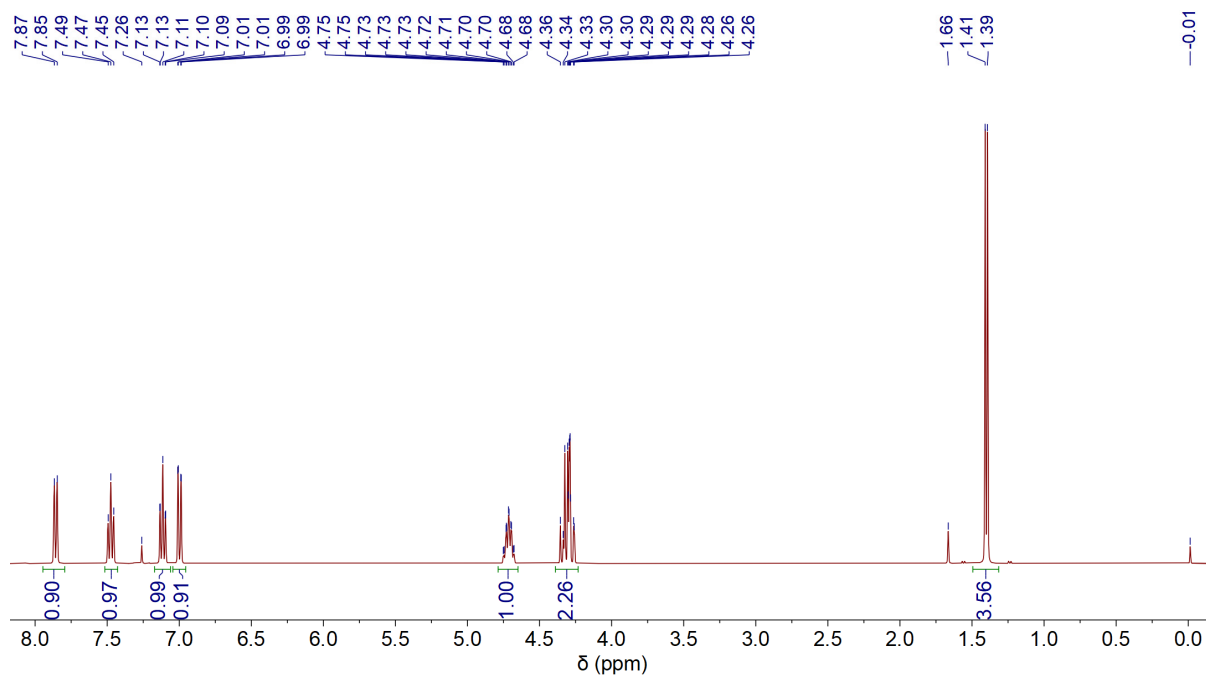


Fig. S1. ¹H NMR (CDCl₃, 25 °C) spectrum of DHB-Me. Residual solvent peaks at 7.26 ppm and 1.66 ppm for CHCl₃ and H₂O, respectively.

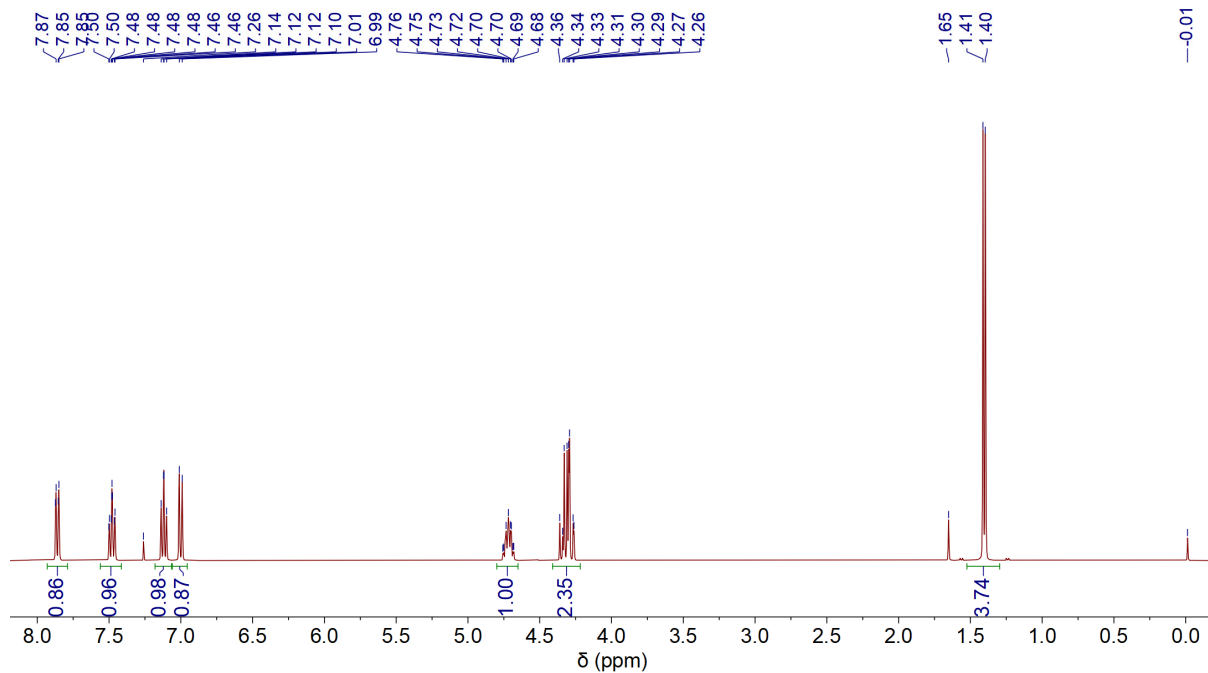


Fig. S2. ^1H NMR (CDCl_3 , 25 $^\circ\text{C}$) spectrum of (*R*)-DHB-Me. Residual solvent peaks at 7.26 ppm and 1.65 ppm for CHCl_3 and H_2O , respectively.

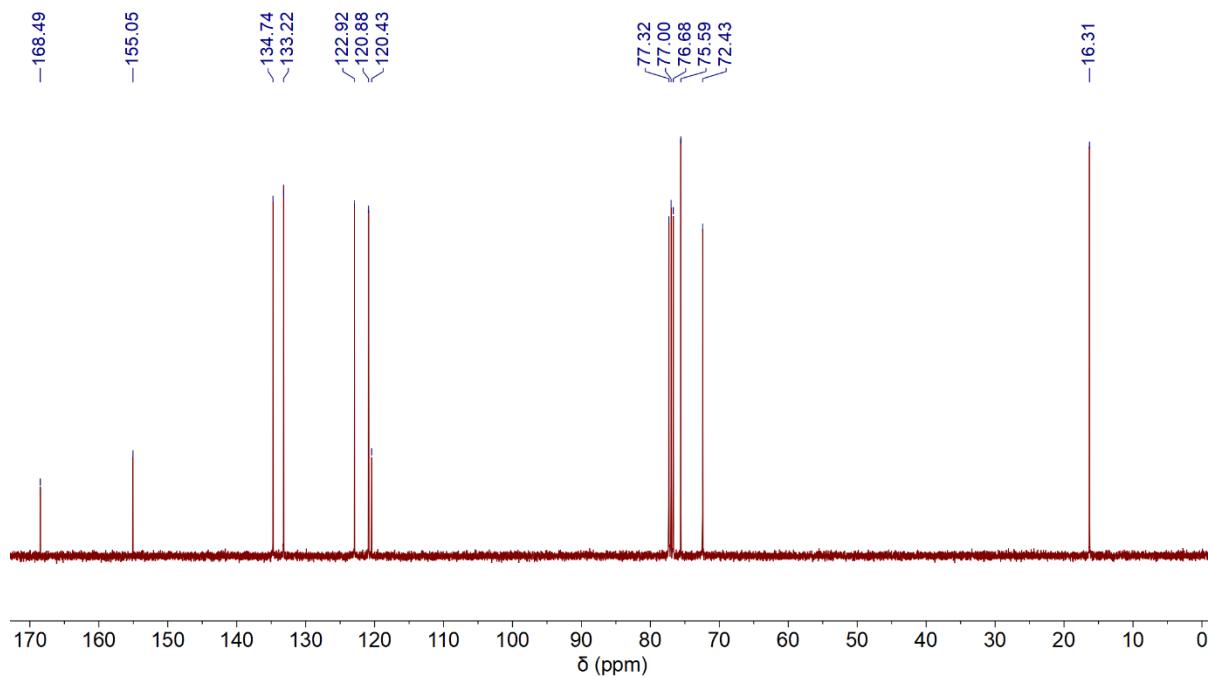


Fig. S3. ^{13}C NMR (CDCl_3 , 25 $^\circ\text{C}$) spectrum of (*R*)-DHB-Me.

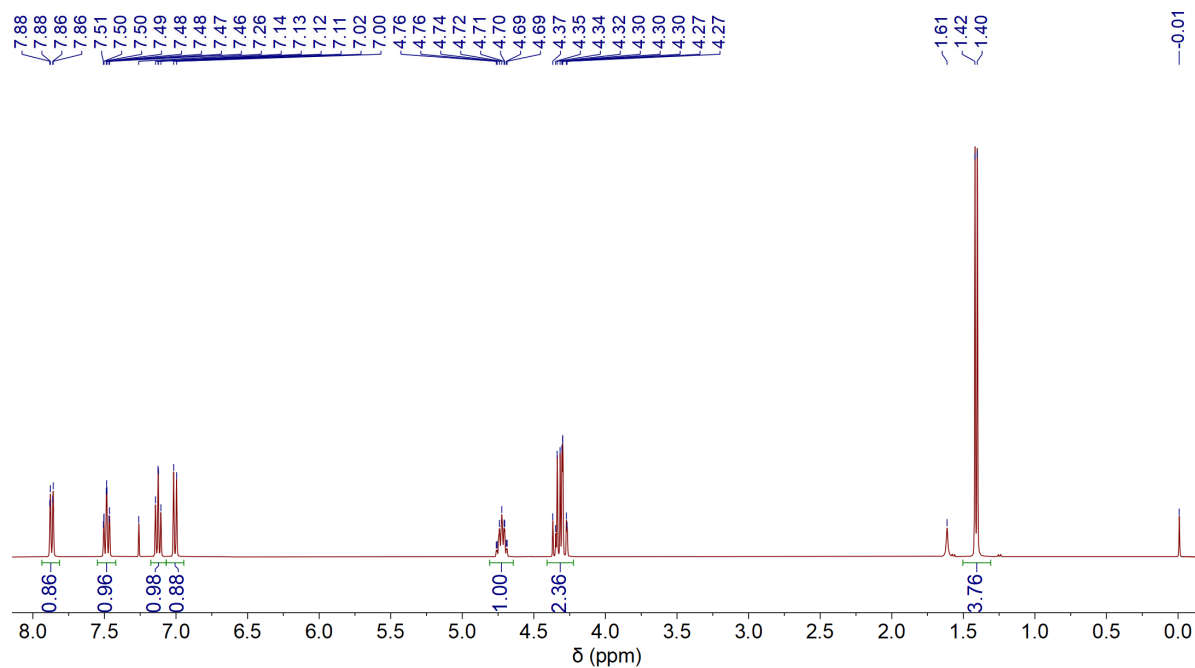


Fig. S4. ^1H NMR (CDCl_3 , 25 $^\circ\text{C}$) spectrum of (*S*)-DHB-Me. Residual solvent peaks at 7.26 ppm and 1.61 ppm for CHCl_3 and H_2O , respectively.

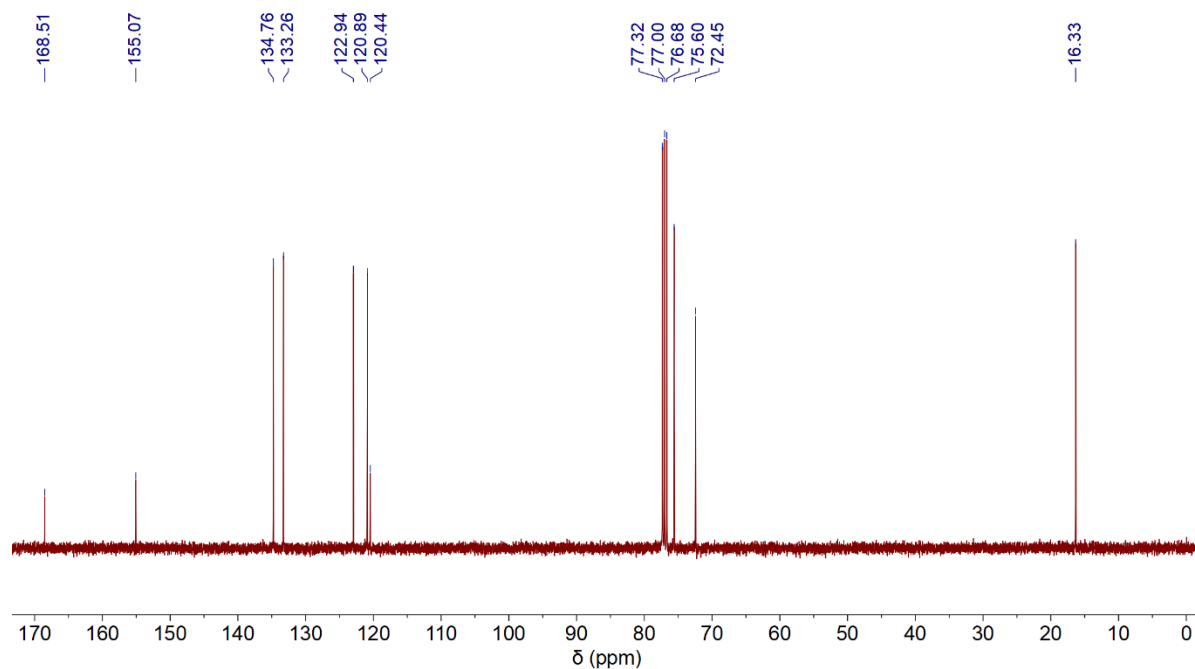


Fig. S5. ^{13}C NMR (CDCl_3 , 25 $^\circ\text{C}$) spectrum of (*S*)-DHB-Me.

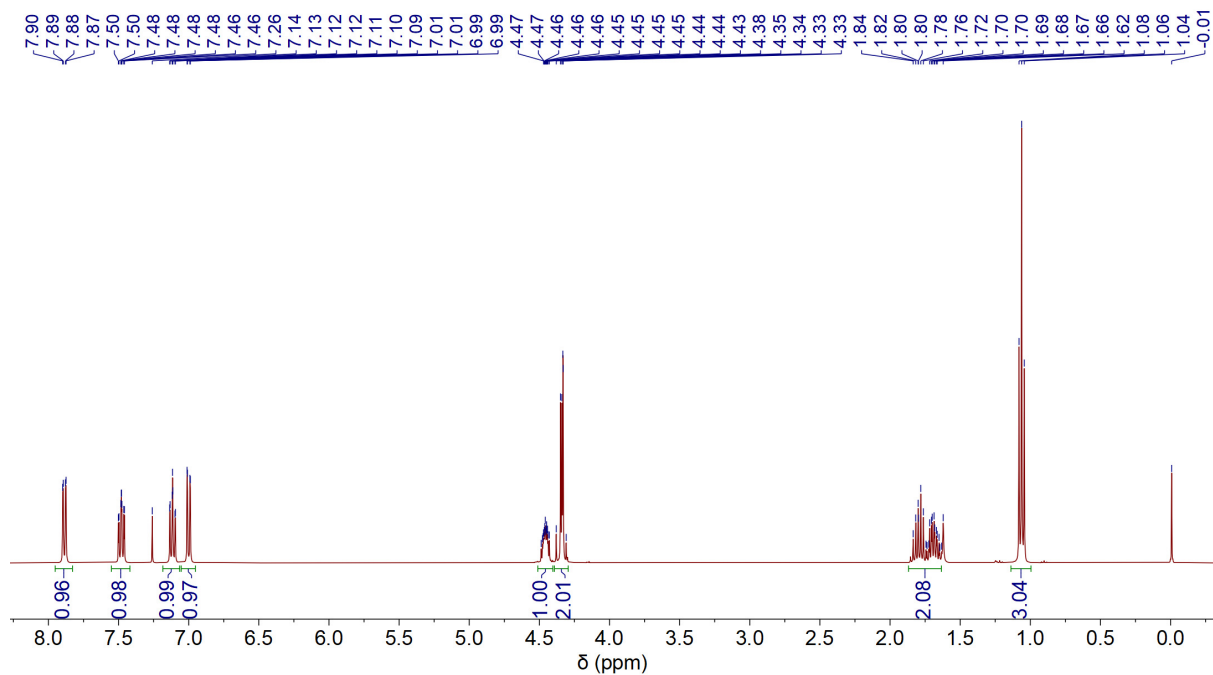


Fig. S6. ^1H NMR (CDCl_3 , 25 $^\circ\text{C}$) spectrum of DHB-Et. Residual solvent peaks at 7.26 ppm and 1.62 ppm for CHCl_3 and H_2O , respectively.

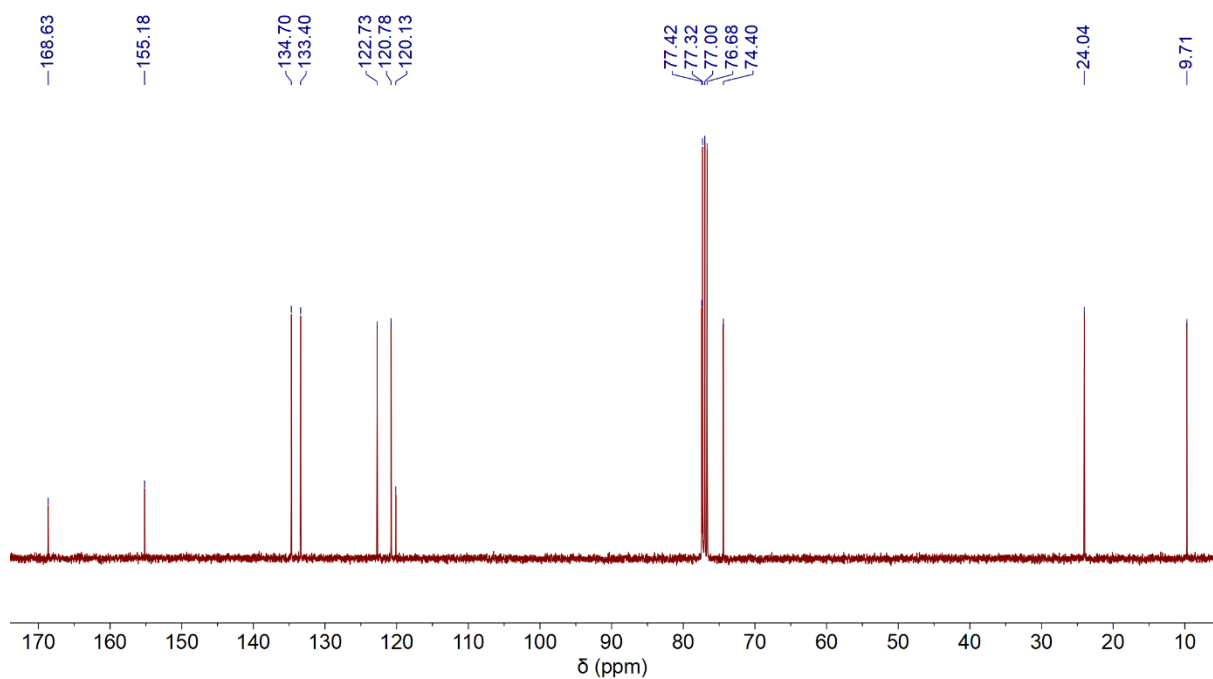


Fig. S7. ^{13}C NMR (CDCl_3 , 25 $^\circ\text{C}$) spectrum of DHB-Et.

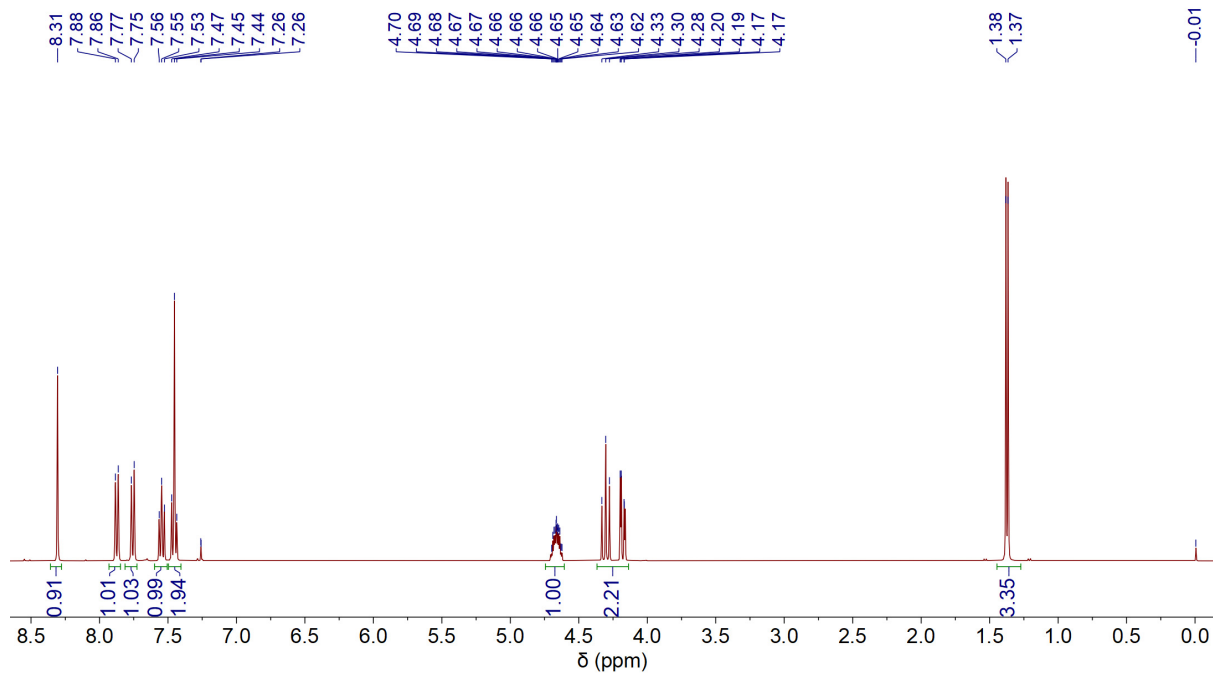


Fig. S8. ^1H NMR (CDCl_3 , 25 $^\circ\text{C}$) spectrum of DHN-Me. Residual solvent peaks at 7.26 ppm for CHCl_3 .

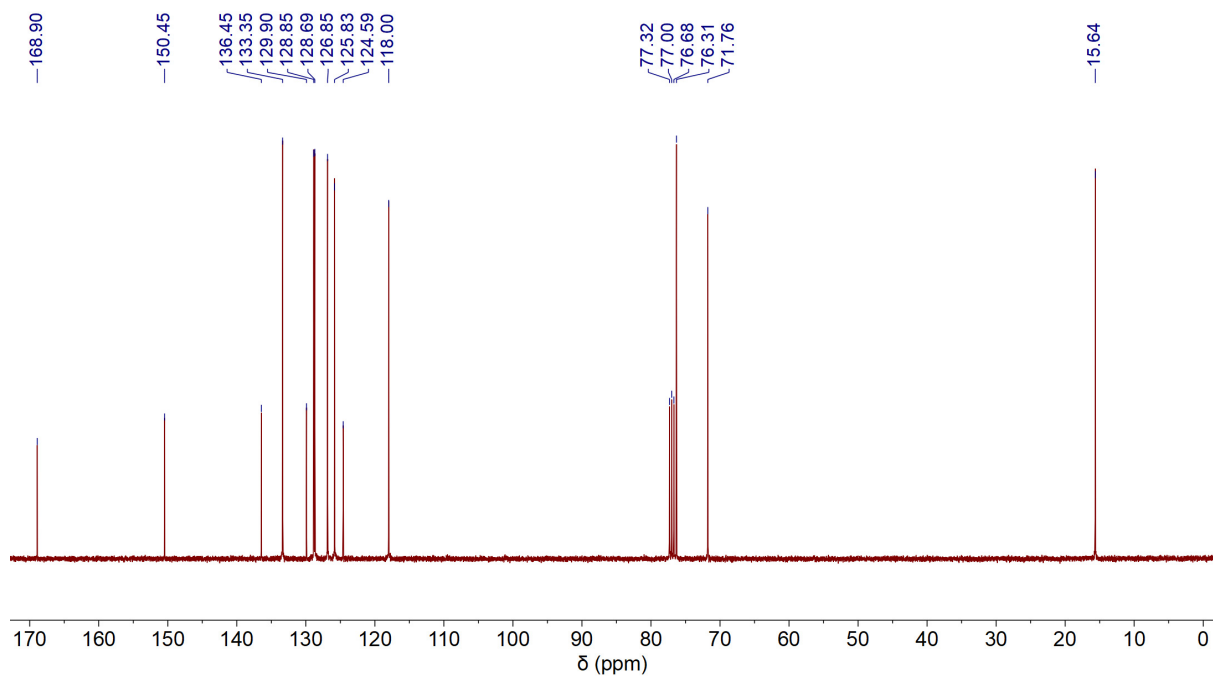


Fig. S9. ^{13}C NMR (CDCl_3 , 25 $^\circ\text{C}$) spectrum of DHN-Me.

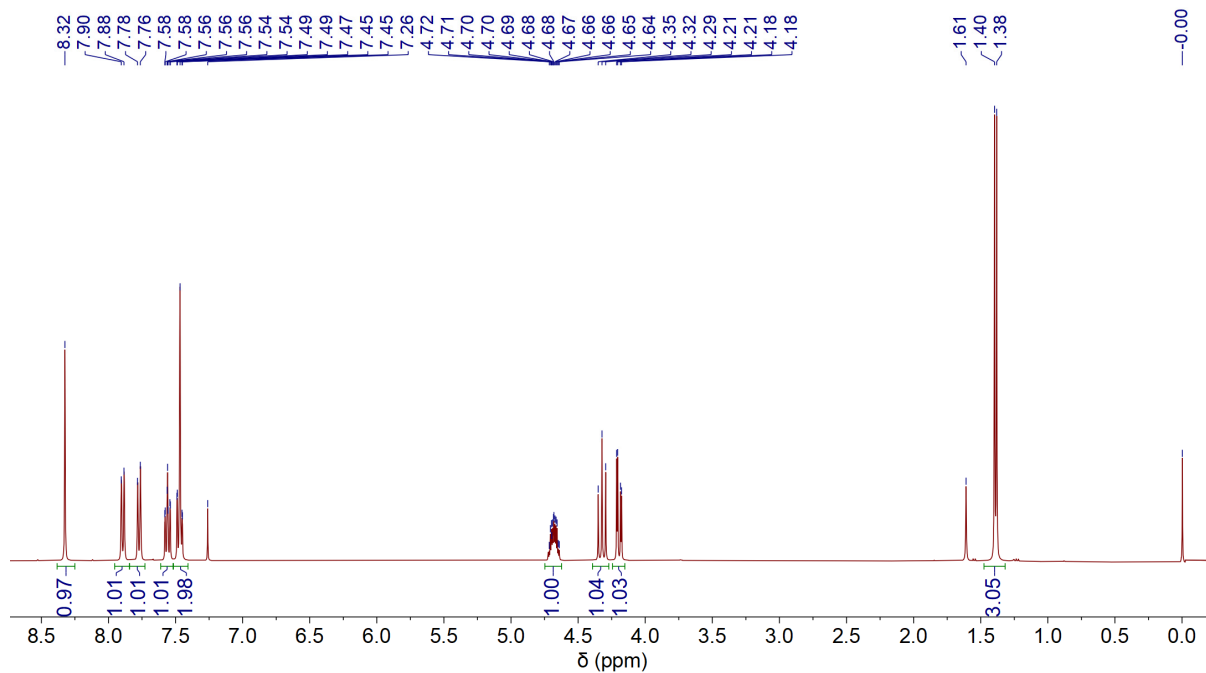


Fig. S10. ^1H NMR (CDCl_3 , 25 $^\circ\text{C}$) spectrum of (*R*)-DHN-Me. Residual solvent peaks at 7.26 ppm and 1.61 ppm for CHCl_3 and H_2O , respectively.

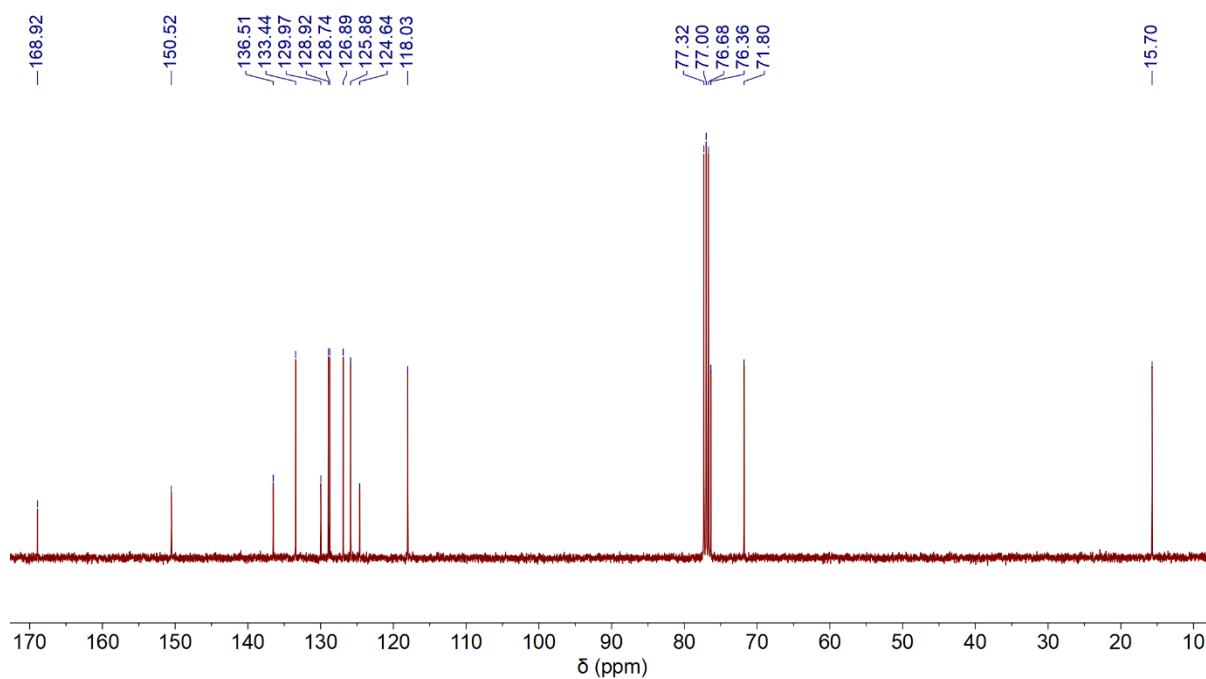


Fig. S11. ^{13}C NMR (CDCl_3 , 25 $^\circ\text{C}$) spectrum of (*R*)-DHN-Me.

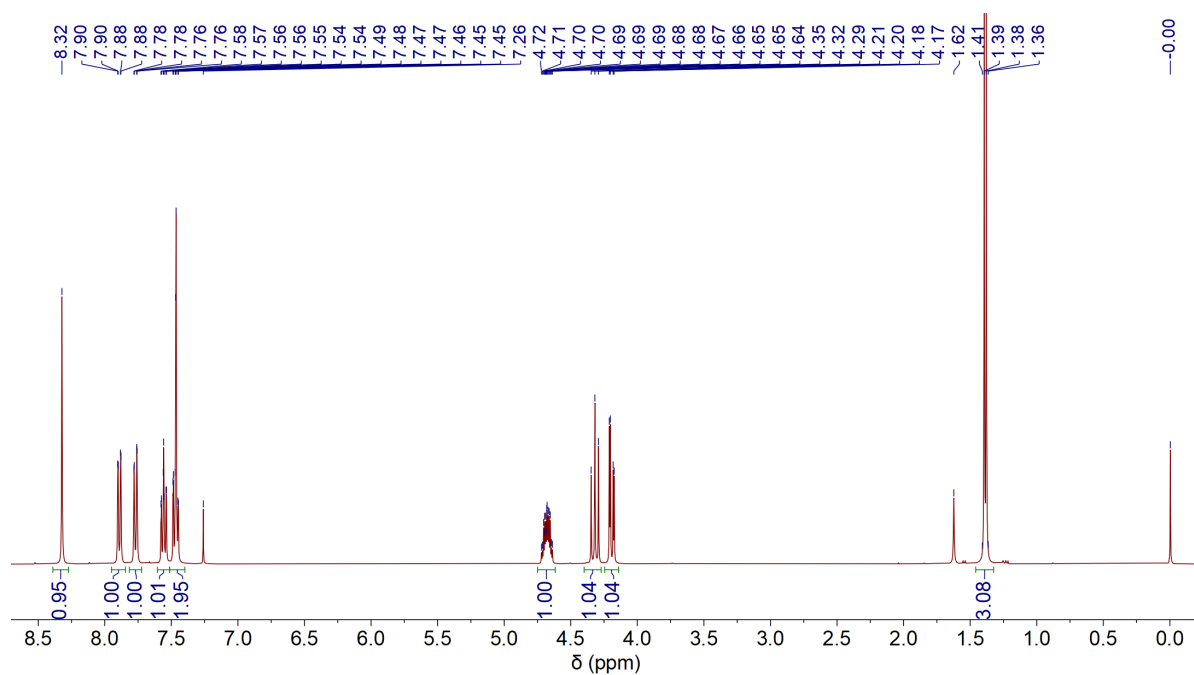


Fig. S12. ^1H NMR (CDCl_3 , 25 °C) spectrum of (*S*)-DHN-Me. Residual solvent peaks at 7.26 ppm and 1.62 ppm for CHCl_3 and H_2O , respectively.

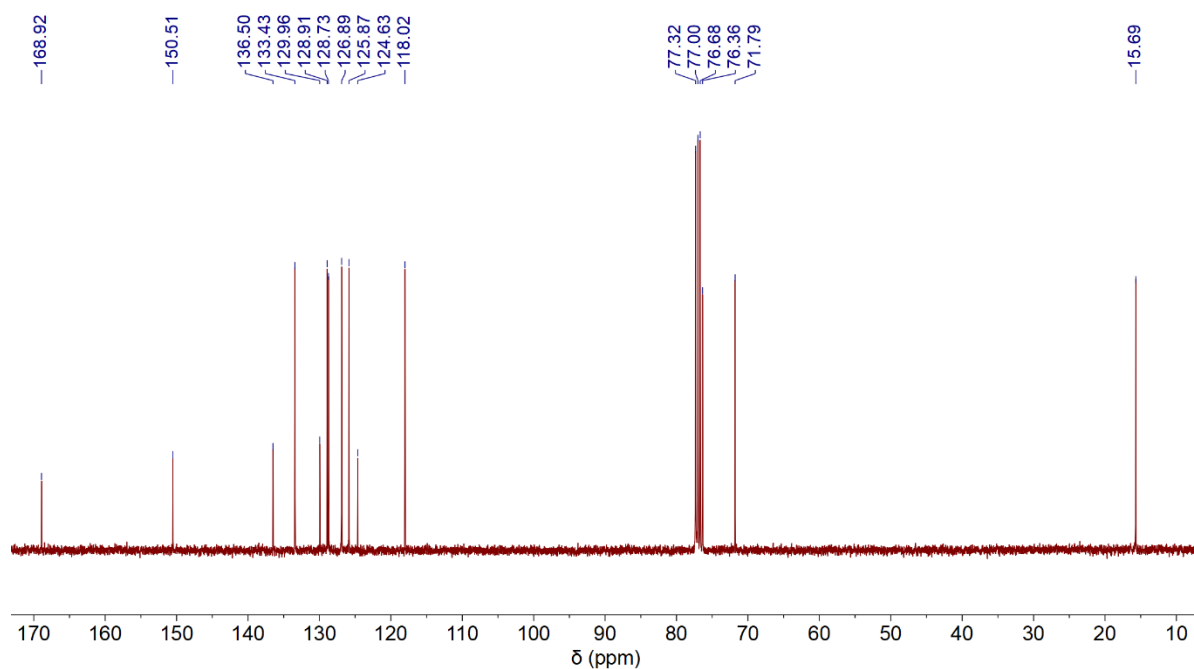


Fig. S13. ^{13}C NMR (CDCl_3 , 25 °C) spectrum of (*S*)-DHN-Me.

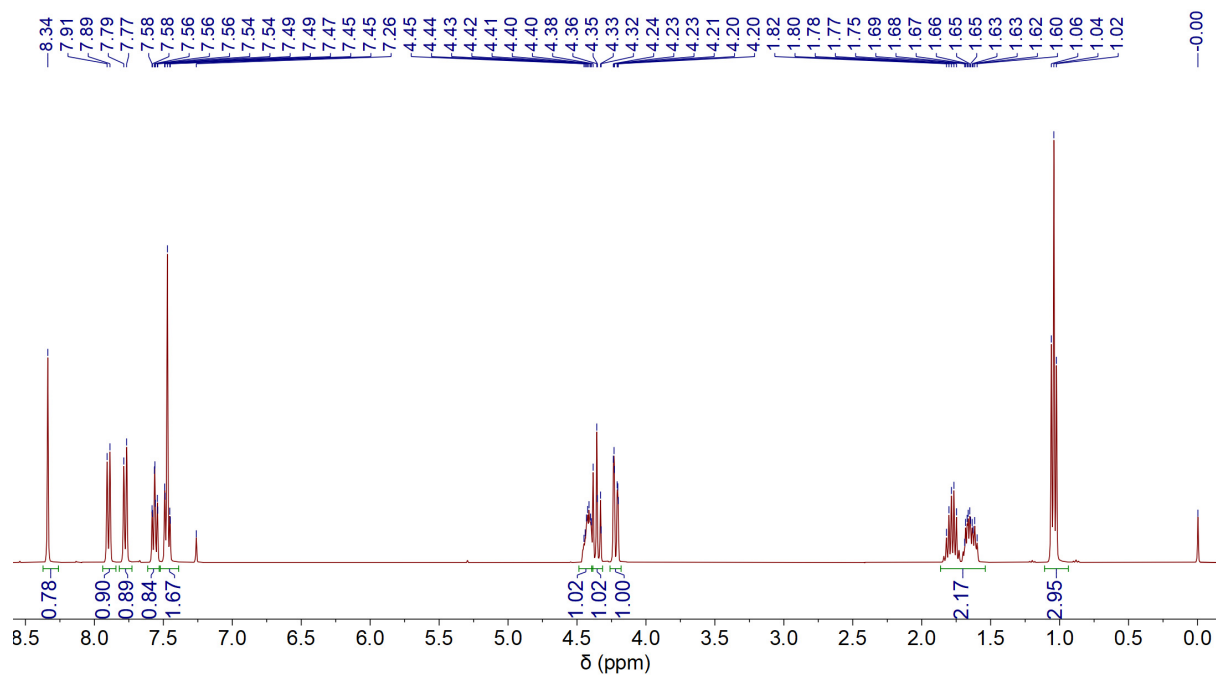


Fig. S14. ^1H NMR (CDCl_3 , 25 °C) spectrum of DHN-Et. Residual solvent peak at 7.26 ppm for CHCl_3 .

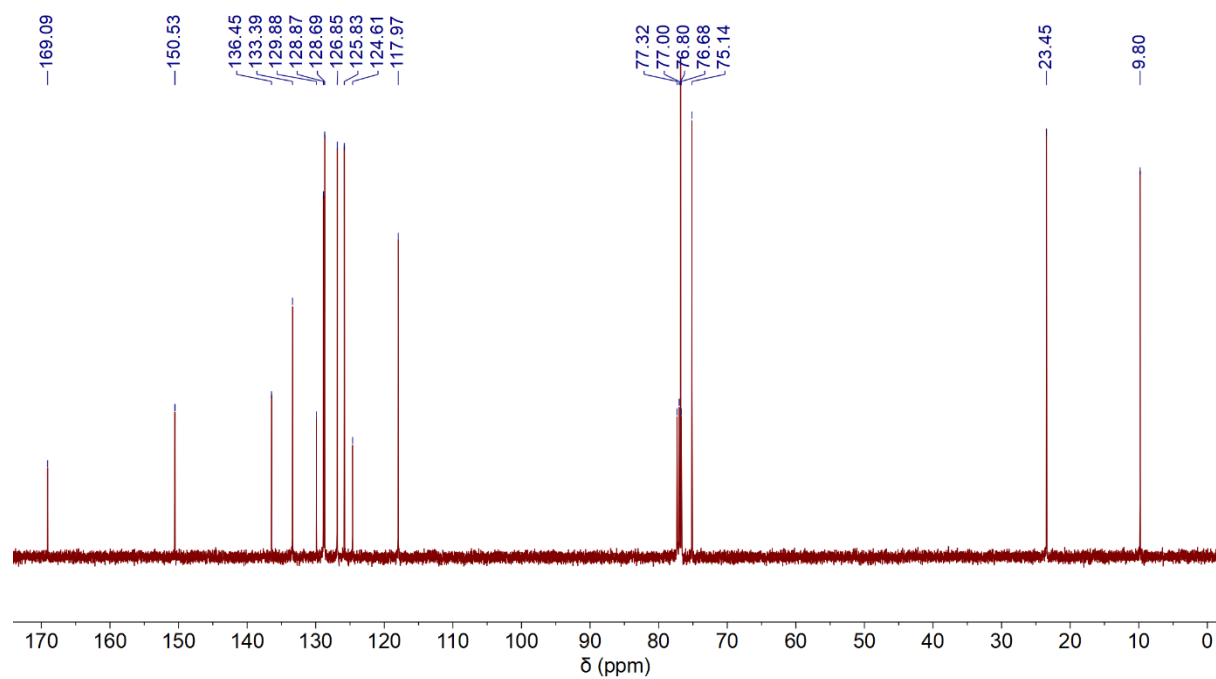


Fig. S15. ^{13}C NMR (CDCl_3 , 25 °C) spectrum of DHN-Et.

General Polymerization Procedures

Note: Prior to polymerization, DHB-Me, (*R*)-DHB-Me and DHB-Et were further purified via recrystallization from ethanol and sublimation at 100 °C twice. DHN-Me, (*R*)-DHN-Me and DHN-Et were further purified via recrystallization from ethanol twice, dried in a vacuum oven at 60 °C for 24 h and washed with extra dry *n*-hexane in glovebox.

Polymerizations were performed in 4 mL vials at 70 °C or 100 °C inside the glovebox, or in 25 mL Schlenk flasks interfaced to a dual-manifold Schlenk line with oil bath for runs. As for DHB-Me and DHB-Et, the catalyst was added to the vigorously stirred prepared monomer and initiator (*p*-tolylmethanol) under bulk condition. As for DHN-Me and DHN-Et, the solution of catalyst in toluene was added to the vigorously stirred prepared monomer and initiator (*p*-tolylmethanol) solution (toluene). After a desired period of time, the polymerization was quenched by addition of 0.5 mL CHCl₃ containing benzoic acid (1 wt %). The quenched mixture was dissolved in CHCl₃ and precipitated into 100 mL of cold methanol, filtered, and washed with cold methanol; then the polymer was dissolved in CHCl₃ and precipitated into 100 mL cold *n*-hexane to ensure any catalyst residue or unreacted monomer was removed. All polymers were dried in a vacuum oven at 60 °C to a constant weight.

Table S1. Results for the copolymerization of DHB-Me and DHB-Et.^a

| Entry | [DHB-Me]/[DHB-Et]/[ZnI]/[I] | Conv. ^b (%) | | DHB-Me content ^b (%) | M_n^c (kDa) | D^c | T_g^d (°C) | T_d^e (°C) |
|-------|-----------------------------|------------------------|--------|---------------------------------|---------------|-------|--------------|--------------|
| | | DHB-Me | DHB-Et | | | | | |
| 1 | 50:1000:1:1 | 76 | 58 | 7 | 57.5 | 1.13 | 50 | 342 |

^aReaction conditions: Initiator (I) = *p*-tolylmethanol, bulk condition, 70 °C, reaction time = 6 h. ^bMonomer conversion measured by ¹H NMR of the quenched solution, DHB-Me content measured by ¹H NMR of resulting polymers. ^cNumber-average molecular weight (M_n) and dispersity index ($D = M_w/M_n$) determined by SEC at 40 °C in THF. ^d T_g measured by differential scanning calorimetry (DSC) from the second heating-scan curves with the cooling and second heating rate of 10 °C min⁻¹. ^e T_d measured by thermal gravimetric analysis (TGA) at a heating rate of 10 °C min⁻¹.

Polymer Characterizations

P(DHB-Me):

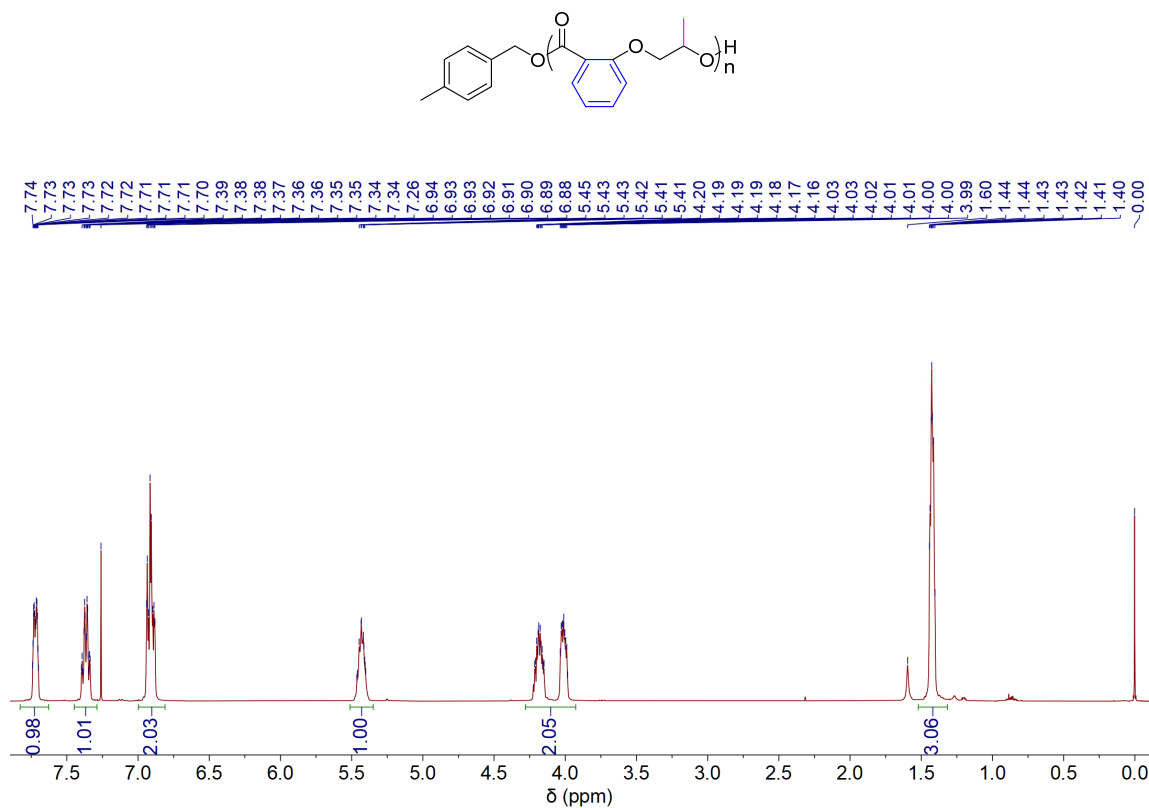


Fig. S16. ¹H NMR (CDCl₃, 25 °C) spectrum of P(DHB-Me) obtained by [DHB-Me]/[TBD]/[I] = 100/1/1.

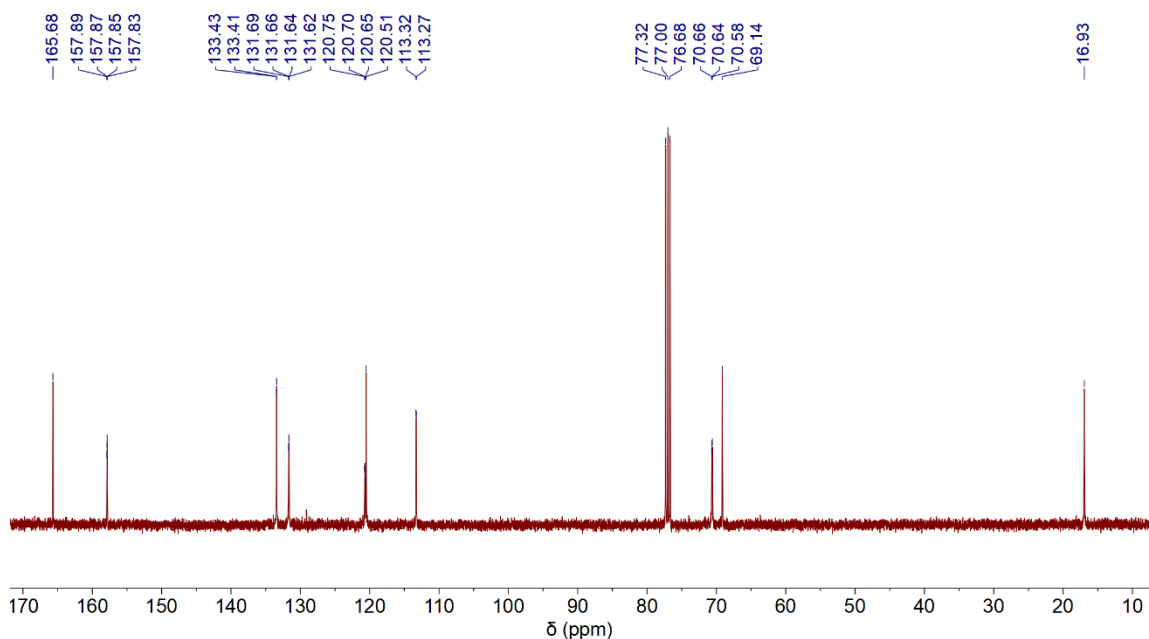


Fig. S17. ¹³C NMR (CDCl₃, 25 °C) spectrum of P(DHB-Me) obtained by [DHB-Me]/[TBD]/[I] = 100/1/1.

P[(*R*)-DHB-Me]:

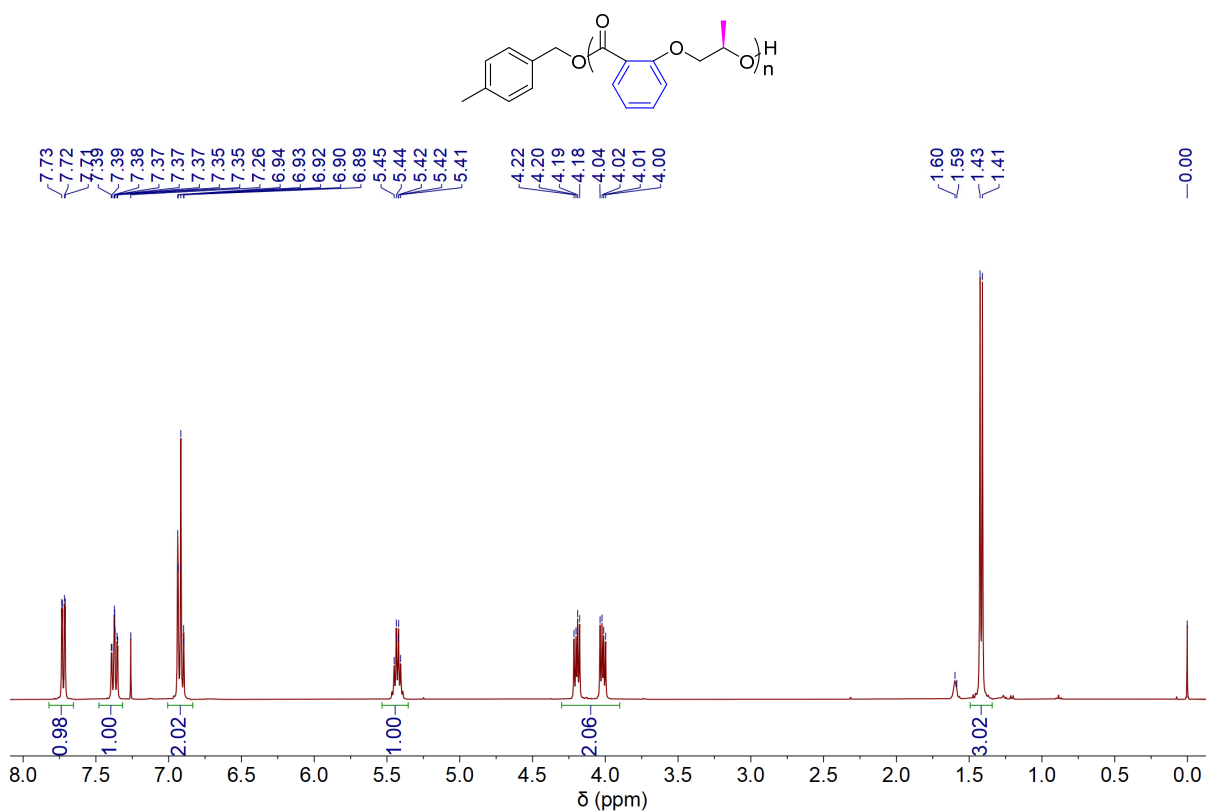


Fig. S18. ¹H NMR (CDCl₃, 25 °C) spectrum of P[(*R*)-DHB-Me] obtained by [(*R*)-DHB-Me]/[Zn1]/[I] = 500/1/1.

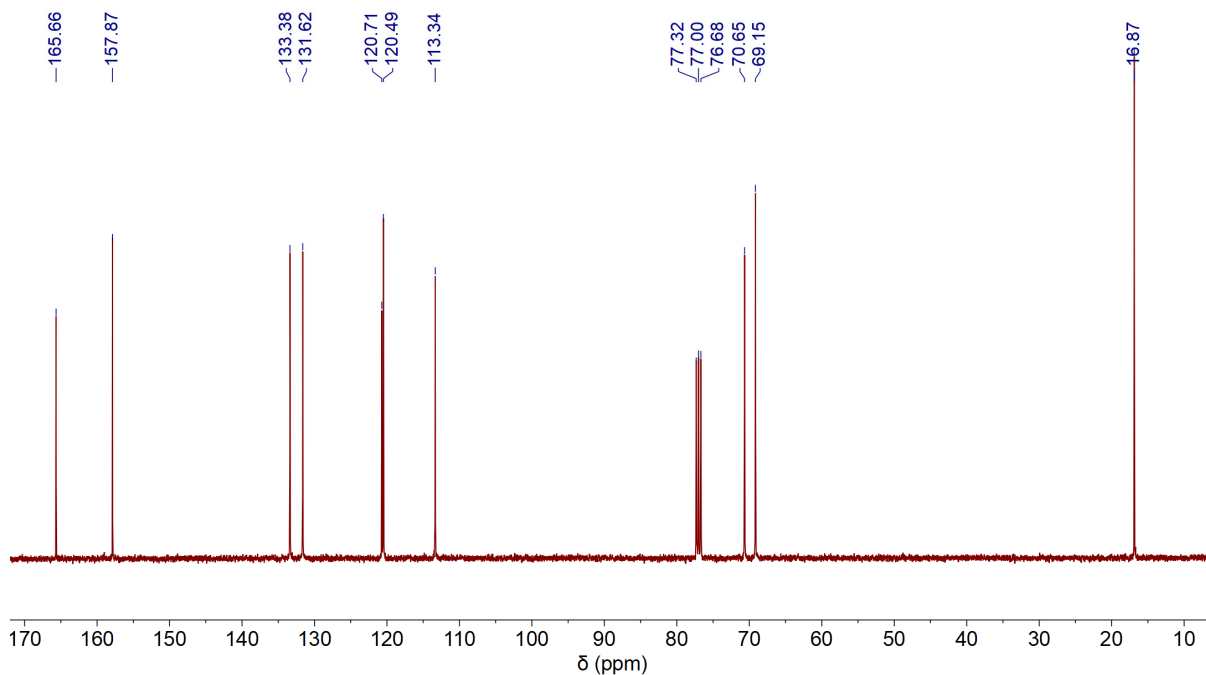


Fig. S19. ¹³C NMR (CDCl₃, 25 °C) spectrum of P[(*R*)-DHB-Me] obtained by [(*R*)-DHB-Me]/[Zn1]/[I] = 500/1/1.

P[(S)-DHB-Me]:

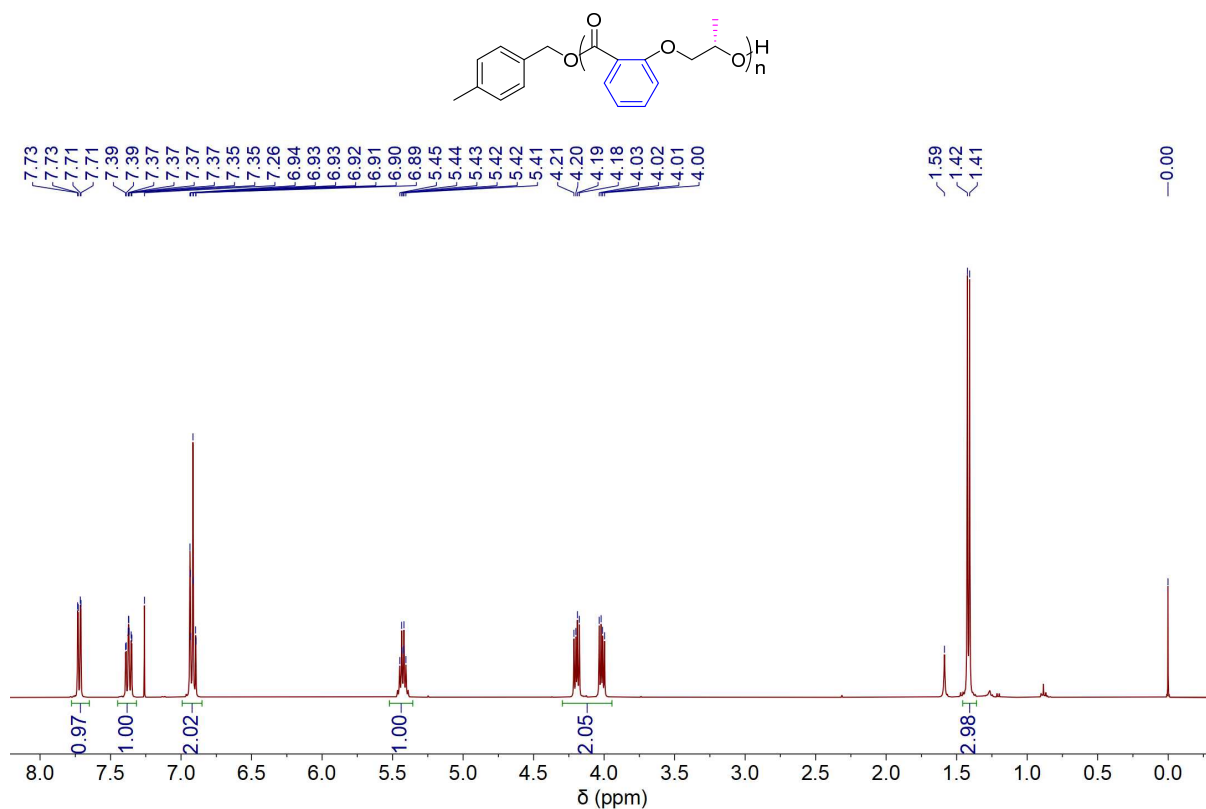


Fig. S20. ¹H NMR (CDCl₃, 25 °C) spectrum of P[(S)-DHB-Me] obtained by [(S)-DHB-Me]/[TBD]/[I] = 500/1/1.

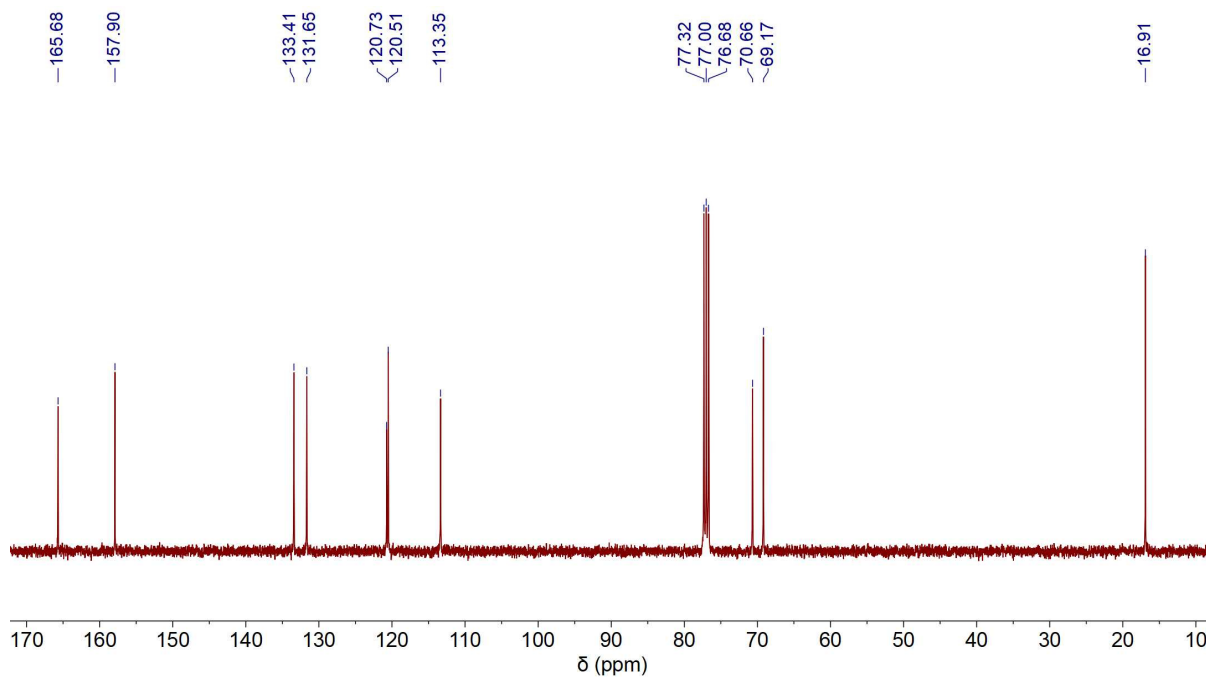


Fig. S21. ¹³C NMR (CDCl₃, 25 °C) spectrum of P[(S)-DHB-Me] obtained by [(S)-DHB-Me]/[TBD]/[I] = 500/1/1.

P(DHB-Et):

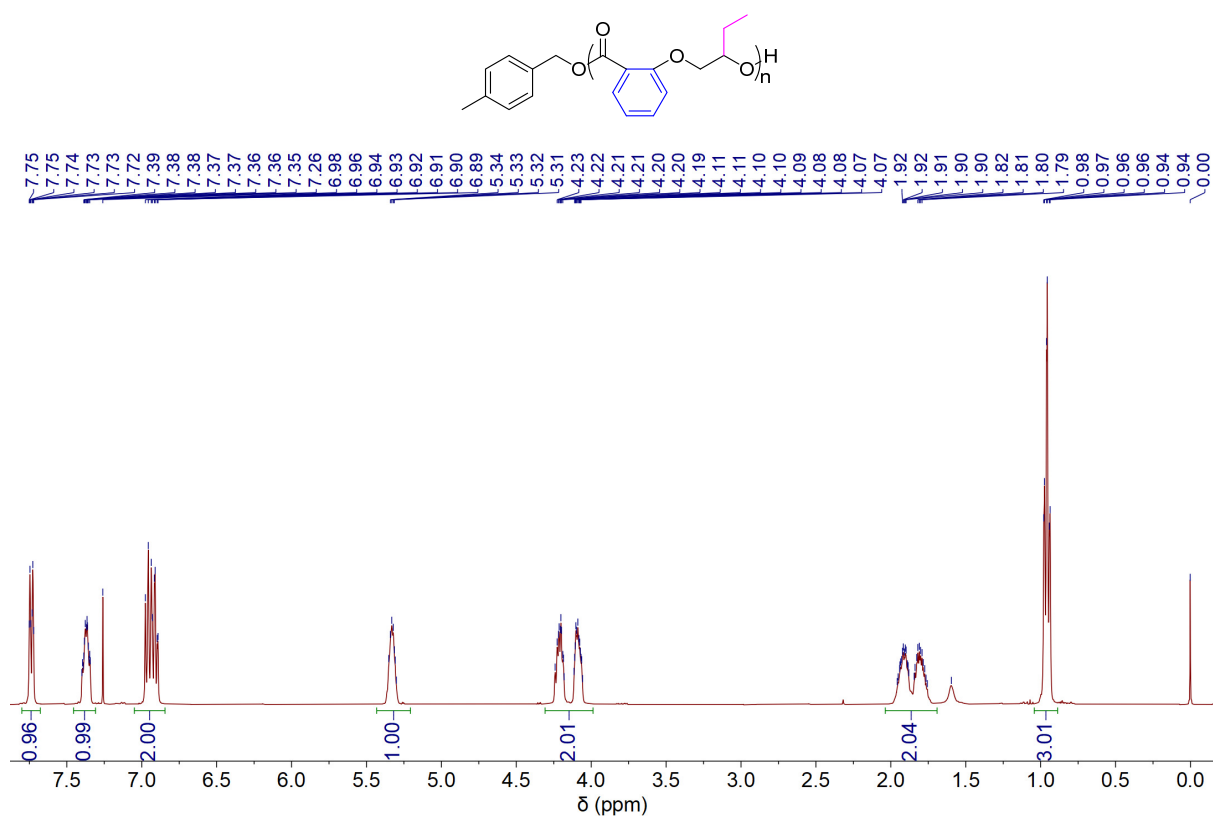


Fig. S22. ¹H NMR (CDCl₃, 25 °C) spectrum of P(DHB-Et) obtained by [DHB-Et]/[TBD]/[I] = 500/1/1.

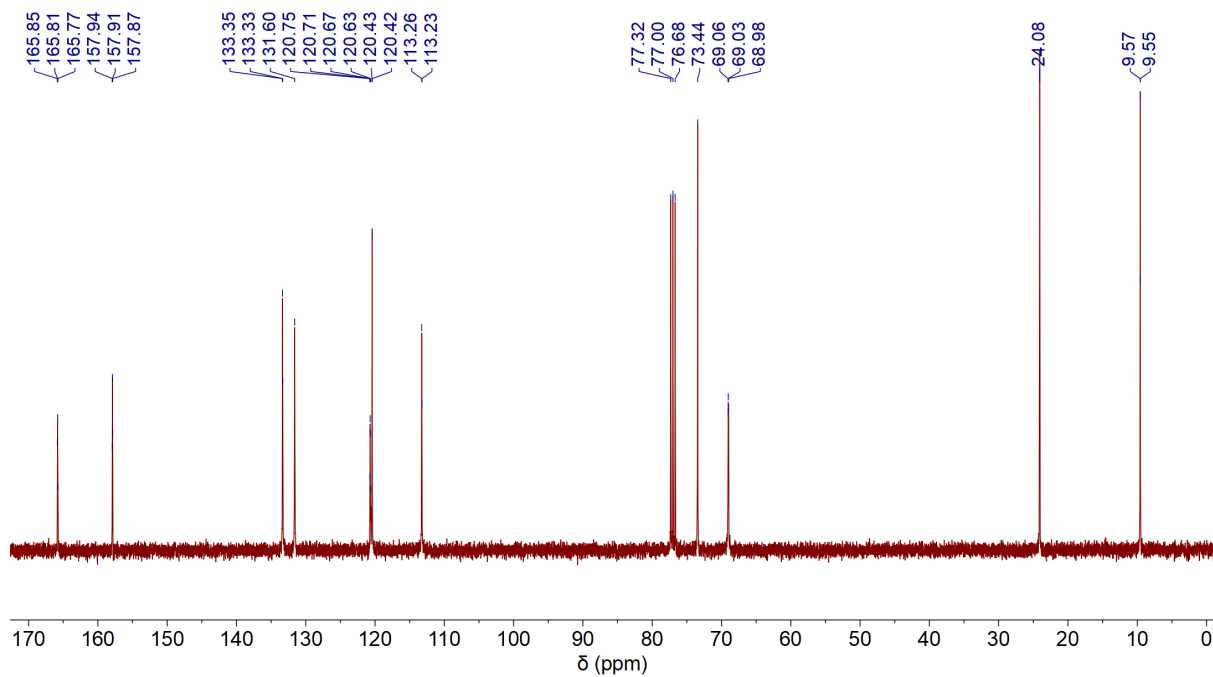


Fig. S23. ¹³C NMR (CDCl₃, 25 °C) spectrum of P(DHB-Et) obtained by [DHB-Et]/[TBD]/[I] = 500/1/1.

P(DHN-Me):

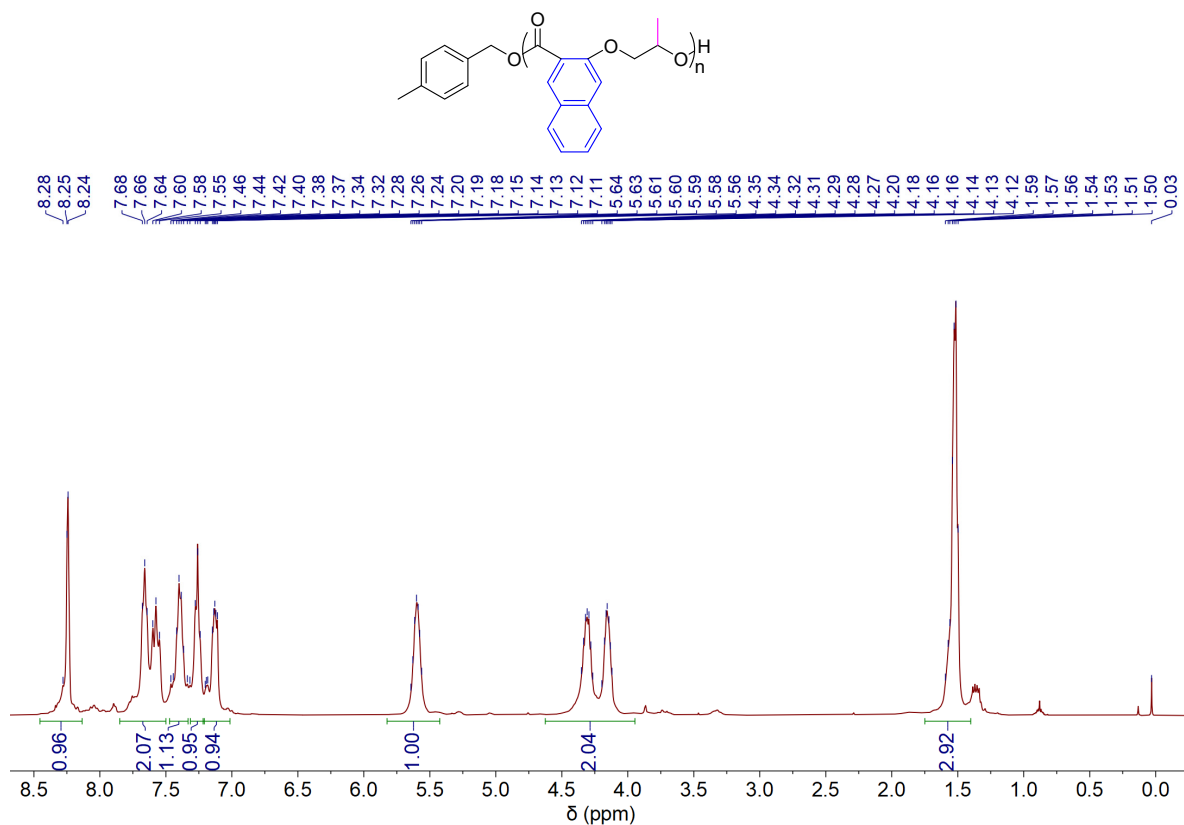


Fig. S24. ^1H NMR (CDCl_3 , 25 °C) spectrum of P(DHN-Me) obtained by $[\text{DHN-Me}]/[\text{Zn1}]/[\text{I}] = 1000/1/1$.

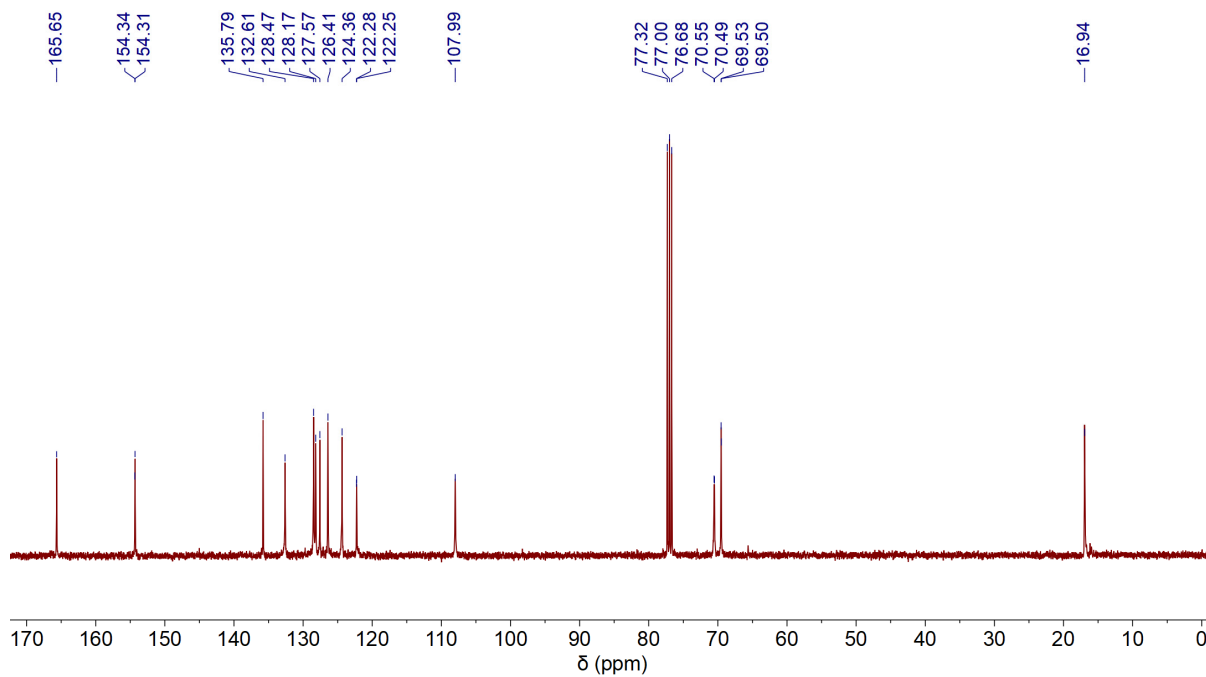


Fig. S25. ^{13}C NMR (CDCl_3 , 25 °C) spectrum of P(DHN-Me) obtained by $[\text{DHN-Me}]/[\text{Zn1}]/[\text{I}] = 1000/1/1$.

P[(*R*)-DHN-Me]:

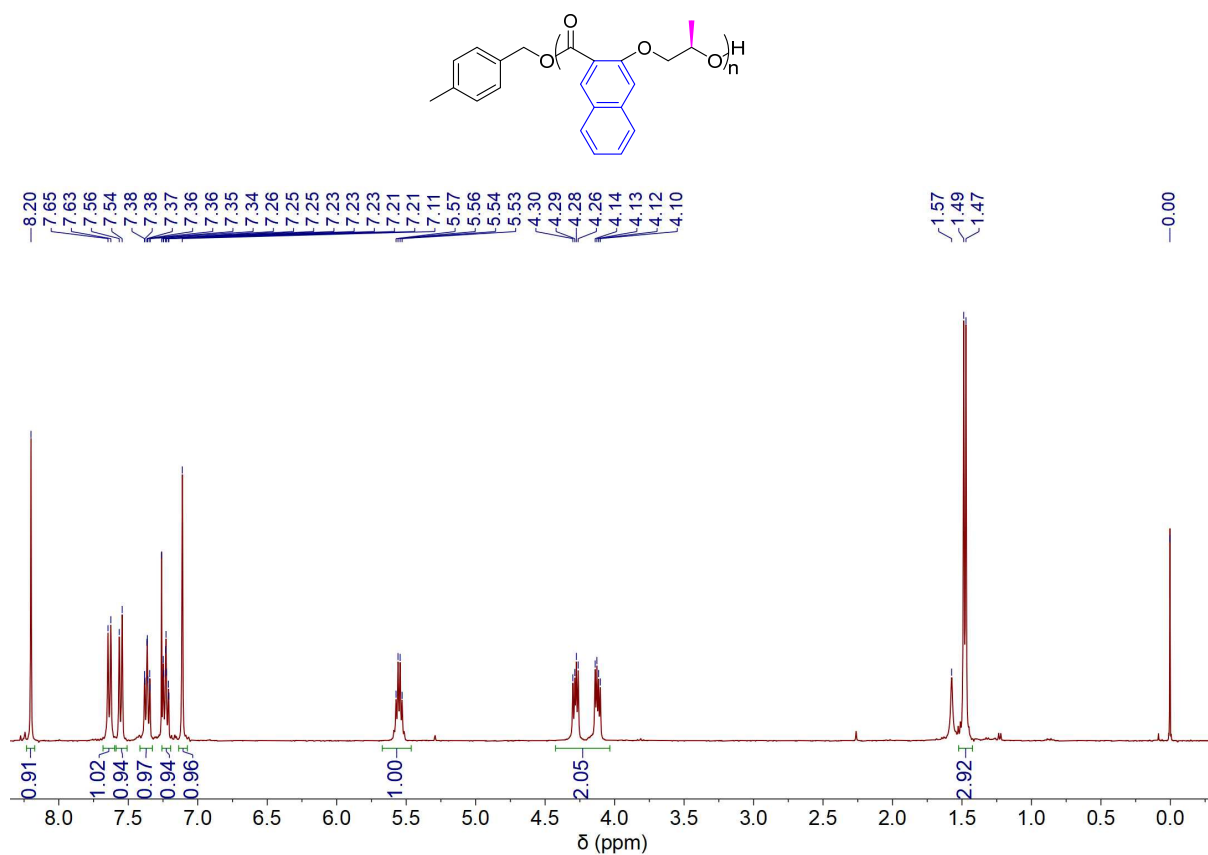


Fig. S26. ¹H NMR (CDCl₃, 25 °C) spectrum of P[(*R*)-DHN-Me] obtained by [(*R*)-DHN-Me]/[Zn1]/[I] = 100/1/1.

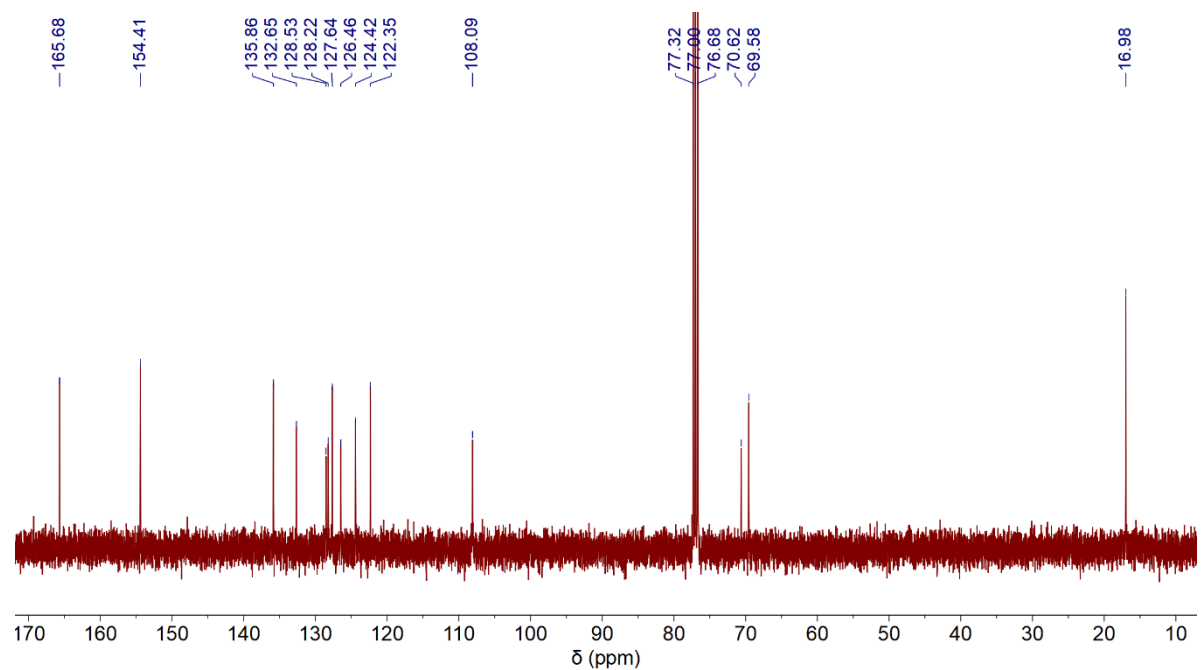


Fig. S27. ¹³C NMR (CDCl₃, 25 °C) spectrum of P[(*R*)-DHN-Me] obtained by [(*R*)-DHN-Me]/[Zn1]/[I] = 100/1/1.

P[(S)-DHN-Me]:

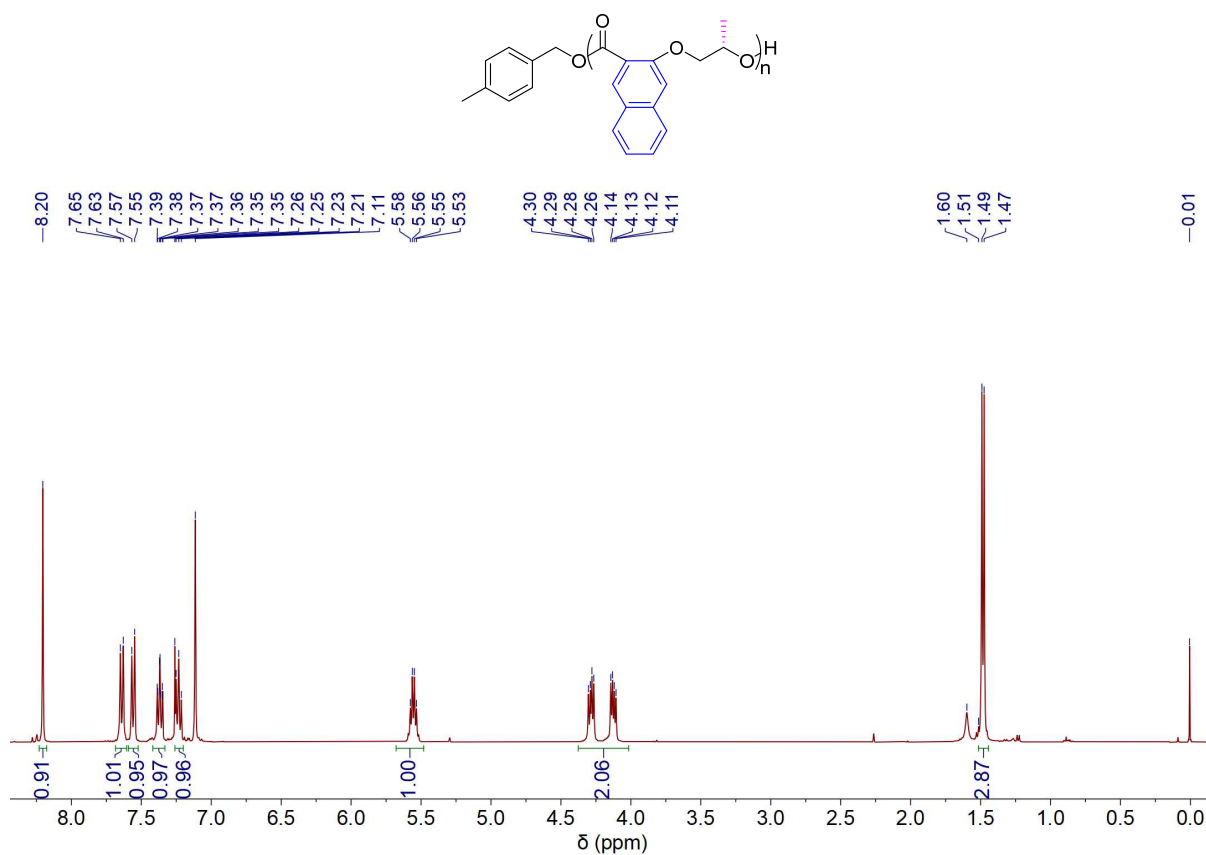


Fig. S28. ¹H NMR (CDCl₃, 25 °C) spectrum of P[(S)-DHN-Me] obtained by [(S)-DHN-Me]/[Zn1]/[I] = 100/1/1.

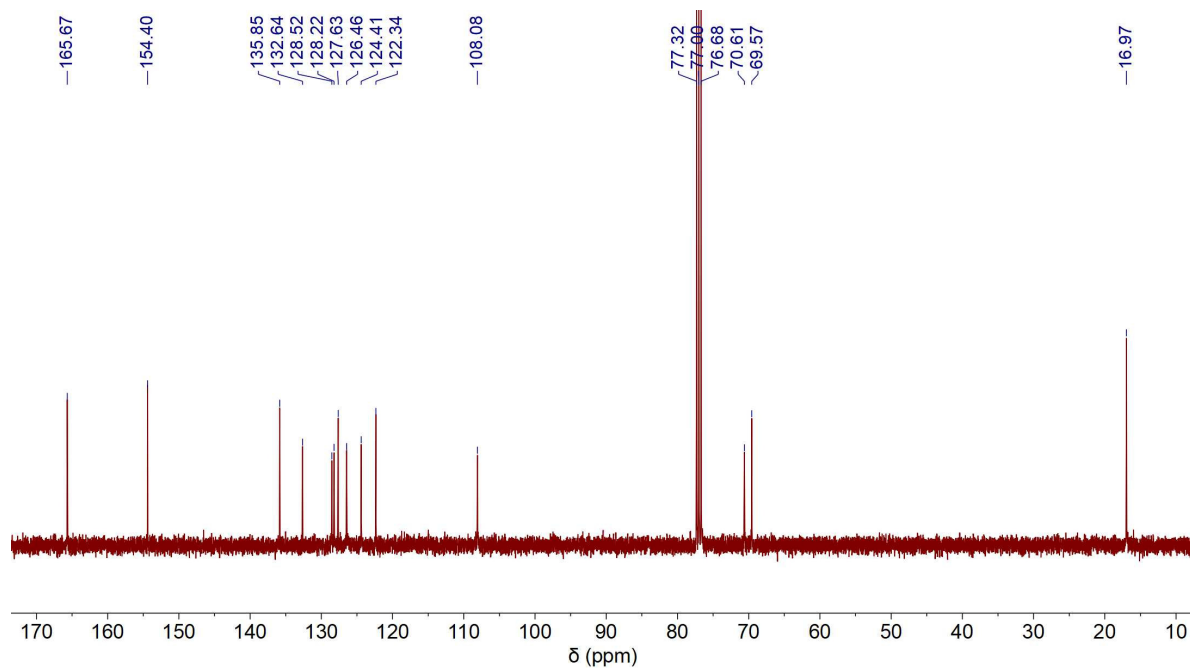


Fig. S29. ¹³C NMR (CDCl₃, 25 °C) spectrum of P[(S)-DHN-Me] obtained by [(S)-DHN-Me]/[Zn1]/[I] = 100/1/1.

P(DHN-Et):

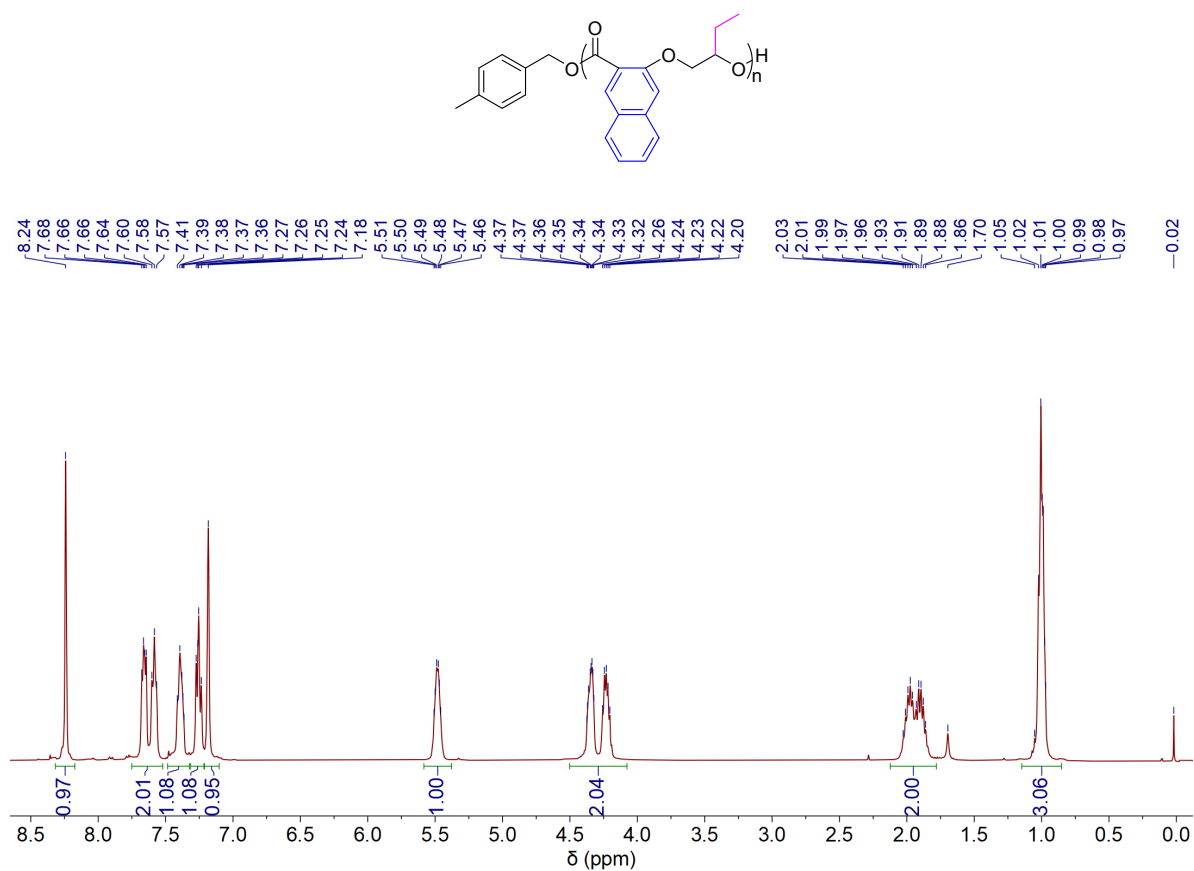


Fig. S30. ^1H NMR (CDCl_3 , 25 $^\circ\text{C}$) spectrum of P(DHN-Et) obtained by $[\text{DHN-Et}]/[\text{Zn1}]/[\text{I}] = 500/1/1$.

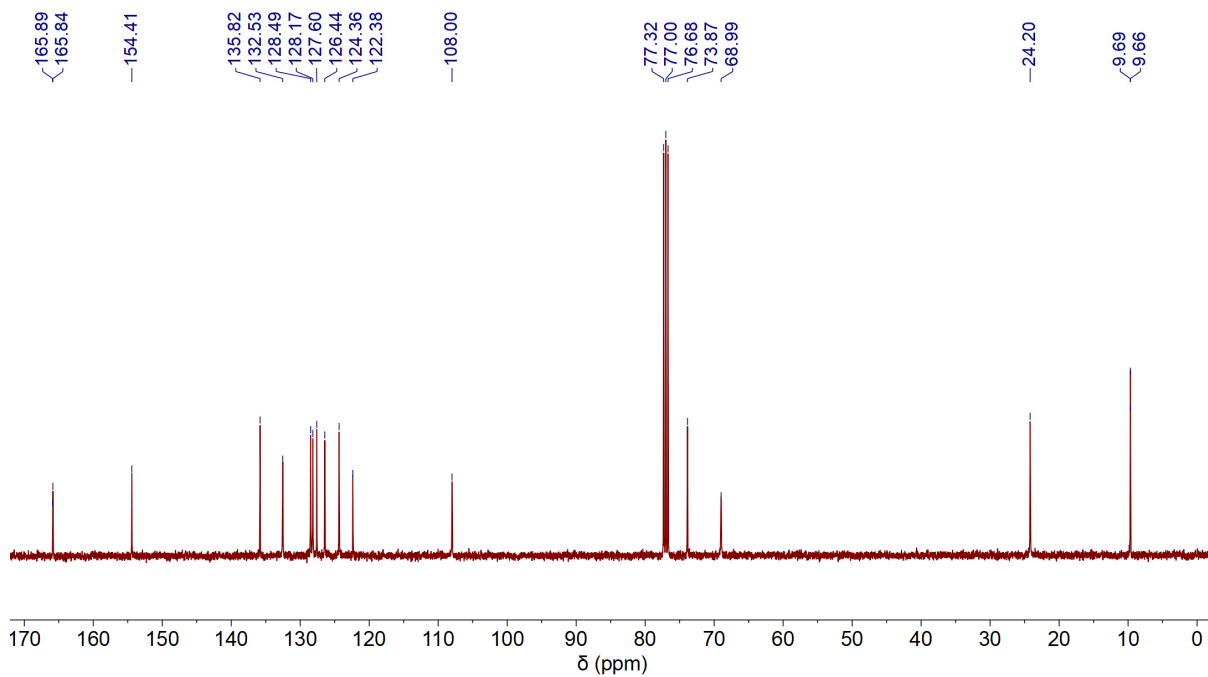


Fig. S31. ^{13}C NMR (CDCl_3 , 25 $^\circ\text{C}$) spectrum of P(DHN-Et) obtained by $[\text{DHN-Et}]/[\text{Zn1}]/[\text{I}] = 500/1/1$.

P(DHB-Me-co-DHB-Et):

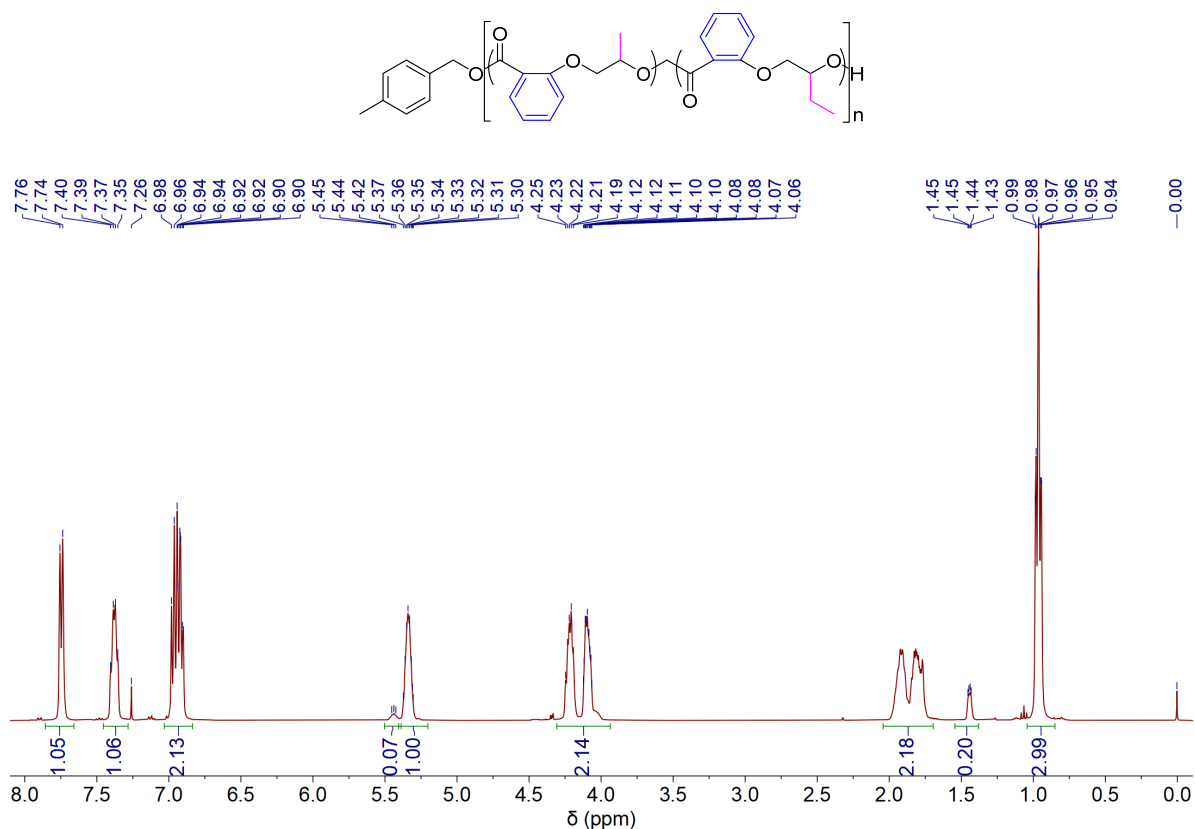


Fig. S32. ^1H NMR (CDCl_3 , 25 °C) spectrum of P(DHB-Me-co-DHB-Et) obtained by $[\text{DHB-Me}]/[\text{DHB-Et}]/[\text{Zn1}]/[\text{I}] = 50/1000/1/1$.

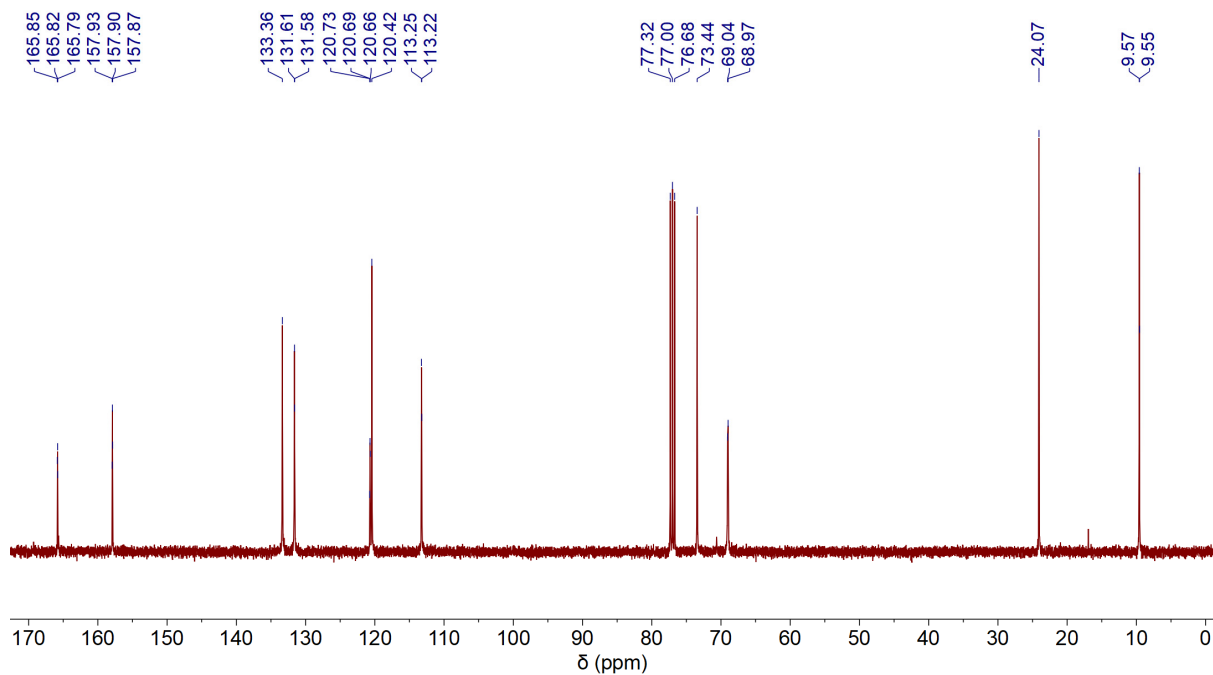


Fig. S33. ^{13}C NMR (CDCl_3 , 25 °C) spectrum of P(DHB-Me-co-DHB-Et) obtained by $[\text{DHB-Me}]/[\text{DHB-Et}]/[\text{Zn1}]/[\text{I}] = 50/1000/1/1$.

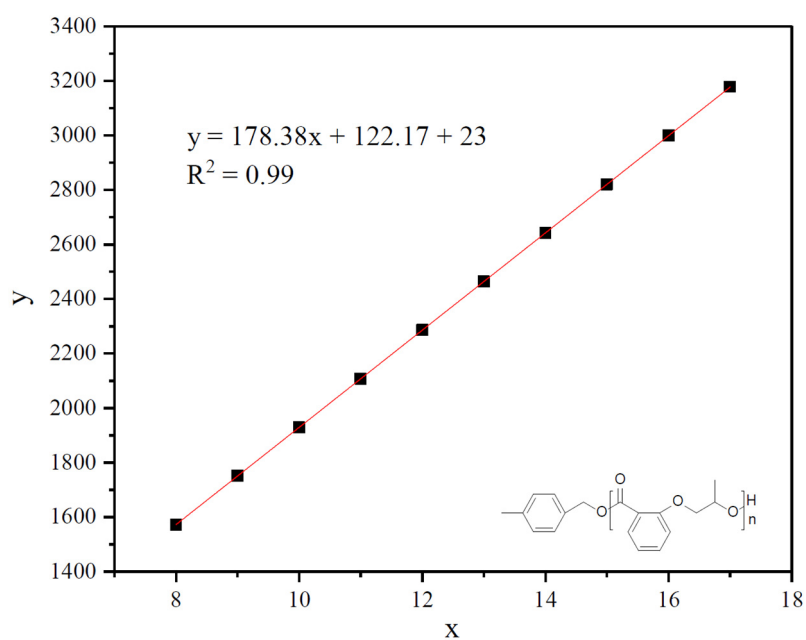
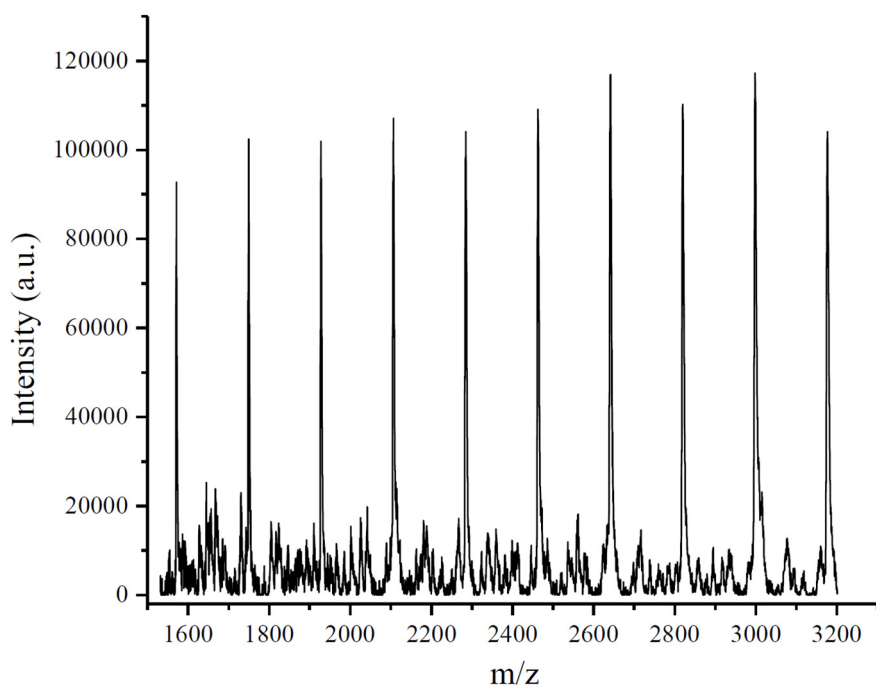


Figure S34. a) MALDI-TOF MS spectrum of the low-molecular-weight P(DHB-Me) produced by [DHB-Me]/[Zn1]/[I] = 50/1/1. b) linear plot of m/z values (y) vs the number of DHB-Me repeat units (x).

The spacing between the two neighboring molecular ion peaks corresponding to the exact molar mass of the repeat unit, DHB-Me [mass/charge ratio (m/z) = 178.06], as shown by the slope of the linear plot of m/z values (y axis) versus the number of DHB-Me repeat units (x axis). The intercept of the plot, $122.17 + 23$, represents the total mass of chain ends plus the mass of Na^+ [$M_{\text{end}} = 122.17$ ($\text{CH}_3\text{C}_6\text{H}_4\text{CH}_2\text{OH}$) g/mol + 23 (Na^+) g/mol], corresponding to linear structure $\text{CH}_3\text{C}_6\text{H}_4\text{CH}_2\text{O}-[\text{DHB-Me}]_n-\text{H}$.

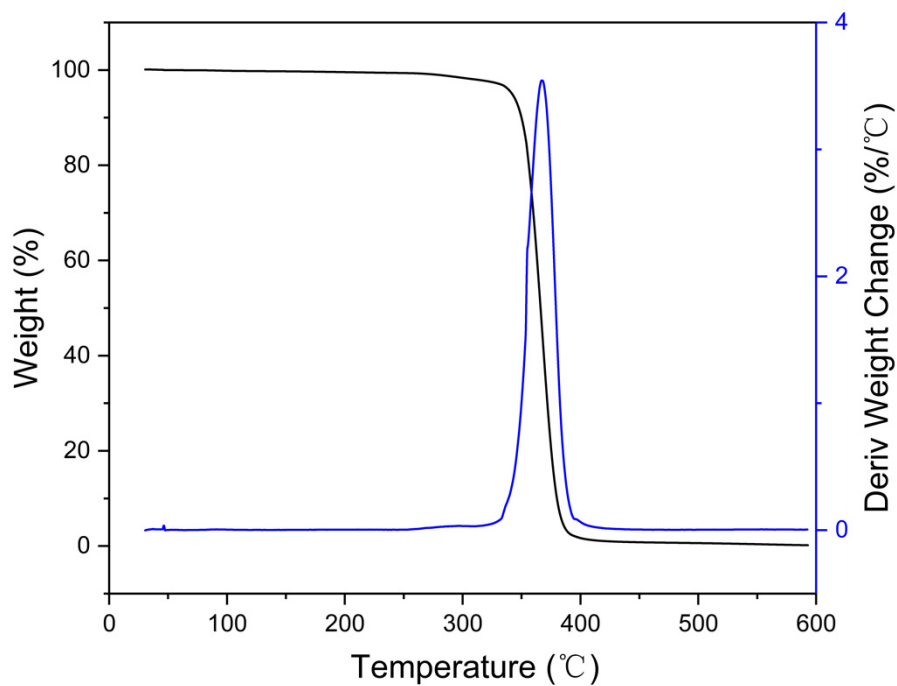


Fig. S35. TGA and DTG curves for P(DHB-Me) obtained by $[\text{DHB-Me}]/[\text{Zn1}]/[\text{I}] = 500/1/1$, $T_d = 342\text{ }^\circ\text{C}$, $T_{\text{max}} = 367\text{ }^\circ\text{C}$.

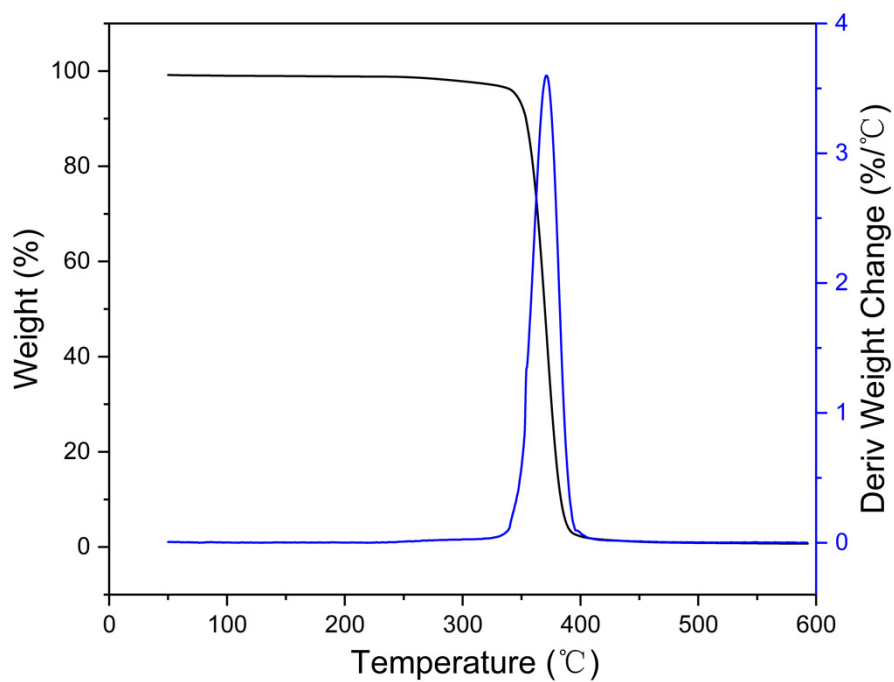


Fig. S36. TGA and DTG curves for P[(R)-DHB-Me] obtained by $[(R)\text{-DHB-Me}]/[\text{Zn1}]/[\text{I}] = 500/1/1$, $T_d = 345\text{ }^\circ\text{C}$, $T_{\text{max}} = 371\text{ }^\circ\text{C}$.

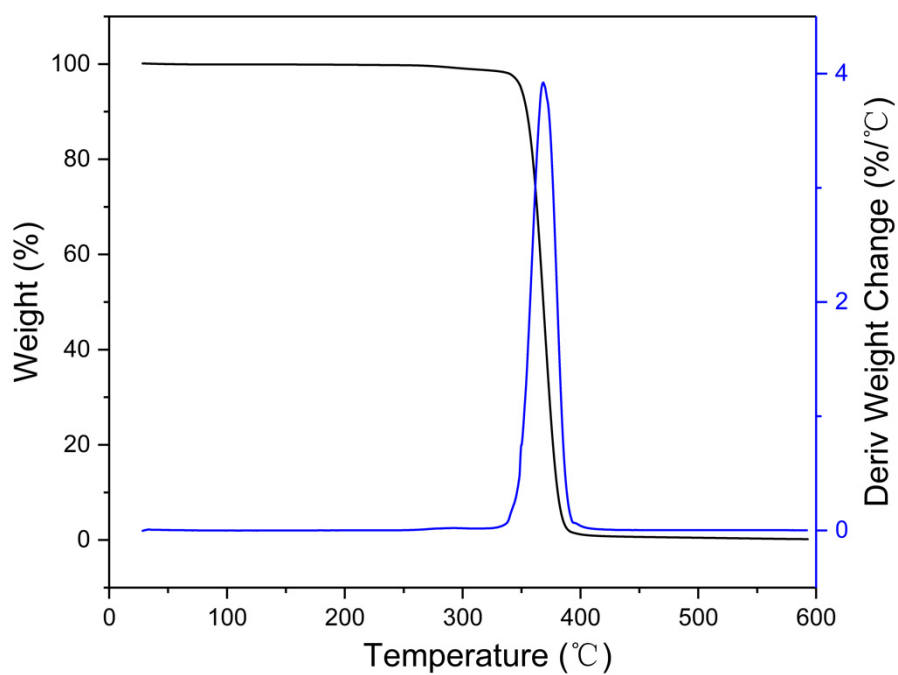


Fig. S37. TGA and DTG curves for P(DHB-Et) obtained by [DHB-Et]/[Zn1]/[I] = 500/1/1, $T_d = 349\text{ }^\circ\text{C}$, $T_{\max} = 368\text{ }^\circ\text{C}$.

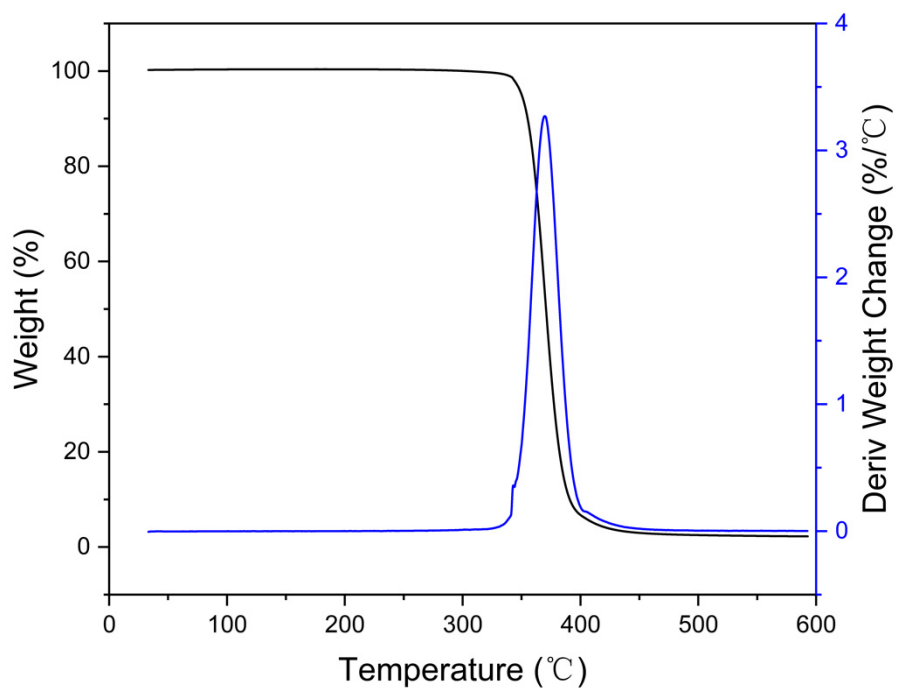


Fig. S38. TGA and DTG curves for P(DHN-Me) obtained by [DHN-Me]/[Zn1]/[I] = 500/1/1, $T_d = 336\text{ }^\circ\text{C}$, $T_{\max} = 369\text{ }^\circ\text{C}$.

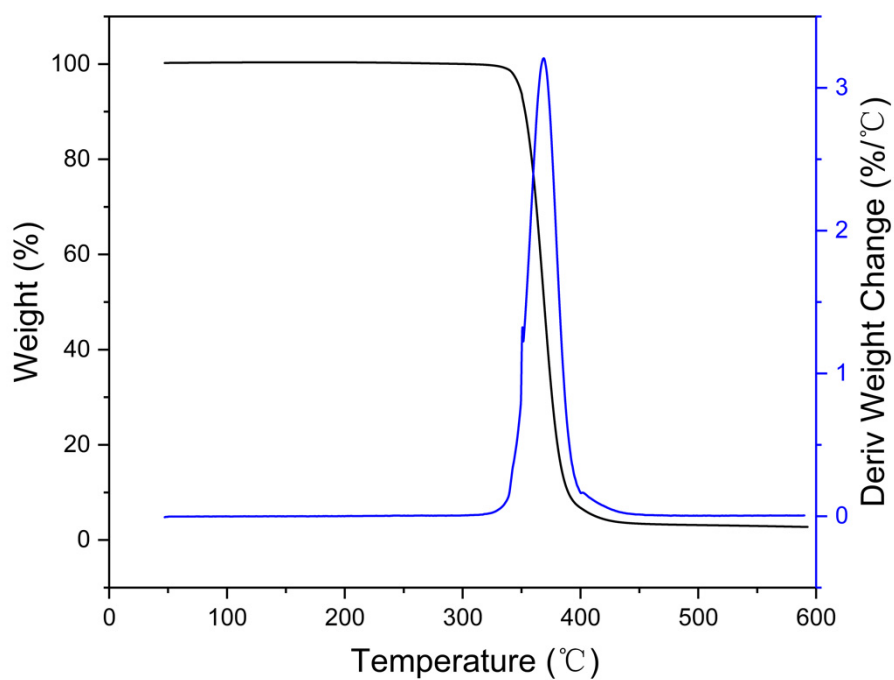


Fig. S39. TGA and DTG curves for P[(*R*)-DHN-Me] obtained by [(*R*)-DHN-Me]/[Zn1]/[I] = 500/1/1, $T_d = 349\text{ }^\circ\text{C}$, $T_{max} = 369\text{ }^\circ\text{C}$.

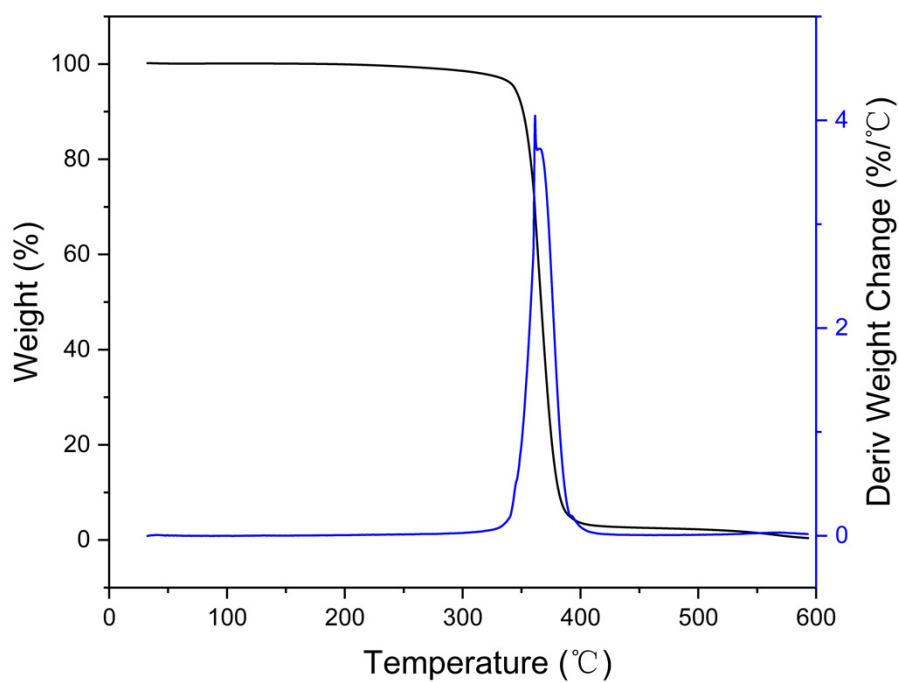


Fig. S40. TGA and DTG curves for P(DHN-Et) obtained by [DHN-Et]/[Zn1]/[I] = 500/1/1, $T_d = 344\text{ }^\circ\text{C}$, $T_{max} = 361\text{ }^\circ\text{C}$.

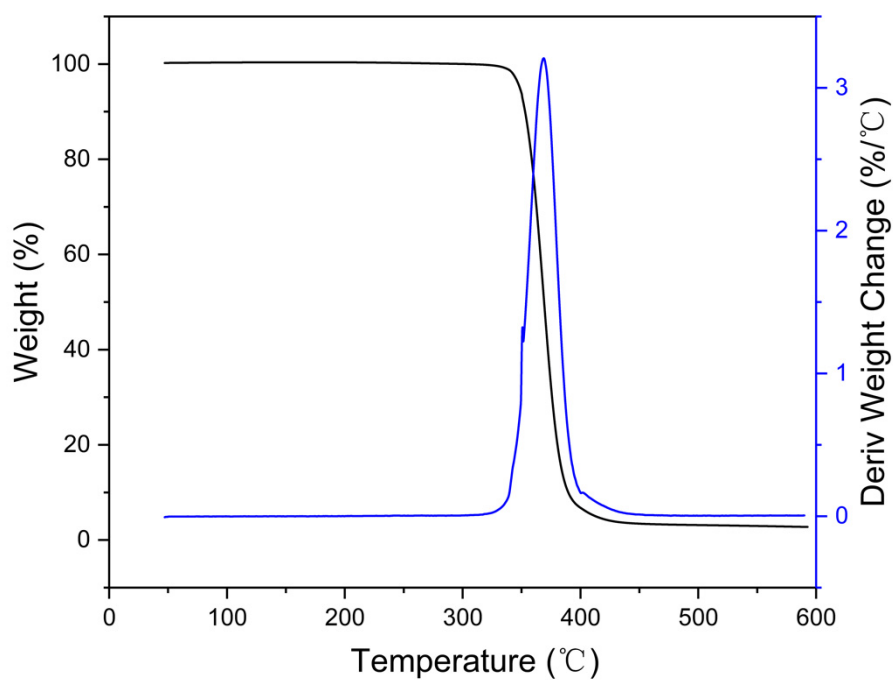


Fig. S41. TGA and DTG curves for P(DHB-Me-co-DHB-Et) obtained by [DHB-Me]/[DHB-Et]/[Zn1]/[I] = 50/1000/1/1, $T_d = 342$ °C, $T_{max} = 366$ °C.

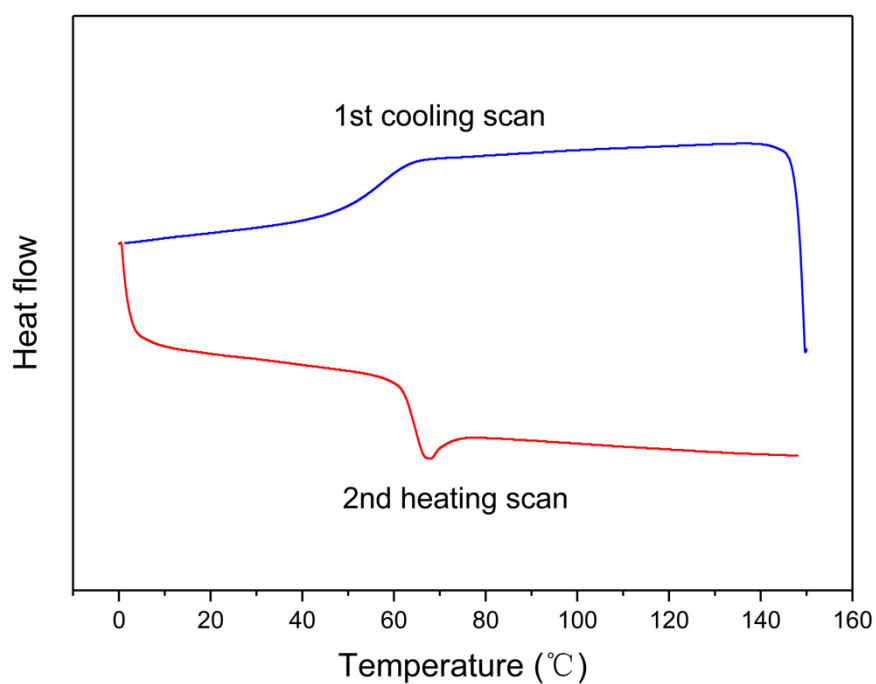


Fig. S42. DSC curves for P(DHB-Me) obtained by [DHB-Me]/[Zn1]/[I] = 500/1/1, $T_g = 65$ °C.

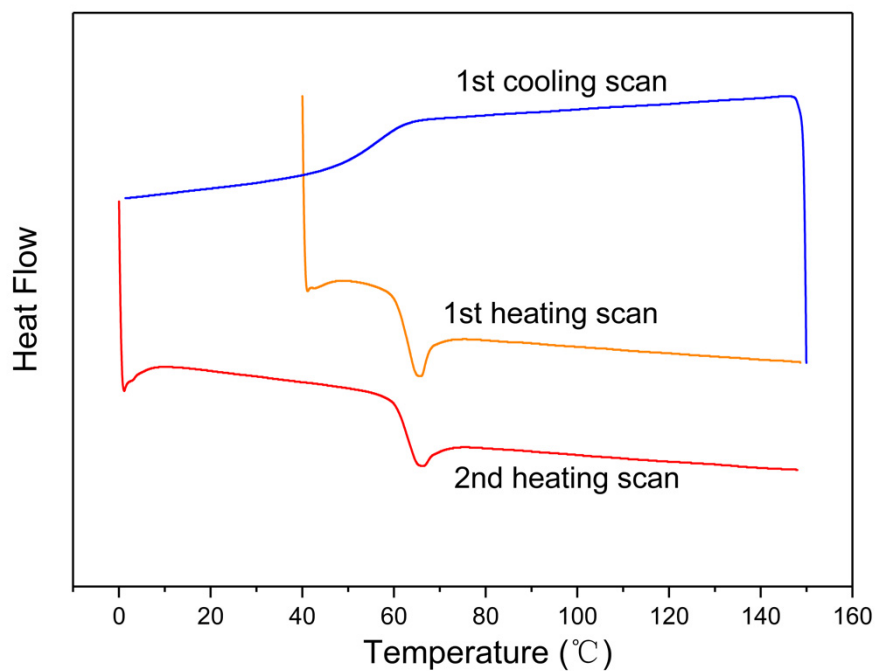


Fig. S43. DSC curves for P[(R)-DHB-Me] obtained by [(R)-DHB-Me]/[Zn1]/[I] = 500/1/1, $T_g = 63$ °C.

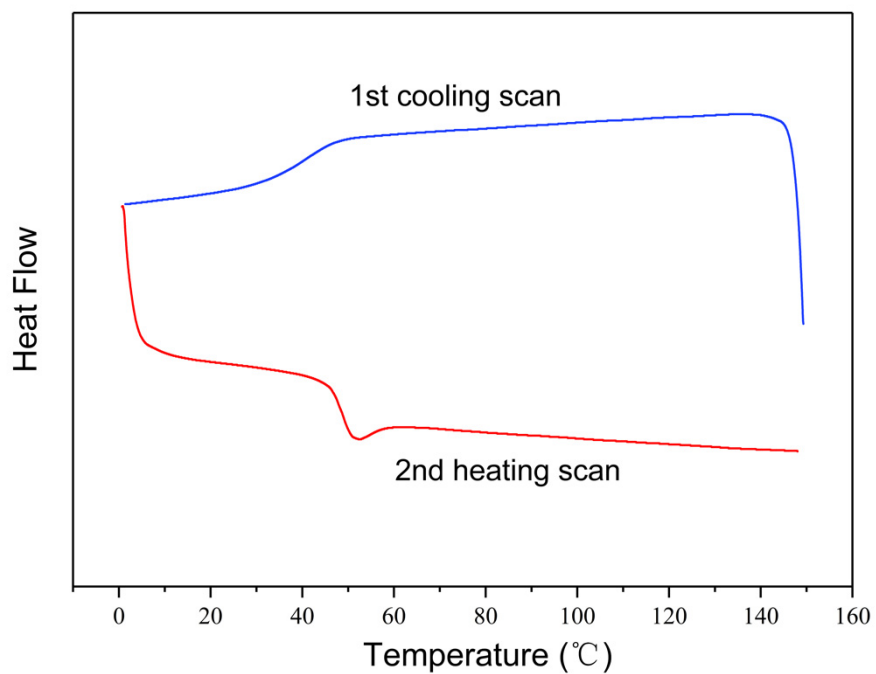


Fig. S44. DSC curves for P(DHB-Et) obtained by [DHB-Et]/[Zn1]/[I] = 500/1/1, $T_g = 49$ °C.

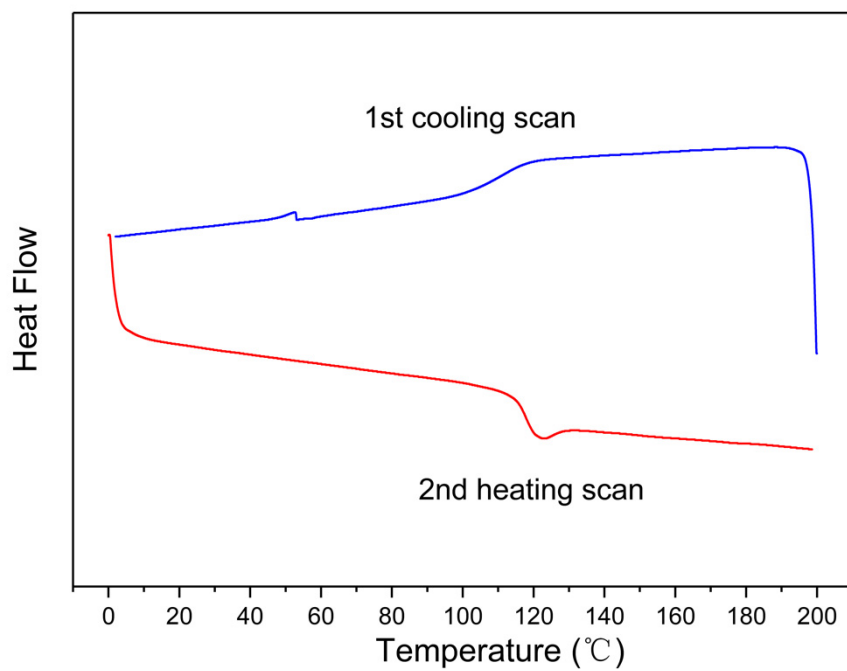


Fig. S45. DSC curves for P(DHN-Me) obtained by $[\text{DHN-Me}]/[\text{Zn1}]/[\text{I}] = 500/1/1$, $T_g = 118$ °C.

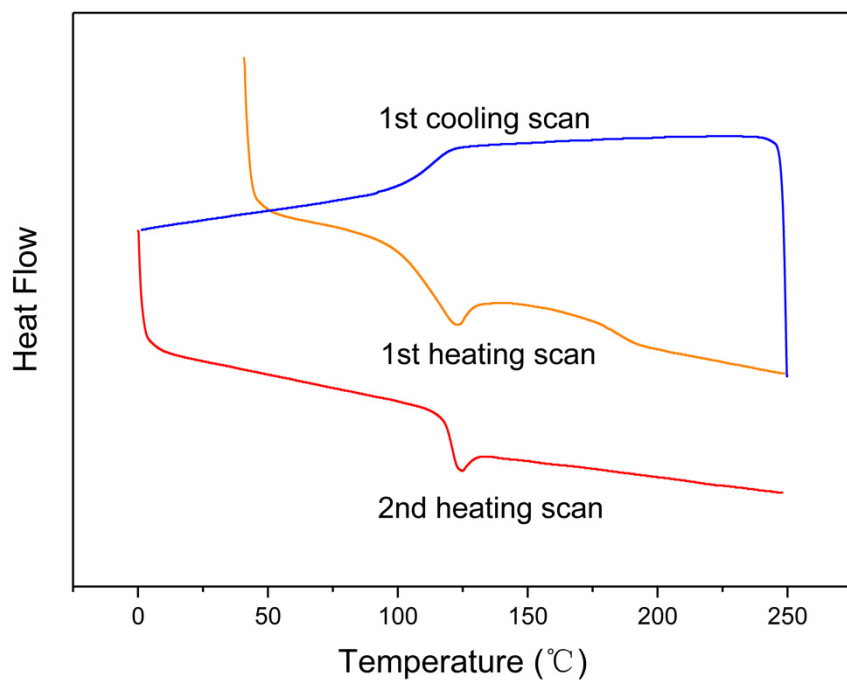


Fig. S46. DSC curves for P[(R)-DHN-Me] obtained by $[(R)\text{-DHN-Me}]/[\text{Zn1}]/[\text{I}] = 500/1/1$, $T_g = 121$ °C.

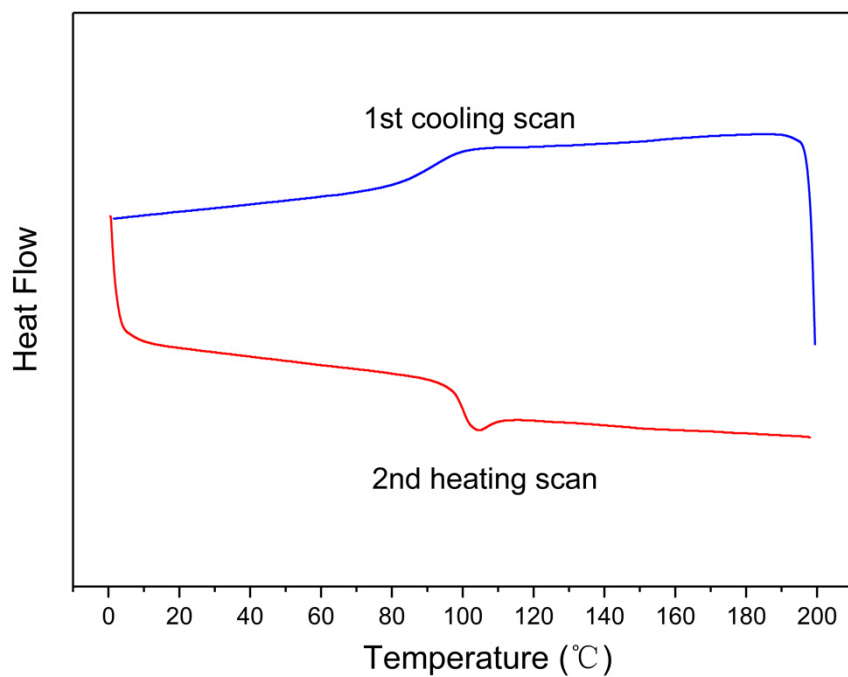


Fig. S47. DSC curves for P(DHN-Et) obtained by $[\text{DHN-Et}]/[\text{Zn1}]/[\text{I}] = 500/1/1$, $T_g = 100\text{ }^\circ\text{C}$.

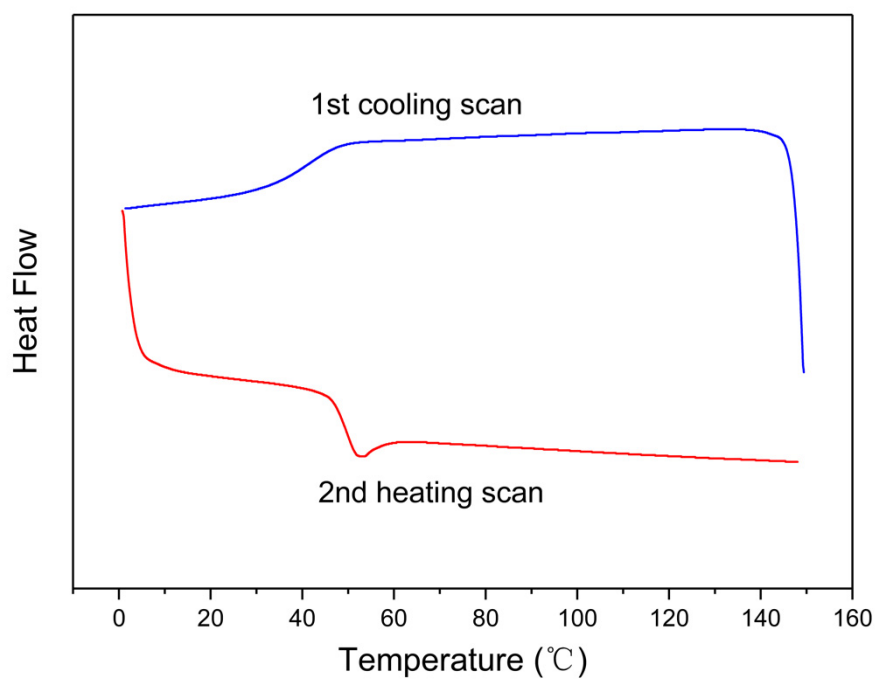


Fig. S48. DSC curves for P(DHB-Me-co-DHB-Et) obtained by $[\text{DHB-Me}]/[\text{DHB-Et}]/[\text{Zn1}]/[\text{I}] = 50/1000/1/1$, $T_g = 50\text{ }^\circ\text{C}$.

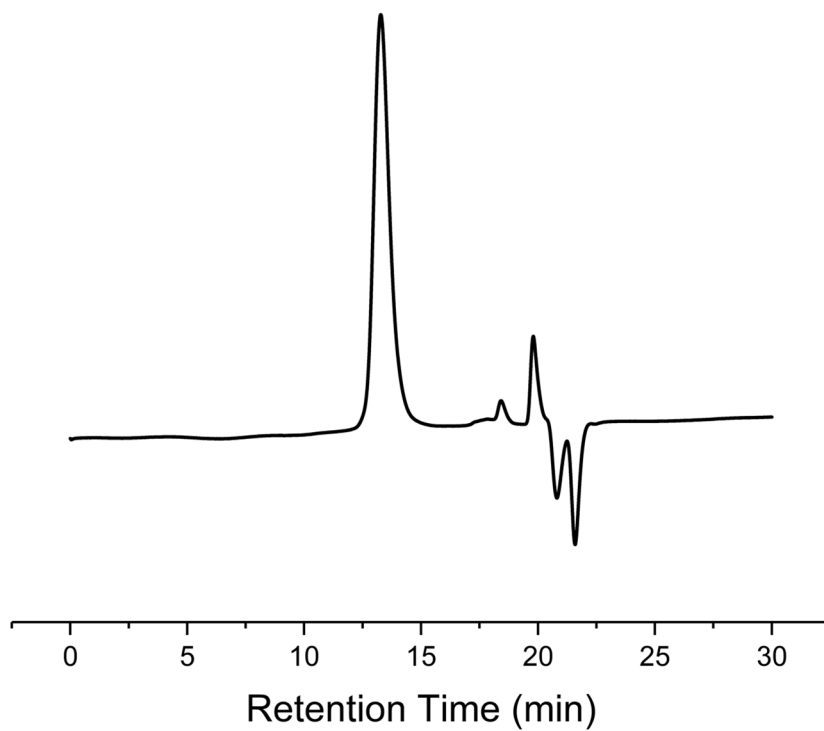


Fig. S49. GPC trace of P(DHB-Me) obtained by $[\text{DHB-Me}]/[\text{Zn1}]/[\text{I}] = 1000/1/1$, $M_n = 97.6 \text{ kg. mol}^{-1}$, $\bar{D} = 1.19$ (Table 1, entry 4).

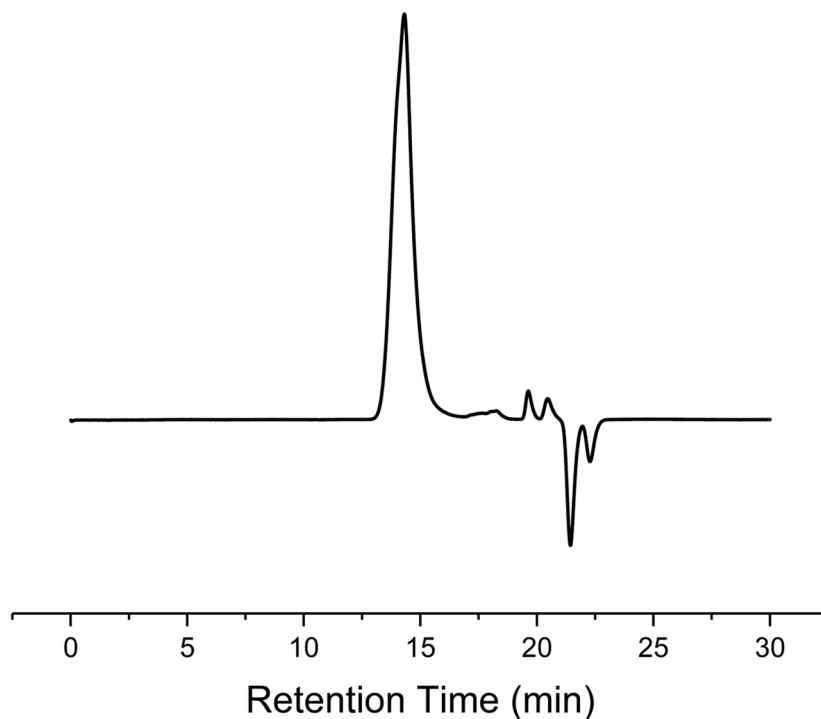


Fig. S50. GPC trace of P[(R)-DHB-Me] obtained by $[(R)\text{-DHB-Me}]/[\text{Zn1}]/[\text{I}] = 500/1/1$, $M_n = 36.6 \text{ kg. mol}^{-1}$, $\bar{D} = 1.25$ (Table 1, entry 6).

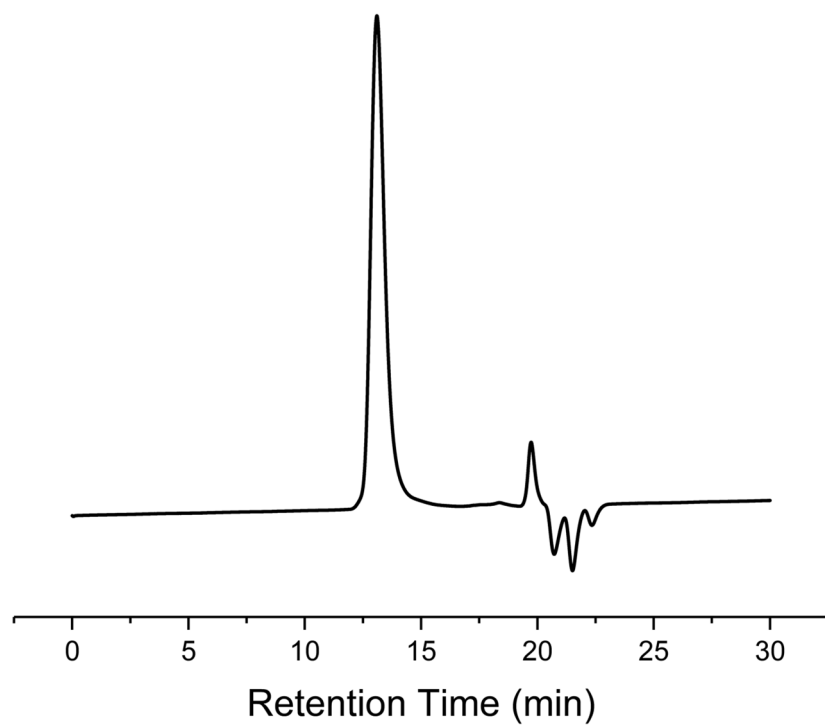


Fig. S51. GPC trace of P(DHB-Et) obtained by [DHB-Et]/[Zn1]/[I] = 1000/1/1, $M_n = 123$ kg. mol⁻¹, $\bar{D} = 1.17$ (Table 1, entry 12).

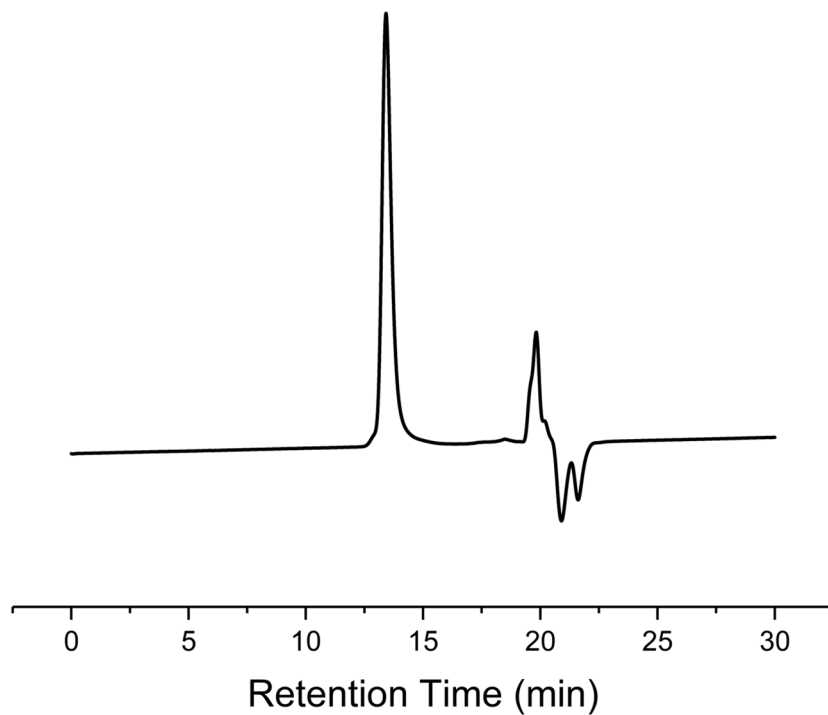


Fig. S52. GPC trace of P(DHN-Me) obtained by [DHN-Me]/[Zn1]/[I] = 500/1/1, $M_n = 66.0$ kg. mol⁻¹, $\bar{D} = 1.13$ (Table 1, entry 14).

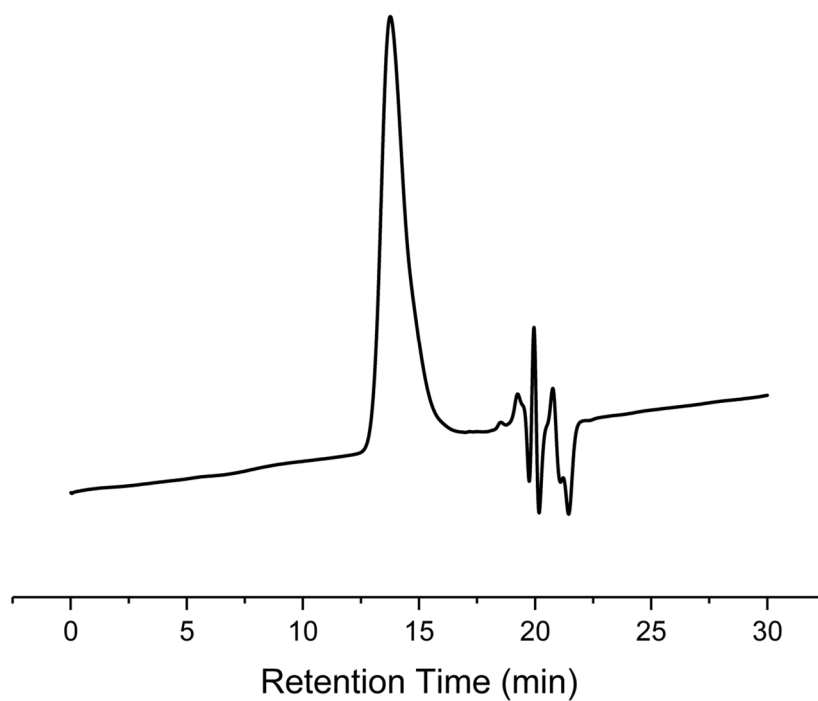


Fig. S53. GPC trace of P[(*R*)-DHN-Me] obtained by [(*R*)-DHN-Me]/[Zn1]/[I] = 500/1/1, $M_n = 42.5 \text{ kg. mol}^{-1}$, $\mathcal{D} = 1.57$ (Table 1, entry 17).

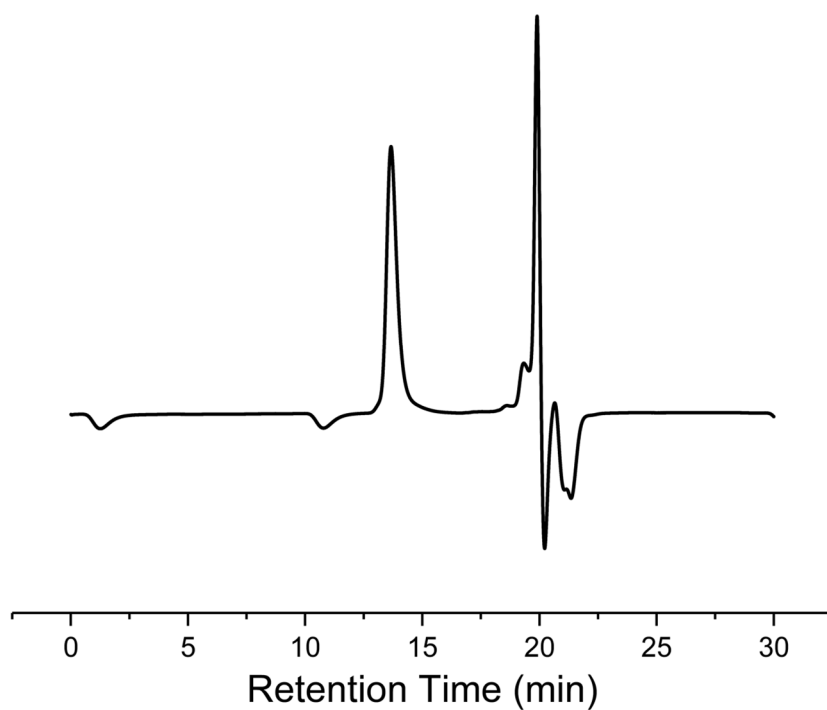


Fig. S54. GPC trace of P(DHN-Et) obtained by [DHN-Et]/[Zn1]/[I] = 1000/1/1, $M_n = 66.7 \text{ kg mol}^{-1}$, $\mathcal{D} = 1.10$ (Table 1, entry 21).

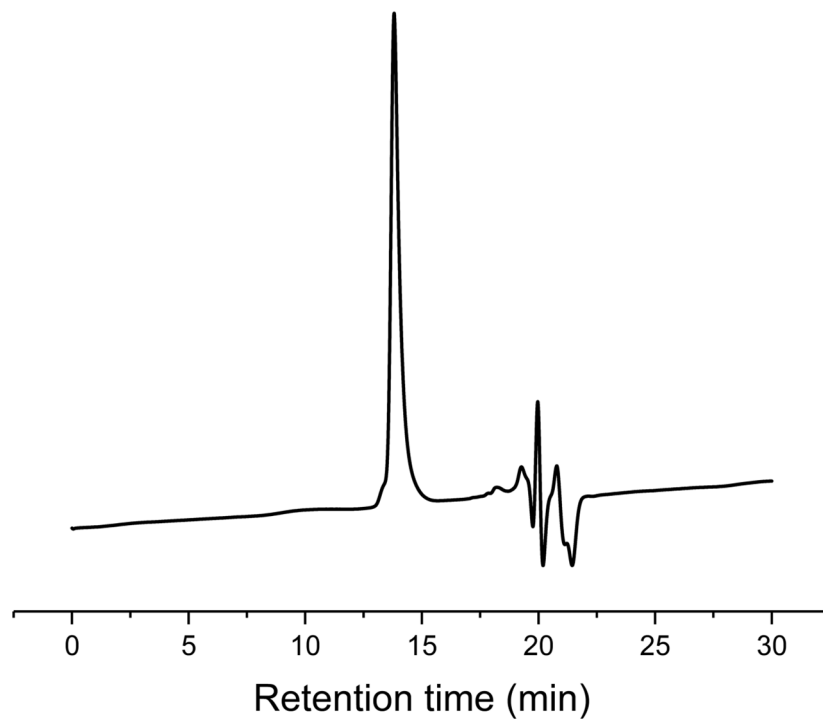


Fig. S55. GPC trace of P(DHB-Me-co-DHB-Et) obtained by [DHB-Me]/[DHB-Et]/[Zn1]/[I] = 50/1000/1/1, $M_n = 57.5 \text{ kg mol}^{-1}$, $\mathcal{D} = 1.13$ (Table S1, entry 1).

General Stereocomplexation Procedures

Stereocomplexes were prepared from a mixture of isotactic (*R*)-polymer and (*S*)-polymer in a 1:1 molar ratio (approximately 100 mg total). The solid polymer sample was dissolved in CHCl_3 (20 mg mL^{-1}), filtered through a plastic frit ($0.22 \mu\text{m}$ pore size nylon filter), and allowed to evaporate slowly and undisturbedly for 3–7 days. The obtained crystalline solid was collected and dried in a vacuum oven at $60 \text{ }^\circ\text{C}$ to a constant weight.

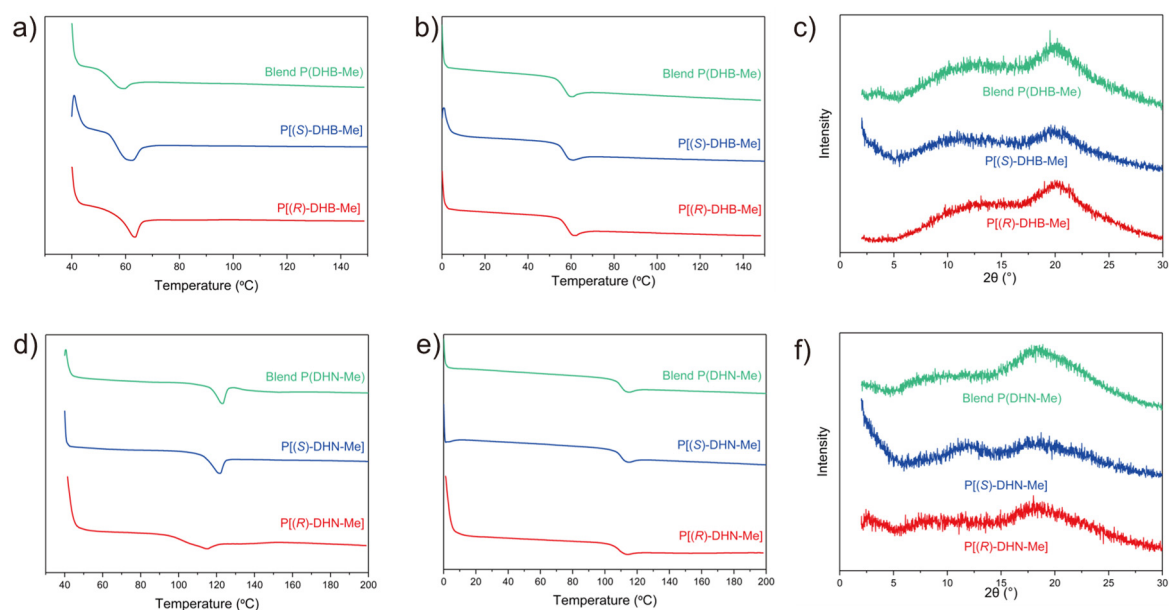


Fig. S56. a) DSC curves for P(DHB-Me)s (first heating, $10^\circ\text{C min}^{-1}$); b) DSC curves for P(DHB-Me)s (second heating, $10^\circ\text{C min}^{-1}$); c) PXRD spectra of P(DHB-Me)s; d) DSC curves for P(DHN-Me)s (first heating, $10^\circ\text{C min}^{-1}$); e) DSC curves for P(DHN-Me)s (second heating, $10^\circ\text{C min}^{-1}$); f) PXRD spectra of P(DHN-Me)s.

Mechanical Property

Table S2. Summary of mechanical properties of polymers. ^a

| Polymer | M_n /KDa | E/GPa | σ_y /MPa | σ_B /MPa | Elongation/% |
|---------------------|------------|-------------|-----------------|-----------------|----------------|
| P(DHB-Me) | 97.6 | 2.17 ± 0.36 | - | 33.69 ± 5.39 | 10.91 ± 2.15 |
| P(DHB-Et) | 123 | 0.74 ± 0.17 | 5.78 ± 2.91 | 3.16 ± 0.57 | 762.63 ± 94.40 |
| P(DHN-Me) | 88.7 | 2.11 ± 0.34 | - | 45.35 ± 1.94 | 3.10 ± 0.45 |
| P(DHN-Et) | 66.7 | 0.98 ± 0.11 | - | 35.18 ± 1.58 | 4.30 ± 0.62 |
| P(DHB-Me-co-DHB-Et) | 57.5 | 0.82 ± 0.11 | - | 38.16 ± 3.56 | 5.86 ± 0.56 |

^aCondition: Tested by uniaxial tensile tests. Strain rate of 10 mm/min, E: Tensile modulus, σ_y : yield strength, σ_B : break strength.

Table S3. Summary of mechanical properties of P(DHB-Me). ^a

| Sample | E/MPa | σ_B /MPa | Elongation/% |
|--------|---------|-----------------|--------------|
| 1 | 1832.32 | 33.61 | 14.25 |
| 2 | 2889.78 | 44.42 | 11.84 |
| 3 | 1806.38 | 33.36 | 9.97 |
| 4 | 2195.33 | 34.68 | 9.41 |
| 5 | 2104.90 | 33.76 | 9.08 |

^aCondition: Tested by uniaxial tensile tests. Strain rate of 10 mm/min, E: Tensile modulus, σ_B : break strength.

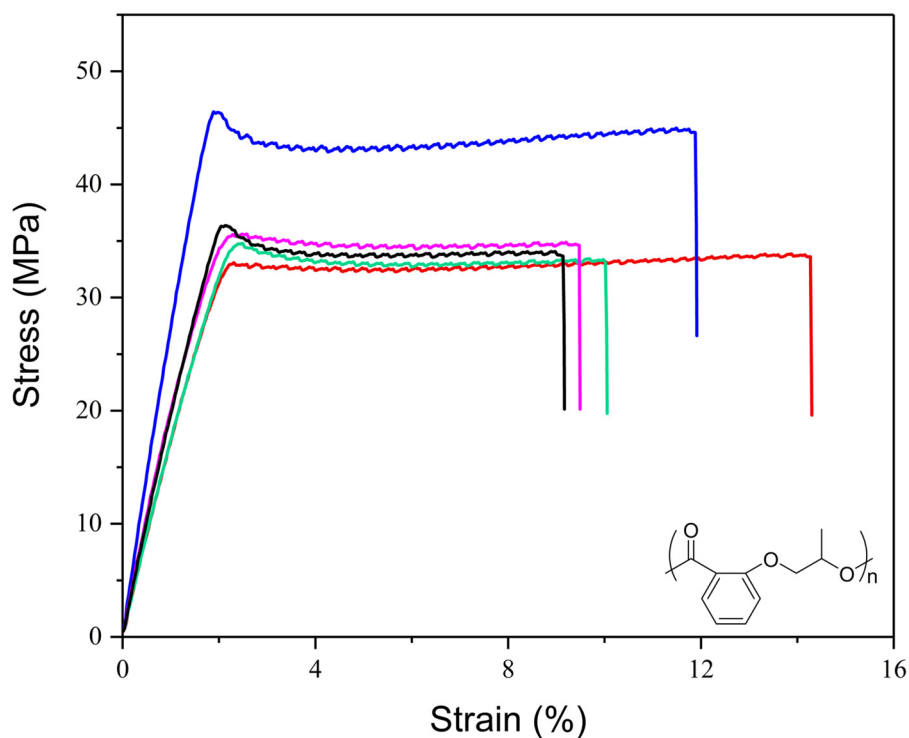


Figure S57. Stress-strain curves of P(DHB-Me).

Table S4. Summary of mechanical properties of P(DHB-Me)s.

| Polymer | M_n /KDa | E/GPa | σ_b /MPa | Elongation/% |
|---------------|------------|-----------------|------------------|-----------------|
| P(DHB-Me) | 35.0 | 2.28 ± 0.20 | 39.30 ± 1.31 | 2.89 ± 0.27 |
| P[(R)-DHB-Me] | 36.6 | 2.40 ± 0.14 | 31.30 ± 1.82 | 1.73 ± 0.24 |
| P[(S)-DHB-Me] | 36.6 | 2.51 ± 0.14 | 35.69 ± 4.27 | 1.96 ± 0.21 |

[a] Condition: Tested by uniaxial tensile tests. Strain rate of 5 mm/min, E: Tensile modulus, σ_y : yield strength, σ_b : break strength.

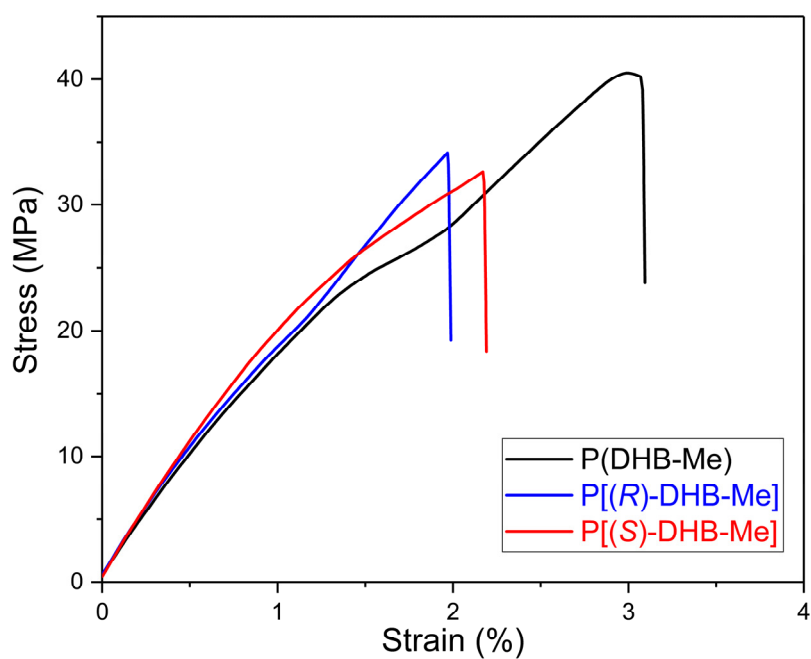


Fig S58. Stress-Strain curves of P(DHB-Me)s.

Table S5. Summary of mechanical properties of P(DHB-Et).^a

| Sample | E/MPa | σ_Y /MPa | σ_B /MPa | Elongation/% |
|--------|--------|-----------------|-----------------|--------------|
| 1 | 719.29 | 7.66 | 2.87 | 719.29 |
| 2 | 498.07 | 2.41 | 2.43 | 885.31 |
| 3 | 702.43 | 3.51 | 3.16 | 852.97 |
| 4 | 977.22 | 9.50 | 3.97 | 680.84 |
| 5 | 803.47 | 5.80 | 2.99 | 700.44 |

^aCondition: Tested by uniaxial tensile tests. Strain rate of 10 mm/min, E: Tensile modulus, σ_Y : yield strength, σ_B : break strength.

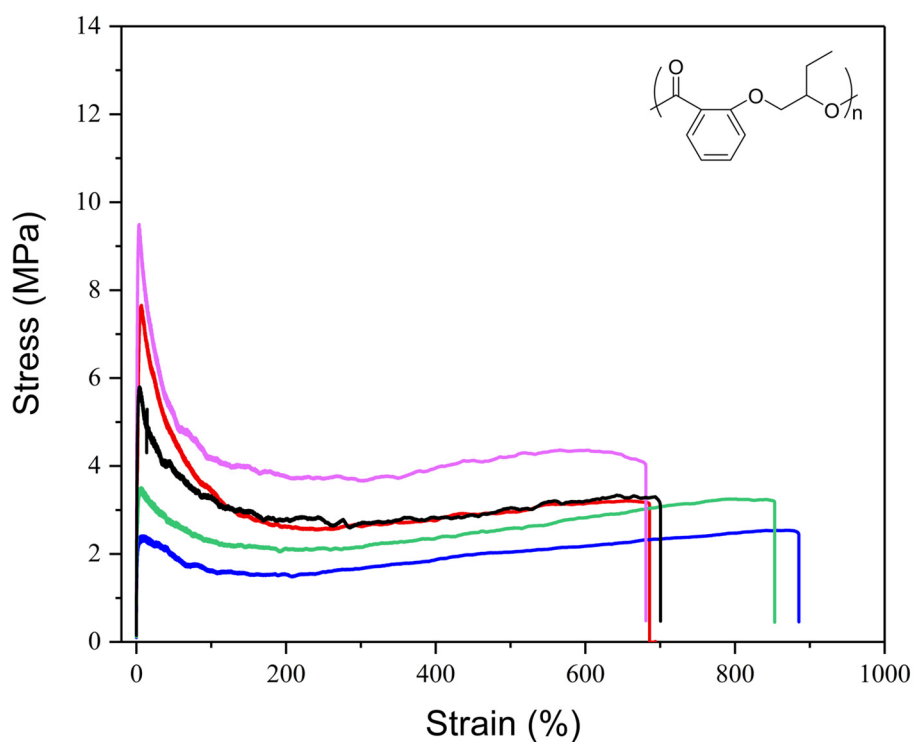


Figure S59. Stress-strain curves of P(DHB-Et).

Table S6. Summary of mechanical properties of P(DHN-Me).^a

| Sample | E/MPa | σ_B /MPa | Elongation/% |
|--------|---------|-----------------|--------------|
| 1 | 1948.34 | 42.23 | 3.66 |
| 2 | 2014.98 | 46.11 | 2.74 |
| 3 | 2338.01 | 46.48 | 2.66 |
| 4 | 2074.36 | 44.80 | 3.47 |
| 5 | 2176.40 | 47.13 | 2.95 |

^aCondition: Tested by uniaxial tensile tests. Strain rate of 10 mm/min, E: Tensile modulus, σ_B : break strength.

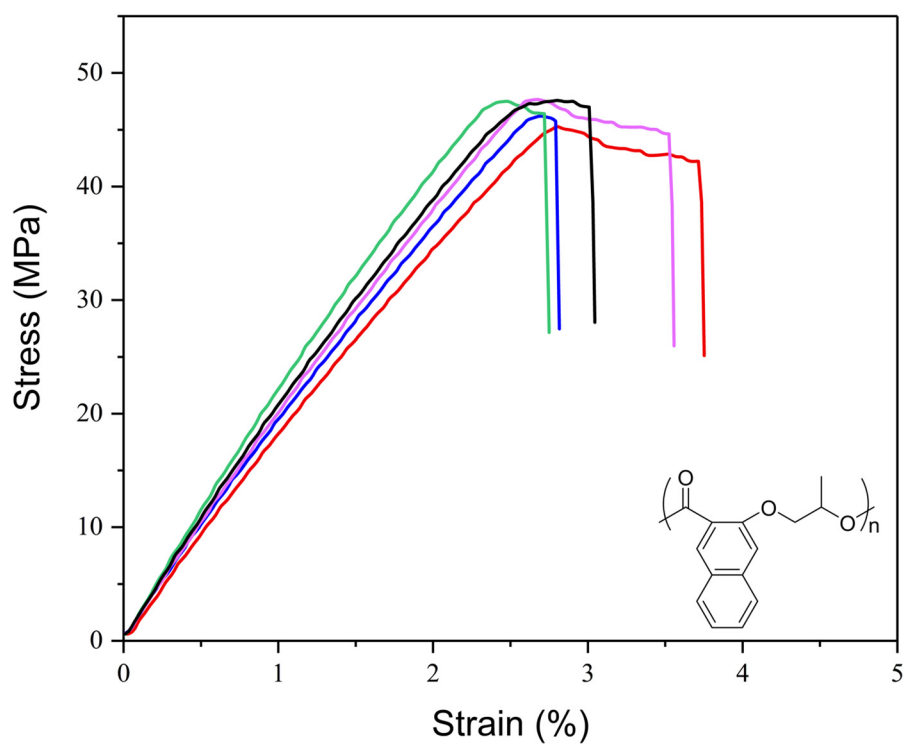


Figure S60. Stress-strain curves of P(DHN-Me).

Table S7. Summary of mechanical properties of P(DHN-Et).^a

| Sample | E/MPa | σ_B /MPa | Elongation/% |
|--------|---------|-----------------|--------------|
| 1 | 947.96 | 36.69 | 4.93 |
| 2 | 841.30 | 34.79 | 4.78 |
| 3 | 961.53 | 33.67 | 3.99 |
| 4 | 1017.85 | 36.98 | 4.40 |
| 5 | 1135.20 | 33.77 | 3.40 |

^aCondition: Tested by uniaxial tensile tests. Strain rate of 10 mm/min, E: Tensile modulus, σ_B : break strength.

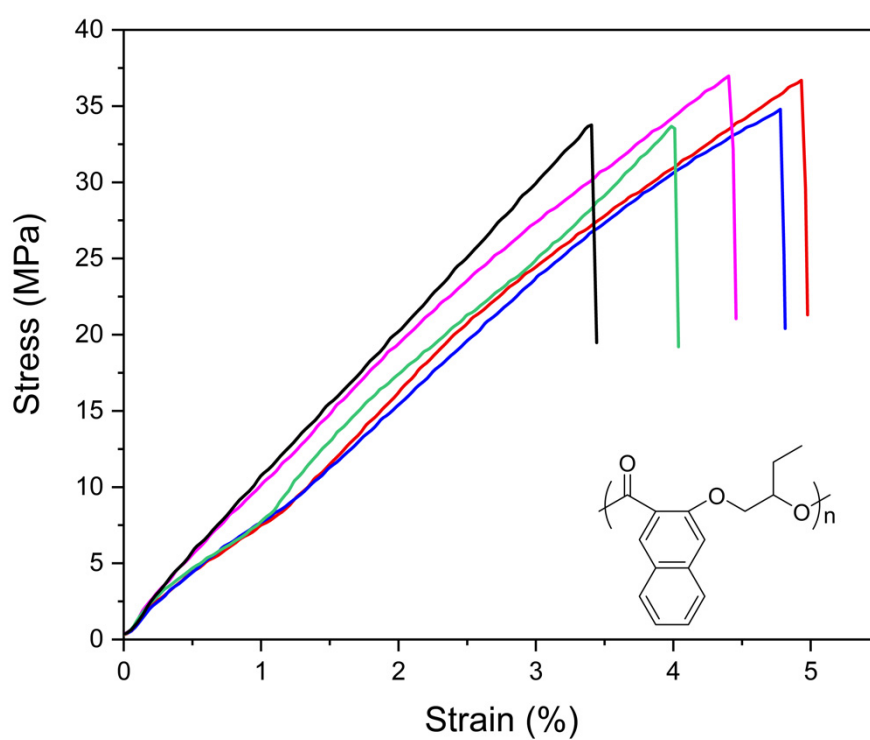


Figure S61. Stress-strain curves of P(DHN-Et).

Table S8. Summary of mechanical properties of P(DHB-Me-co-DHB-Et).^a

| Sample | E/MPa | σ_B /MPa | Elongation/% |
|--------|--------|-----------------|--------------|
| 1 | 881.97 | 41.55 | 5.70 |
| 2 | 635.25 | 32.10 | 6.64 |
| 3 | 931.03 | 38.88 | 5.19 |
| 4 | 837.59 | 39.14 | 5.59 |
| 5 | 810.76 | 39.11 | 6.17 |

^aCondition: Tested by uniaxial tensile tests. Strain rate of 10 mm/min, E: Tensile modulus, σ_B : break strength.

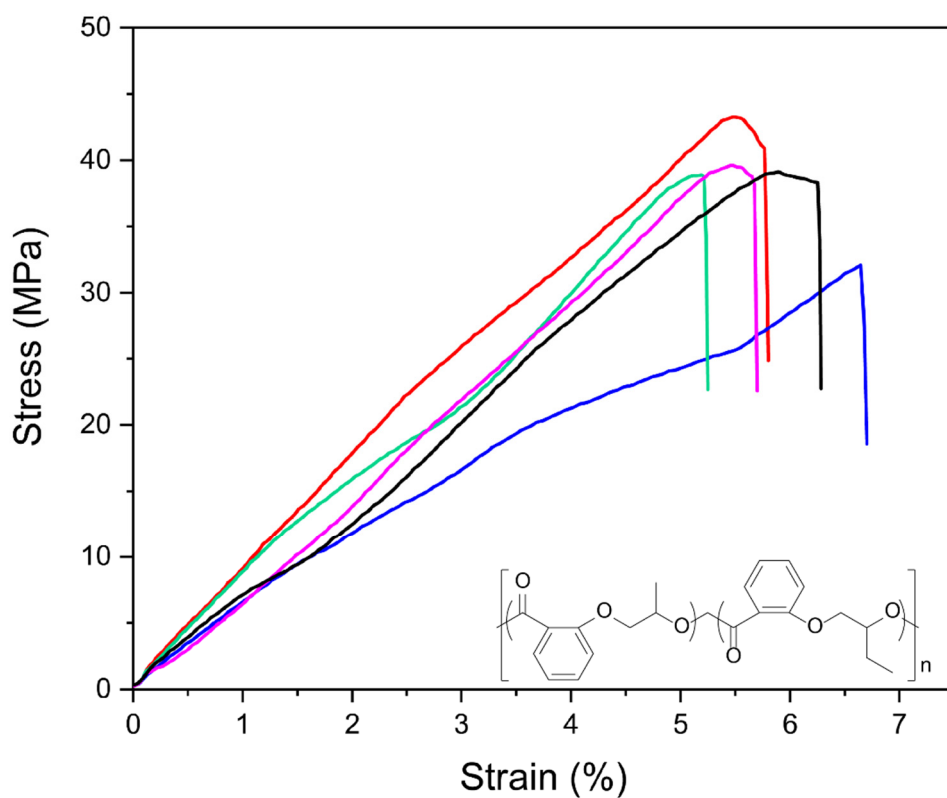


Figure S62. Stress-strain curves of P(DHB-Me-co-DHB-Et).

Thermodynamic study

In an argon-filled glovebox, a toluene stock solution of DHB-Me (712.2 mg, 4 mmol), *p*-tolylmethanol (4.9 mg, 0.04 mmol) and **Zn1** (23.6 mg, 0.04 mmol) was prepared in a 2 mL volumetric flask. The stock solution was divided equally to 4 vials (2 mL). Then the vials were sealed and brought outside of glovebox. After stirring at specific temperature for 5 h, the reaction was quenched by addition of 0.3 mL CDCl_3 containing benzoic acid (1 wt%). The polymerization reaction reached equilibrium at 45–75 °C and the conversion of DHB-Me was monitored by ^1H NMR. The equilibrium monomer concentration, $[\text{DHB-Me}]_{\text{eq}}$, was measured to be 0.68, 0.80, 0.94 and 1.10 mol. L^{-1} for 45 °C, 55 °C, 65 °C and 75 °C. The Van't Hoff plot of $\ln[\text{DHB-Me}]_{\text{eq}}$ versus $1/T \times 10^3$ gave a linear fitting with a slope of -1.78 and an intercept of 5.21, from which the thermodynamic parameters were calculated to be $\Delta H_p^\circ = -14.8 \text{ kJ. mol}^{-1}$ and $\Delta S_p^\circ = -43.3 \text{ J. mol}^{-1.} \text{ K}^{-1}$, based on the equation $\ln[\text{DHB-Me}]_{\text{eq}} = \Delta H_p^\circ/RT - \Delta S_p^\circ/R$, where R is the molar gas constant. T_c was calculated to be 69 °C at $[\text{DHB-Me}]_0 = 1 \text{ mol/L}$, based on the equation $T_c = \Delta H_p^\circ/(\Delta S_p^\circ + R \ln [\text{DHB-Me}]_0)$.

Table S9. Raw data over equilibrium conversion at various temperatures for DHB-Me.^a

| Entry | T (K) | Conv. ^b (%) | M_0 (mol/L) | $T^{-1} \times 10^3$ (K^{-1}) | $[M]_{\text{eq}}$ (mol/L) | $\ln[M]_{\text{eq}}$ (mol/L) |
|-------|-------|------------------------|---------------|--|---------------------------|------------------------------|
| 1 | 318.3 | 66 | 2.0 | 3.14 | 0.68 | -0.3857 |
| 2 | 328.3 | 60 | 2.0 | 3.05 | 0.80 | -0.2231 |
| 3 | 338.3 | 53 | 2.0 | 2.96 | 0.94 | -0.0619 |
| 4 | 348.3 | 45 | 2.0 | 2.87 | 1.10 | 0.0953 |

^aReaction conditions: Catalyst = **Zn1**, initiator (I) = *p*-tolylmethanol, toluene, $[\text{DHB-Me}]/[\text{Zn1}]/[\text{I}] = 100/1/1$, $[M]_0 = 2 \text{ mol. L}^{-1}$. ^bMonomer conversion measured by ^1H NMR of the quenched solution.

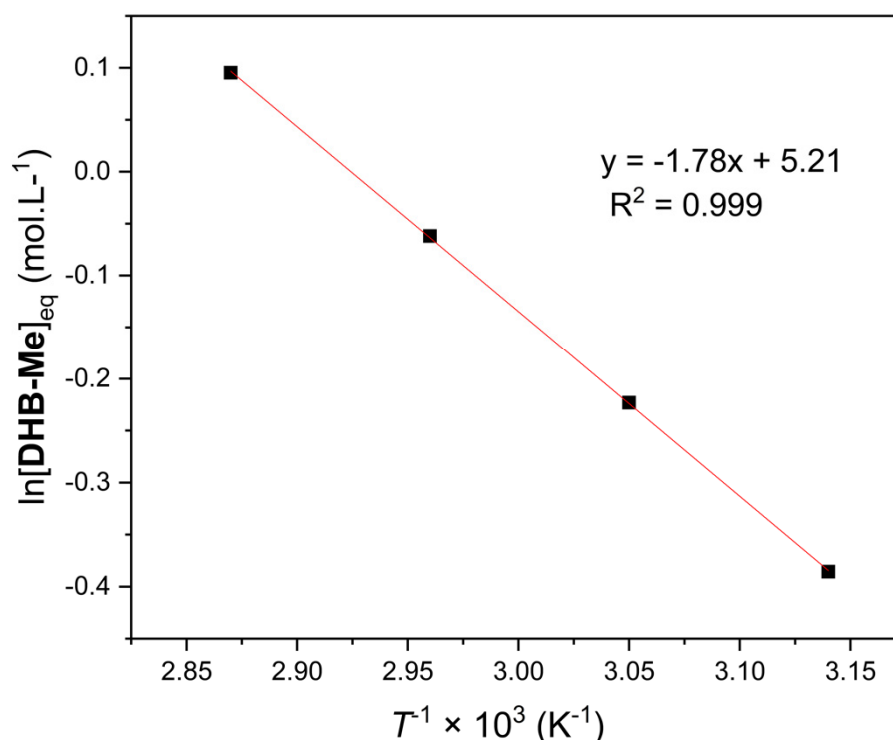


Fig. S63. Van't Hoff plot of $\ln[\text{DHB-Me}]_{\text{eq}}$ vs. reciprocal of the absolute temperature (T^{-1}).

General procedure for the depolymerization of polymers in dilute solutions

The depolymerization was conducted at 120 °C or 140 °C with **Zn1** or TBD as the catalyst. Depolymerization of P(DHB-Me) was used as an example. Inside an argon-filled glovebox, a 15 mL pressure tube was charged with the purified P(DHB-Me) (18 mg), **Zn1** (5 mol%) and toluene (5 mL). The reactor was sealed, taken out of the glovebox, and immersed in the oil bath. The mixture was stirred at 120 °C for 0.5 h. The reaction mixture (3 mL) was withdrawn and concentrated under reduced pressure to determine the conversion by ¹H NMR spectroscopy.

Table S10. Results for depolymerization of polymers in dilute solutions.^a

| Entry | Polymer | Catalyst | Catalyst loading (mol %) | Temperature (°C) | Time (h) | Conv. ^b (%) |
|-------|-----------|----------|--------------------------|------------------|----------|------------------------|
| 1 | P(DHB-Me) | Zn1 | 5 | 120 | 0.5 | 96 |
| 2 | P(DHB-Me) | TBD | 10 | 120 | 12 | 63 |
| 3 | P(DHB-Et) | Zn1 | 5 | 120 | 0.5 | 94 |
| 4 | P(DHB-Et) | TBD | 10 | 120 | 12 | 74 |
| 5 | P(DHN-Me) | Zn1 | 5 | 140 | 0.5 | 80 |
| 6 | P(DHN-Me) | TBD | 10 | 140 | 12 | 93 |
| 7 | P(DHN-Et) | Zn1 | 5 | 140 | 0.5 | 83 |
| 8 | P(DHN-Et) | TBD | 10 | 140 | 12 | 98 |

^aReaction conditions: [M] = 0.2 M, toluene. ^bPolymer conversion measured by ¹H NMR of the solution.

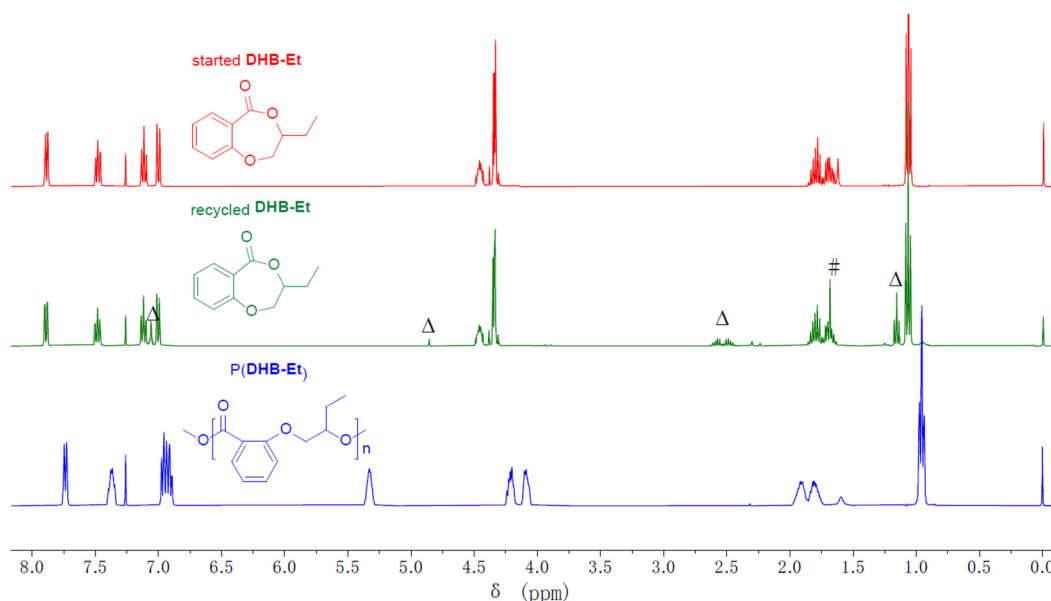


Fig. S64. ¹H NMR spectra of P(DHB-Et) prepared by [DHB-Et]/[**Zn1**]/[I] = 100/1/1 (bottom), recycled DHB-Et after depolymerization (middle) and clean starting DHB-Et for comparison (top). (*solvent toluene impurity, Δ catalyst **Zn1** residual, # H₂O)

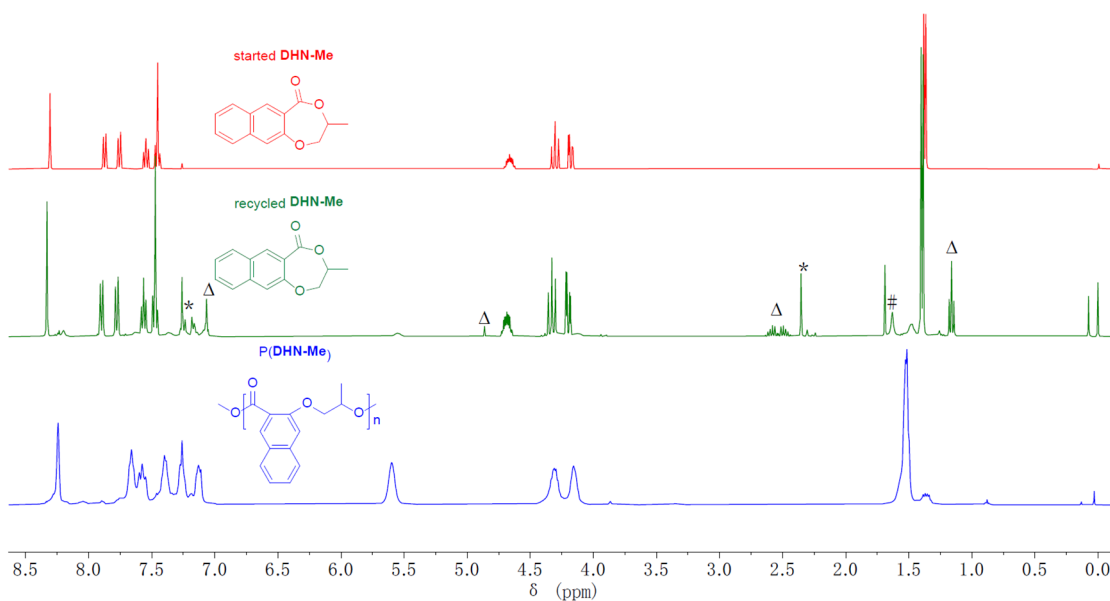


Fig. S65. ^1H NMR spectra of P(DHN-Me) prepared by $[\text{DHN-Me}]/[\text{Zn1}]/[\text{I}] = 100/1/1$ (bottom), recycled DHN-Me after depolymerization (middle) and clean starting DHN-Me for comparison (top). (*solvent toluene impurity, Δ catalyst **Zn1** residual, # H_2O)

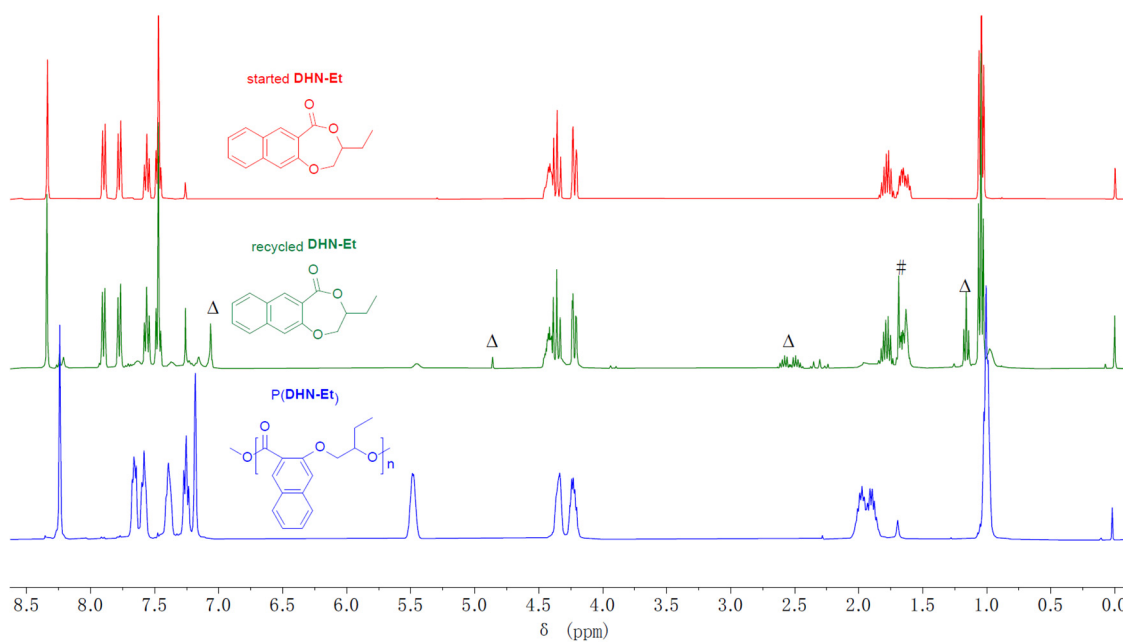


Fig. S66. ^1H NMR spectra of P(DHN-Et) prepared by $[\text{DHN-Et}]/[\text{Zn1}]/[\text{I}] = 100/1/1$ (bottom), recycled DHN-Et after depolymerization (middle) and clean starting DHN-Et for comparison (top). (Δ catalyst **Zn1** residual, # H_2O)

Reference

- [1] M. Cheng, D. R. Moore, J. J. Reczek, B. M. Chamberlain, E. B. Lobkovsky, G. W. Coates, *J. Am. Chem. Soc.* **2001**, *123*, 8738-8749.